Molecular analysis of pancreatic cancer metastasis in a genetically engineered mouse model

Dissertation

zur

Erlangung des Doktorgrades (Dr. rer. nat.)

der

Fakultät Wissenschaftszentrum Weihenstephan für Ernährung, Landnutzung und Umwelt der Technischen Universität München

vorgelegt von

Annegret Gohlke

TECHNISCHE UNIVERSITÄT MÜNCHEN
Lehrstuhl für Humanbiologie

Molecular analysis of pancreatic cancer metastasis in a genetically engineered mouse model

Annegret Gohlke

Vollständiger Abdruck der von der Fakultät Wissenschaftszentrum Weihenstephan für Ernährung, Landnutzung und Umwelt der Technischen Universität München zur Erlangung des akademischen Grades eines

Doktors der Naturwissenschaften

genehmigten Dissertation.

Vorsitzende:		Univ.-Prof. A. Schnieke, Ph.D.
Prüfer der Dissertation:	1.	Univ.-Prof. Dr. M. Schemann
	2.	Univ.-Prof. Dr. R. M. Schmid
	3.	Priv.-Doz. Dr. J. Beckers

Die Dissertation wurde am 10.08.2010 bei der Technischen Universität München eingereicht und durch die Fakultät Wissenschaftszentrum Weihenstephan für Ernährung, Landnutzung und Umwelt am 08.12.2010 angenommen.

So eine Arbeit wird eigentlich nie fertig,
man muss sie für fertig erklären,
wenn man nach Zeit und Umständen
das Möglichste getan hat.

(Johann Wolfgang von Goethe)

Table of contents

Table of Figures

Abbreviations

ALSV-A	avian leukosis sarcoma virus subgroup A
BSA	bovine serum albumine
CSC	cancer stem cells
CGH	comparative genomic hybridisation
DNA	deoxyribonucleid acid
EGFP	enhanced green fluorescent protein
EMT	epithelial to mesenchymal transition
FBS	fetal bovine serum
fluc	firefly luciferase
GSEA	gene set enrichment analysis
h	hour
HE	Haematoxylin and Eosin
IGF	Insulin like Growth Factor
LOH	loss of heterozygozity
LSL	lox-stop-lox
Min	minute(s)
miRNA	microRNA
PanIN	pancreatic interepithelial neoplasia
PBS	phosphate buffered saline
PCR	polymerase chain reaction
OI	orthotopic implantation
PDAC	pancreatic ductal adenocarcinoma
TGF-β	transforming growth factor β
RNA	ribonucleid acid
RNase	ribonuclease
rpm	rotations per minute
RCAS	avian leukosis virus long terminal repeat with splice acceptor
RCASBP(A)	RCAS vector with Bryan-RSV polymerase and subgroup A envelope
RT	Room temperature
RT-PCR	Real-time PCR
TVA	Subgroup A avian leukosis virus receptor

WT	Wild type
µg	Microgram
µL	Microliter

1 Introduction

1.1. Pancreatic ductal adenocarcinoma (PDAC)

Pancreatic cancer is the fourth leading cause of cancer associated death in the western world (Jemal et al., 2009). About 60000 cases are diagnosed with this highly malignant tumour each year in Europe and incidence almost equals mortality. The most common pancreatic tumour is pancreatic ductal adenocarcinoma (PDAC) which accounts for more than 85 % of pancreatic neoplasms (Warshaw and Fernandez-del Castillo, 1992). In 60 % of cases PDAC arises in the head of the pancreas. PDAC is characterized by a high degree of desmoplasia, a stroma that is built up by fibroblasts and cells of the inflammatory response. It penetrates surrounding tissues like lymphatics, spleen and the peritoneum. Typically PDAC metastasizes to the liver and lung.

The 5-year survival rate is below 5 % and median survival is below six months. This is due to very late diagnosis as the disease causes unspecific and hard to identify symptoms such as pain in the upper abdomen, loss of appetite, significant weight loss or jaundice (National Cancer Institute, 2002). Only 10 % of tumours are resectable because surgery can only be performed in the minority of cases in which the tumour is localised and has not yet invaded surrounding tissue or metastasized. In regard to these cases the 5-year survival rate is approximately at 20 % which leads to overall survival of less than 2 %. In addition pancreatic cancer is extensively resistant to chemo- and radiotherapy (Schneider et al., 2005). Complete remission is extremely rare.

1.1.1 Carcinogenesis

Development of PDAC occurs through graded progression through well characterised precursor lesions, namely pancreatic intraepithelial neoplasia (PanIN) (Klimstra and Longnecker, 1994). The development of the earliest precursor lesion PanIN 1A is characterized by columnar, mucinous epithelium which acquires a papillary architecture as it proceeds to PanIN 1B stage (see Figure 1-1). These lesions are present in up to 40 % of non-malignant pancreata of patients from 50 years onward (Hruban et al., 2004). During progression of PanINs to stages 2 and 3 they obtain increasing amounts of nuclear atypia and structural abnormalities like

budding of cells into the lumen of ducts. In line with the morphological changes PanINs also acquire multiple genetic alterations ultimately leading to PDAC (Hruban et al., 2000).

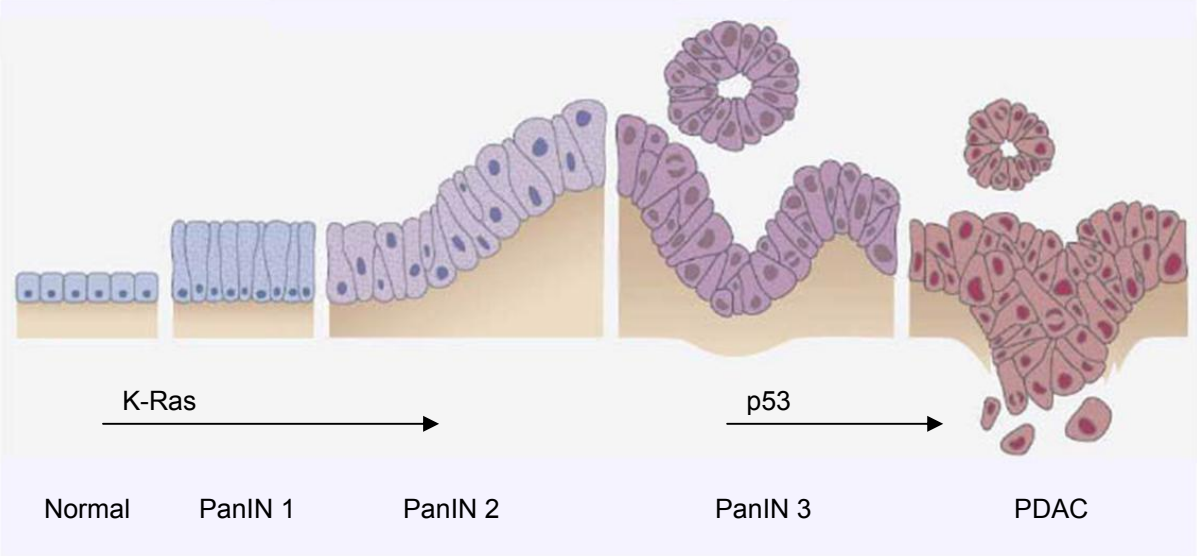

Figure 1-1 Tumour progression model of human PDAC adapted after Hezel et al. (2006) and Hruban et al. (2000) showing the morphology of augmenting PanIN stages and PDAC and onset of *K-Ras* and *p53* mutations

One of the first and most frequent mutations is the activating *K-Ras* point mutation at codon 12 (Almoguera et al., 1988; Klimstra and Longnecker, 1994; Terhune et al., 1998). Substitutions from GGT to GAT or GTT, and more rarely CGT result in exchange of glycine with aspartate, valine or arginine. Up to 40 % of early PanIN lesions and nearly 100 % of PDAC carry this hotspot mutation.

K-RAS belongs to the family of GTPases. Mutation at codon 12 leads to a constitutively active state of the protein and therefore its functions on proliferation, differentiation and survival (Campbell et al., 1998; Malumbres and Barbacid, 2003) can not be attenuated by hydrolysis of GTP. Accordingly, these functions are independent of growth factor stimulation. With development of higher grade lesions more mutations and genetic alterations such as aneuploidy and chromosomal rearrangements are accumulated.

Another gene locus important for progression of pancreatic cancer is the *INK4A* and *ARF* containing 9p21 locus *Cyclin-dependent kinase inhibitor 2A (CDKN2A)*. In 80 % to 95 % of PDAC cases its function is lost subsequently to *K-Ras* mutation (Rozenblum et al., 1997). INK4A indirectly inhibits phosphorylation of RB thereby

blocking cell cycle progression into S phase. ARF on the other hand inhibits MDM2 which tags p53 for proteasomal degradation.

Other noteworthy mutations occurring in later stages of PanINs are missense mutations of the DNA-binding domain of the tumour suppressor *p53*. They arise in over 50 % of PDAC cases (Boschman et al., 1994; Rozenblum et al., 1997). Mutation of *p53* often goes along with loss of heterozygosity and therefore loss of wildtype function (Barton et al., 1991; Boschman et al., 1994). This leads to impaired growth checkpoints and deficient protection against genomic rearrangements. As loss of p53 wildtype function cooperates with telomere dysfunction in pancreatic cancer as well as multiple other carcinomas (Chin et al., 1999) this accounts for the high degree of intratumoural genomic heterogeneity.

Furthermore, the transcription factor SMAD4 (DPC4 named for "deleted in pancreatic carcinoma") is lost in PanINs 3 and PDAC through deletion or point mutation with a frequency of up to 66% in carcinomas (Biankin et al., 2001; Hahn et al., 1996; Wilentz et al., 2000). Its central role in the transforming growth factor β (TGF-β) signaling pathway is likely to play a major role in tumorigenesis (Massague et al., 2000). Nevertheless, other TFG-β independent mechanisms might also contribute to tumorigenesis: Restoration of SMAD4 function in pancreatic cancer cells inhibited tumour formation and down-regulated angiogenesis while TGF-β sensitivity was not altered (Schwarte-Waldhoff et al., 2000).

1.1.2 Mouse models of pancreatic cancer

Taking into account that there are significant differences between mice and humans (Rangarajan and Weinberg, 2003) mouse models have nevertheless contributed immensely to our understanding of cancer biology. Broadly altering cancer genes throughout a tissue via cell-specific transgene expression or throughout the entire organism by targeted germline mutations have been extensively applied to examine the early stages of tumourigenesis. To learn more about later molecular and cellular mechanisms of cancer such as angiogenesis, invasion and metastasis, aspects which are critical to understand from the human health perspective, more complex strategies have been devised.

However, the generation of an adequate model mimicking human PDAC has been a major challenge. First attempts from the 1980s on were accomplished targeting the pancreas specific elastase promoter and generating transgenic mice expressing

genes such as *Hras*, *SV40 T antigen*, *c-myc*, and *TGF-α* (Ornitz et al., 1987; Quaife et al., 1987; Sandgren et al., 1990; Wagner et al., 1998). Unfortunately, none of these models exhibited the classic tumour morphology of pancreatic ductal adenocarcinoma resembling the human disease as the oncogenes were expressed mostly in the acinar compartment and developed acinar and at best mixed carcinomas. *Elastase-TGF-α* mice featured tubular complexes derived from acinar-ductal metaplasia, a phenomenon only seldomly seen in human pancreatic pathologies. Moreover, they did not acquire mutations in *Kras* which are significant for development of human PDAC as described above. As a consequence, oncogenic Kras was expressed under the control of the ductal CK-19 promoter (Brembeck et al., 2003) and in a distinct study under the control of the elastase promoter (Grippo et al., 2003). Still, formation of PanINs and PDAC could not be induced. In the *CK-19-K-ras* model only minor morphological changes with occasional focal ductal hyperplastic lesions and lymphocytic infiltrates were detected.

Headway was made when two transcription factors important for pancreatic development were brought into focus: the homeodomain protein PDX-1and the helix-loop-helix protein PTF1, with its major subunit p48. PDX-1 is expressed in pancreatic progenitor cells at E8.5 (Guz et al., 1995; Offield et al., 1996). Shortly after PDX-1 Ptf1a/p48 is expressed at E9.5 also in pancreatic progenitor cells (Krapp et al., 1998). Both transcription factors are key regulators of the pancreatic organogenesis and are active in the common progenitors of all pancreatic cell types with relatively restricted expression outside of the pancreas. PDX-1 first marks pancreatic progenitor cells during embryogenesis, later on it is expressed in acinar and endocrine precursor cells and in adulthood it becomes mainly restricted to polypeptide- (PP) and insulin-expressing β-cells (Miller et al., 1994; Ohlsson et al., 1993). Ptf1a/p48 is required for the anlage of the pancreatic ventral bud along with the outgrowth of early pancreatic branches (Kawaguchi et al., 2002). These two transcription factors were embedded into a new strategy to generate mouse models. They enabled the generation of a refined genetically engineered mouse model that closely mirror many of the genetic and histologic characteristics of the human disease like induction of PanINs and progression to invasive and metastatic PDAC.

Tyler Jack's group generated mice expressing *Kras* with the oncogenic glycine to aspartic acid (G12D) mutation at codon 12 (Jackson et al., 2001). They knocked this construct into the endogenous *Kras* locus. To prevent ubiquitious expression the

oncogene was silenced by a stop cassette flanked by loxP sites upstream of the mutation (*LSL–K-Ras*^{G12D}). This stop cassette can conditionally be excised by a Cre-recombinase thereby activating permanent expression of oncogenic K-Ras in recombined cells – a strategy that has been deduced and modified from approaches to delete various genes of interest which has been effectively applied using the Cre/loxP system in cancer research. (Jonkers et al., 2001; Marino et al., 2000; Xu et al., 1999). This was applied to this pancreatic model by crossing the *LSL–K-Ras*^{G12D} mice either with a knock-in strain expressing Cre under control of the Ptf1a/p48 promoter (Kawaguchi et al., 2002) or with a transgenic strain expressing Cre under control of the PDX-1 promoter. Both models developed PanINs 1-3 with some mice progressing to invasive and metastatic disease states after six to eight months. This for the first time closely recapitulated human PDAC (Hingorani et al., 2003). Because there was such latency until formation of a malignant tumour several groups generated follow up mouse models. Aguirre and colleagues placed concomitant biallelic *Ink4a/Arf* deletion in the context of *Kras*^{G12D} expression (Aguirre et al., 2003) a gene often mutated or silenced in preneoplastic human lesions and PDAC. Mice of this strain developed an aggressive, locally invasive, and poorly differentiated disease accompanied, on occasion, by microscopic metastases. Of note, no further mutations in other tumour suppressors could be detected. Moreover, besides their high local aggressiveness these tumours showed a benign cytogenetic profile and sarcomatoid histology both features seldomly appearing in the human disease. Hingorani and colleagues took a further step to refine the above mentioned *Kras*^{G12D} mouse by employing a mutant *p53* gain of function mouse strain previously described (Olive et al., 2004). This mouse model was designed analogous to the *Kras*^{G12D} mouse – that is with a LSL element upstream of the mutated gene. Concomitant expression of endogenously controlled *Kras*^{G12D} and *Tp53*^{R172H} significantly accelerated tumour progression (Hingorani et al., 2005). The wild-type *p53* allele was lost in this process and macroscopic metastatic disease emerged as early as ten weeks post partum. Interestingly, they found a profound molecular heterogeneity combined with widespread chromosomal instability of the tumours resembling the epithelial cancers typical for humans. This is uncommon in mice. As murine telomeres are four to six times longer compared to human (Jonkers and Berns, 2002) they are believed to contribute to protection from development of carcinomas in mice

which more often develop lymphomas and sarcomas (Artandi et al., 2000; Sharpless and DePinho, 2004).

Another noteworthy approach to induce pancreatic cancer was undertaken by the group of Varmus. They targeted acinar cells using the RCAS-TVA system (Lewis et al., 2003). Transgenic mice expressed TVA – a receptor for the avian leukosis sarcoma virus subgroup A (ALSV-A) – under control of the elastase promoter. In an *Ink4a/Arf* knock-out background they delivered c-Myc or PyMT antigen into acinar cells via this receptor. Although mice yielded pancreatic tumours with histological phenotypes differing considerably from human PDAC this approach to tissue-specific gene delivery is worth being examined in more detail.

1.2. The TVA/RCAS System

Viral vectors have been a potent tool to deliver oncogenes or dominant negative tumour suppressor genes to somatic cells. One system has been engineered to facilitate cell-specific delivery of genes by the avian RCAS-TVA based retrovirus (Fisher et al., 1999). Therefore, mice expressing the TVA receptor under a cell-type specific promoter were engineered. TVA is a receptor normally expressed in avian but not mammalian cells (Bates et al., 1993). It is responsible for susceptibility to the avian leukosis sarcoma virus subgroup A (ALSV-A) and therefore was cloned to enable retroviral somatic gene transfer through an ALSV-A derived avian leukosis virus long terminal repeat with splice acceptor (RCAS) vector. Cell-type specific expression enables restricted infection of a limited number of cells expressing the TVA receptor with the RCAS vector carrying transcripts with a maximum size of 2.5 kb. Viral spread in mammalian cells is precluded due to the replication incompetence in mammalian cells.

Furthermore, this system allows for temporally controlled introduction of various genes of interest – simultaneously or sequentially – an intriguing aspect for modelling cancer in a mouse model. The stochastic infection of a limited number of discrete cells also mimics the incidental acquisition of mutations in sporadic human carcinogenesis. Production of virus in chicken fibroblasts enables generation of a high viral titre before introduction into the host (Himly et al., 1998; Schaefer-Klein et al., 1998). An additional advantage of this system includes the integration of the retrovirus into the host genome thereby leading to constitutive expression of the target gene. However, there are also limitations that have to be mentioned. The

random integration site of the retrovirus into the host genome may influence expression of the target gene as well as this might also disrupt gene expression of a host gene. Moreover, the RCAS virus has an insert limit of 2.5 kb. This can be circumvented by application of pseudotyped lentiviruses, but viral titres are lower in this case.

A major drawback to date is that for tissue-specific gene delivery only a limited number of mouse models have already been generated (Dunn et al., 2001; Dunn et al., 2000; Federspiel et al., 1994; Holland et al., 1998; Holland and Varmus, 1998; Murphy and Leavitt, 1999), thus it is still necessary to generate a new transgene or knock-in mouse model with TVA expressed under control of the new desired promoter.

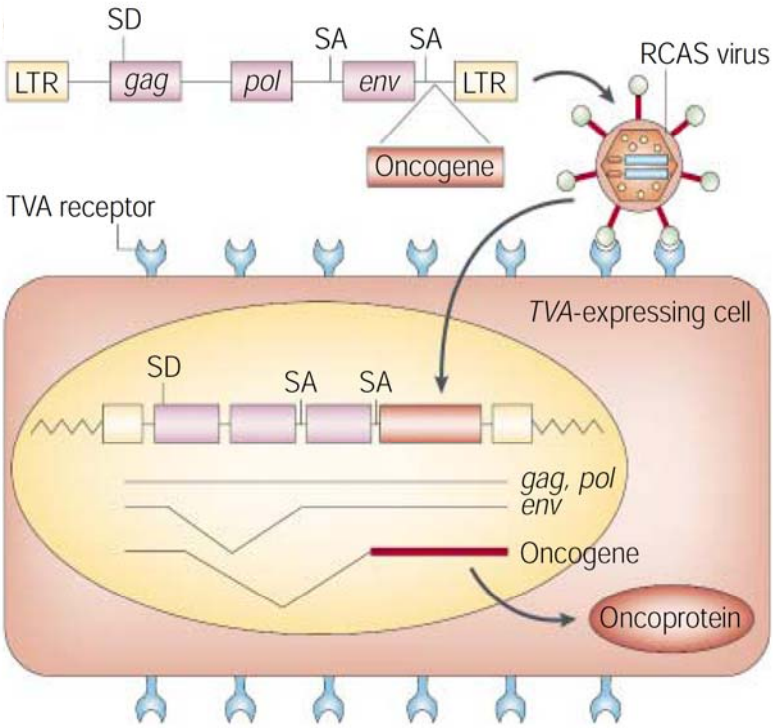

Figure 1-2 TVA/RCAS model of cell-type specific retroviral gene delivery The gene of interest is cloned into the genome of the RCAS virus. The virus then binds to the transgenic TVA receptor, enters the cell and integrates into the host genome. Exclusively cells with transgene-encoded TVA receptor expression can be infected with RCAS viruses, normal mammalian cells do not express the receptor. This allows for introduction of the oncogene into specific cell types or tissues. (Jonkers and Berns, 2002).

1.3. Metastasis and its models

For years metastasis has been considered the final step in carcinogenesis. Genetic and epigenetic changes in the genome of a cancerous cell were thought to be accumulated over time with the result of dissemination. Not the bulk but only a rare subpopulation – most likely the most advanced clone – of primary tumour cells was believed to acquire the mutations enabling metastatic spread to distant sites (Fidler and Kripke, 1977).

Taking into account the numerous somatic mutations and therefore the large genetic heterogeneity this designates a disease of enormous complexity. Prediction of metastatic potential of a tumour might consequently require analysis of a vast array of markers. Traditionally, age, tumour size, axillary node status, histological tumour type and standardized pathologic grade are prognostic and predictive factors relied upon in clinical practice. Recently, however, novel approaches are complementing these factors in search for the right treatment. To identify patterns of gene expression has become a promising technique.

1.3.1 Gene expression profiles

Expression signatures represent a unique biological state or phenotype, e.g. a metastatic or non-metastatic tumour, which is associated with a distinctive pattern of gene expression. If little is known about the underlying biology of this phenotype identifying gene expression signatures with microarray technology is a sophisticated approach to determine the relevant genes that relate to the phenotype. This has been especially useful for the identification of previously unknown clinically discrete subgroups of breast cancer in an unsupervised analysis (Perou et al., 2000).

Considering that tumour subtypes with different clinical behaviour require different treatment, this was very useful for future identification of therapeutic targets that might be shared in the same subgroup.

For many types of tumours comprising serous ovarian cancer, lung adenocarcinoma, non-small cell lung carcinoma, breast cancer, B-cell lymphoma, and prostate cancer the possibility that a certain gene expression pattern can discriminate tumours with the potential for recurrence has been successfully investigated (Beer et al., 2002; Berchuck et al., 2005; Huang et al., 2003; Paik et al., 2004; Pittman et al., 2004; Potti et al., 2006; Ramaswamy et al., 2003; Shipp et al., 2002; Singh et al., 2002; van 't Veer et al., 2002; van de Vijver et al., 2002; West et al., 2001).

These analyses proved that in several incidences the metastasizing primary tumour can be distinguished by its gene expression profile from the one that remains localized indicating that the genes responsible for metastasis are expressed early in tumorigenesis. Of note, application of different microarray platforms revealed separate and hardly overlapping but nonetheless predictive gene expression signatures for breast cancer metastasis (Wang et al., 2005).

A study by Ramaswamy and colleagues supports the concept of good versus bad prognosis signature and takes it one step further. The group identified a 17-gene signature that was associated with metastasis in multiple tumour types of diverse origin including lung, breast, prostate, colorectal, uterus and ovary (Ramaswamy et al., 2003). Complementing to this result Chang and colleagues found a gene expression signature associated with the serum response of fibroblasts based on which metastasis risk could also be predicted in various kinds of tumours such as breast, prostate, lung, gastric and hepatocellular carcinomas (Chang et al., 2004). Importantly, if diagnosis had been based on this prediction 30 % of women with breast cancer would have been spared unnecessary cytotoxic chemotherapy (Chang et al., 2005). To analyze if performance of gene expression signatures is applicable in clinical diagnosis a blinded validation study for early stage lung cancer was performed. Best results were obtained with combined use of clinical and molecular information. Risk scores that substantially correlated with actual subject outcome were produced with several prediction models (Shedden et al., 2008).

With regard to the similarity in gene-expression profile of primary tumours and their distant metastases contradictory findings have been published. While Kuukasjarvi and colleagues showed that remarkable differences exist between the primary tumour and distant metastases (Kuukasjarvi et al., 1997) Ma and colleagues reported that distant metastases, even though they developed years after the primary tumour, were highly similar to their corresponding primary tumour at the transcriptome level independently of their progression level (Ma et al., 2003). This is also true for hematogeneous metastases of colorectal cancer (Al-Mulla et al., 1999).

In some studies even organ-specificity of metastasis has been documented. For breast cancer a subset of genes were found to be related to metastasis to the bone in mice (Kang et al., 2003). However, this could only be demonstrated if analysis was confined to tumours that were known to have metastasized, not for analyses including non-metastasized samples (Minn et al., 2005b). Also, the artificial character of the experiment (a human cell line derived from a pleural metastasis transplanted

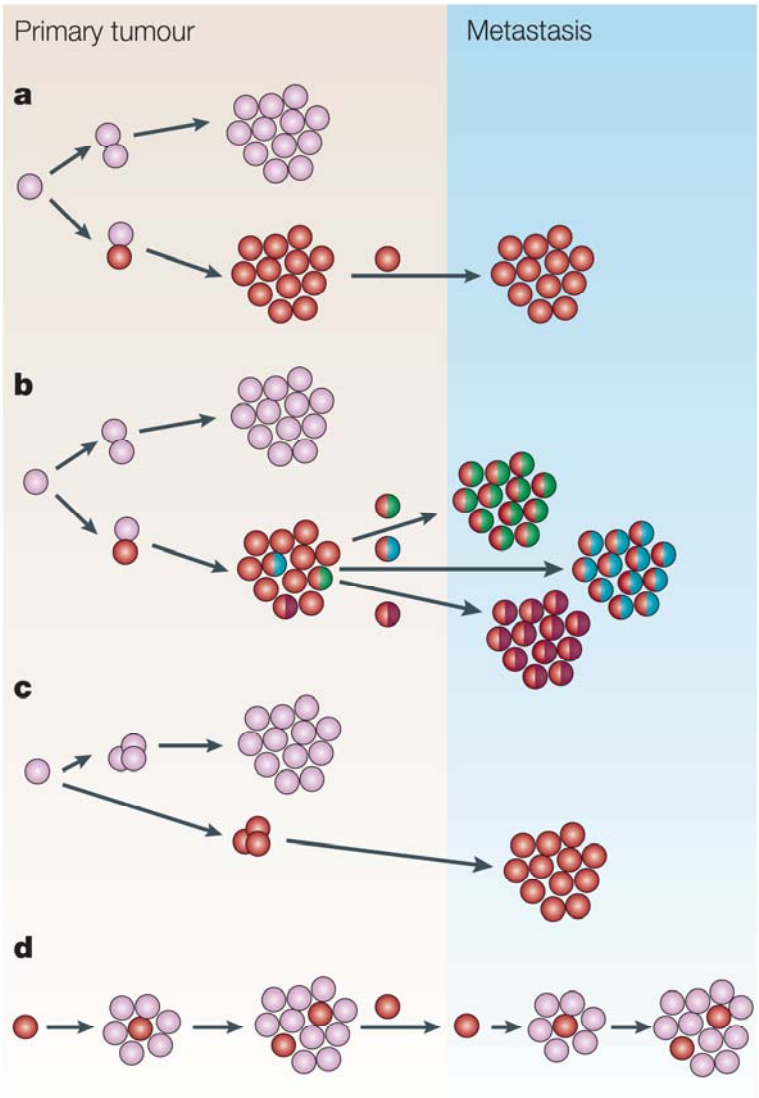

Figure 1-3 Current models of metastasis
a) Metastatic potential can be predicted based on a poor-prognosis (red) versus good-prognosis (pink) gene signature. **b)** Metastatic tumours exhibit a poor-prognosis signature and an additional tissue-specific expression profile predicting the site of metastasis homing. **c)** Dissemination of metastatic cancer cells occurs early in oncogenesis and independently from tumour cells at the primary site. Therefore the expression profile of primary tumours and metastasis are different. **d)** Only cancer stem cells, not the non-tumorigenic bulk of the tumour, have the ability to metastasize and form new tumours. Thus there is no difference in any expression profile detectable with the possible exception of circulating tumour cells.
Adapted from (Weigelt et al., 2005)

into an immune-deficient animal to analyze the development of metastasis to bone) weakens the possible significance of this experiment. Yet, with the discovery of a gene-expression signature specific for metastasis to the bone in a murine mouse model for lung cancer (Vicent et al., 2008) this concept might be worth to be investigated in more detail.

A number of groups have carried out expression profiling of pancreatic cancer cell lines and primary tumours. By this means various novel markers implicated with PDAC progression have been determined (Argani et al., 2001; Crnogorac-Jurcevic et al., 2002; Grutzmann et al., 2003; Han et al., 2002; Iacobuzio-Donahue et al., 2002; Jones et al., 2008; Rosty et al., 2002). Yet, these studies all focused on tumorigenesis rather than metastasis. Missiaglia and colleagues have even aimed to identify a metastatic signature. However, this study was solely able to identify a collection of genes with a potential link to the site of metastasis from which these cell lines were isolated (Missiaglia et al., 2004).

Most investigations on gene expression analysis so far have been done on primary tumour samples rather than on disseminated cells. According to the hypothesis that metastasis stems from the most advanced clone of the primary tumour this seems logical. This model is challenged by emerging evidence that metastasis might already take place early in tumorigenesis. Comparison of chromosomal aberrations of single human disseminated cells from the bone marrow with their corresponding primary breast tumours led to a model proposing that metastasis evolves independently from the primary tumour (Schmidt-Kittler et al., 2003).

This is supported by Hüsemann and colleagues who substantiated that premalignant cells – driven by oncogene activation – have the ability to disseminate even before the emergence of a primary mammary tumour (Husemann et al., 2008). Intriguingly, even phenotypically normal mouse mammary epithelial cells can not only survive in the bloodstream of recipient animals but also rest dormant at distant sites until activation of oncogenes drives metastatic growth (Podsypanina et al., 2008).

1.3.2 Cancer stem cells

The "cell of origin" for most solid tumours is unknown. An attractive model of tumorigenesis presumes that tumours are fed by so called cancer stem cells (CSCs) (Reya et al., 2001). In analogy to normal stem cells these CSCs exhibit stem/progenitor characteristics and are defined by their potential to proliferate, divide

asymmetrically and proximately self-renew or differentiate. Of note, in functional xenograft and allograft studies only a minority of cells is capable to reconstitute the tumour. Additionally, cancers regenerated from purified CSCs recapitulate the heterogeneous histology of the parental tumour (Al-Hajj and Clarke, 2004; Al-Hajj et al., 2003; Bonnet and Dick, 1997). To date, CSCs have been identified in cancer of the breast, brain, lung and prostate based on markers expressed on the cell surface of the presumed cancer stem cells (Al-Hajj et al., 2003; Collins et al., 2005; Kim et al., 2005; Singh et al., 2004). Whether these CSCs arise from adult stem cells or more differentiated progenies is still unknown.

So far, most studies on cancer stem cells focus on early tumorigenesis rather than metastasis. According to the CSC model the only cells capable of dissemination and metastasis formation are the cancer stem cells which build up tumours at distant sites analogous to the primary tumours at the primary site. Among the few studies trying to bridge the gap between CSCs and metastasis Li and Kang propose a model in which cancer malignancy, metastatic potential and tissue tropism are preassigned in cancer stem cells (Li et al., 2007b). Balic and colleagues discovered that in breast cancer early disseminated cancer cells detected in the bone marrow have stem cell properties (Balic et al., 2006) as well as cells isolated from clinically apparent metastatic lesions as concluded in a separate study conducted by Al-Hajj. Up to 10 % of primary or metastatic lesions were reported to be composed of these $CD44^{+}CD24^{-}$ stem cells (Al-Hajj et al., 2003; Ponti et al., 2005). Recently Theodoropoulos identified a subset of circulating tumour cells with a putative CSC phenotype in breast cancer as well (Theodoropoulos et al., 2009).

1.3.2.1 Cancer stem cells in pancreatic cancer

Of late there is accumulating evidence that CSCs might as well play a role in pancreatic cancer. As CD133 was found to be a stem cell marker not only in neural stem cells but also in brain tumours (Singh et al., 2004) this became a marker repeatedly tested for PDAC. Results, however, are controversial. Hermann et al. found CD133 positive cells in the invasive front of human pancreatic tumours which they proposed to determine metastatic potential of the tumour (Hermann et al., 2007). Supporting this hypothesis a correlation was found between CD133 expression and clinical lymph node metastasis (Maeda et al., 2008). This classified CD133 as a powerful prognostic factor as 5-year survival was significantly reduced for CD133 positive patients. However, it did not classify CD133 as an overall

metastasis marker in pancreatic cancer as liver metastasis did not correlate with CD133 expression level. Therefore it rather is a marker for more rapid dissemination. Conversely, Immervoll and colleagues could not establish a correlation between CD133 expression level and patient survival (Immervoll et al., 2008). They conclude that CD133 as a sole marker does not account for stemness. Additionally, a late comparative analysis between primary and recurrent pancreatic cancer could not allocate a significant impact of CD133 expression to metastasis levels either questioning the role of CD133 as a CSC marker (Welsch et al., 2009).

Another group identified a distinctive set of markers which might distinguish pancreatic cancer stem cells based on a xenograft model: $CD44^{+}CD24^{+}ESA^{+}$ (Li et al., 2007a). These cells had a 100-fold increased potential. As few as 100 cells were capable to reconstitute a tumour histologically indistinguishable from the original human counterpart. Metastasis, however, was not assessed in this study.

1.4. Aims of this work

As stated above it is still necessary to date to generate a new transgene or knock-in mouse model with TVA expressed under control of a new desired promoter. This is time consuming and difficult. In our lab a more universal mouse has been designed. A transcriptional stop cassette flanked by two loxP sites is localized upstream of the TVA receptor which is under control of the general Rosa26 promoter (*R26*$^{Tva\text{-}lacZ/+}$, see section 3.1.1). As a reporter gene nuclear LacZ has been inserted downstream regulated by an IRES sequence. By breeding these mice with knock-in mice for Cre recombinase under control of different cell-type specific promoters it should be possible to obtain mice that express the TVA receptor in the desired cell type. Importantly, this would enable to couple them to many already existing mouse models functioning according to the same principle and improve the options to research cancer. In my thesis I want to characterize and thereby establish this new mouse model.

Furthermore, several groups have conducted expression profiling of PDAC cell lines as well as primary tumours but none of them have focused on metastasis. Here, I set out to identify a gene expression signature that predicts metastasis in pancreatic cancer which may help to identify genes that could represent new drug targets. Therefore, I employ a mouse model with characteristics of the human disease and compare metastasized tumours with their corresponding metastases as well as with

non-metastasized tumours, an approach that is not achievable in human PDAC. In this context I likewise investigate putative stem cell markers with regard to pancreatic cancer metastasis which has not been well characterised so far.

2 Materials

2.1. Technical equipment

Technical equipment	Source
ABI 7700 Sequence Detection System	Applied Biosystems Inc., Foster City, CA, USA
Analytical Balance Kern AGB	Gottlieb Kern & Sohn GmbH, Balingen-Frommern
ASP300 Tissue Processor	Leica, Solms
AxioCam MRc	Carl Zeiss AG, Oberkochen
Centrifuge 5417R	Eppendorf AG, Hamburg
CO_2 incubator HERAcell® 240	Heraeus Instruments GmbH, Osterode
Cryotome Microm HM 560	Thermo Scientific, Walldorf
Dewar Carrying Flask, Type B	KGW-Isotherm, Karlsruhe
Electrophoresis-Power Supply Power Pac 200	Bio-Rad Laboratories GmbH, München
Gel doc XR+ documentaion system	Bio-Rad Laboratories GmbH, München
Gene Amp PCR System 9700	Applied Biosystems Inc., Foster City, CA, USA
Homogenizer Silent Crusher M with tool 6F	Heidolph Instruments GmbH, Schwabach
Horizontal Gel Electrophoresis	GIBCO BRL Life Technologies, Neu Apparatus
Laminar Flow Hera Safe	Heraeus Instruments GmbH, Hanau
Luminometer Lumat LB 9501	Berthold Technologies GmbH, Bad Wildbad
Magnetic Stirrer COMBIMAG	IKA-Werke GmbH, Staufen
Microscope Axiovert 25	Carl Zeiss AG, Oberkochen
Microscope DM LB	Leica, Solms
Microtome Microm HM 355S	Thermo Scientific, Walldorf
Microwave	Siemens, München

Technical equipment	Source
Paraffin Tissue Floating Bath	Thermo Fisher Scientific Inc., Waltham, Microm SB80
PCR-Thermocycler T-1	Biometra biomedizinische Analytik GmbH, Göttingen
pH-Meter	WTW GmbH, Weilheim
Pipettes	Eppendorf AG, Hamburg
Power supply E844, E832, EV243	Consort, Turnhout, Belgium
Precision Balance Kern FTB	Gottlieb Kern & Sohn GmbH, Balingen-Frommern
Spectrophotometer ND-1000	PEQLAB Biotechnologie GmbH, Erlangen
Stereomicroscope Stemi SV 11	Carl Zeiss AG, Oberkochen
Thermomixer compact	Eppendorf AG, Hamburg
Thermoshake	Gerhardt GmbH, Königswinter
Vortex VF2	IKA-Werke GmbH, Staufen
Vortex Reax 2000	Heidolph Instruments GmbH, Schwabach
Water bath 1003	GFL Gesellschaft für Labortechnik GmbH, Burgwedel

2.2. Disposables

Disposable	Source
27-gauge needles	BD Biosciences, Franklin Lakes, NJ, USA
Cell culture plastics	BD Biosciences, Franklin Lakes, NJ, USA, TPP Tissue Culture Labware, Trasadingen, CH
Cell scrapers	TPP Tissue Culture Labware, Trasadingen, CH
Cover slips	Menzel-Gläser, Braunschweig
Cryotubes	Nunc™ Brand Products, Napeville, IL, USA

Disposable	Source
Ethilon 5-0	Ethicon, Johnson & Johnson MEDICAL GmbH, Norderstedt
Microtome blades S35, C35	Feather Safety Razor CO, LTD., Osaka, Japan
PCR reaction tubes	Eppendorf AG, Hamburg
Pipet tips	PEQLAB Biotechnologie GmbH, Erlangen
Polystyrene tubes	Sarstedt AG, Nümbrecht
Reaction tubes 1.5 and 2 ml	Eppendorf AG, Hamburg
Safe-Lock reaction tubes BioPur	Eppendorf AG, Hamburg
Serological pipettes	BD Biosciences, Franklin Lakes, NJ, USA
Single use syringes	CODAN Medizinische Geräte GmbH, Lensahn
Sterile Pipet tips	Biozym Scientific GmbH, Hessisch Oldendorf
Superfrost®Plus glass slides	Menzel-Gläser, Braunschweig
Wound clips	MEDICON eG, Tuttlingen

2.3. Reagents and enzymes

All reagents and chemicals which are not listed seperately were purchased from the following companies: Biochrom KG (Berlin), Boehringer (Mannheim), BioRad (München), Fluka Feinchemikalien GmbH (Neu-Ulm), GibcoBRL (Eggenstein), Merck (Darmstadt), Amersham/Pharmacia (Freiburg), Roth (Karlsruhe), Seromed (Berlin), Serva (Heidelberg), Sigma Chemie GmbH (Deisenhofen), Delta.Pharma (Pfullingen). Restriction endonucleases were obtained from New England Biolabs (Frankfurt).

Reagent	Source
1 kb DNA ladder	New England Biolabs, Frankfurt
100 bp DNA ladder	New England Biolabs, Frankfurt
10 x PBS	Invitrogen GmbH, Karlsruhe

Reagent	Source
Agarose	PEQLAB Biotechnologie GmbH, Erlangen
Ampicillin 100 mg/ml	Carl Roth GmbH, Karlsruhe
DAB	Vector Laboratories, Burlingame, CA, USA
DAPI	Linaris GmbH, Wertheim-Bettingen
DNase I	Qiagen GmbH, Hilden
Ethanol (100 %)	Carl Roth GmbH, Karlsruhe
Ethidiumbromid (10 mg/mL)	Inivitrogen, Karlsruhe
Glutaraldehyde	Merck KGaA, Darmstadt
Glycerin	Sigma-Aldrich Chemie GmbH, Steinheim
Isofluran Forene	Abbott GmbH, Wiesbaden
Isopropanol	Merck KGaA, Darmstadt
Isotonic NaCl-Solution	DeltaSelect GmbH, Munich
Kanamycin	Carl Roth GmbH, Karlsruhe
LB Broth Luria/Miller	Carl Roth GmbH, Karlsruhe
LB Agar Luria/Miller	Carl Roth GmbH, Karlsruhe
β-Mercaptoethanol	Sigma-Aldrich, Taufkirchen
Metacam	Boehringer Ingelheim Pharma GmbH, Ingelheim am Rhein
Novalgin	Sanofi-Aventis Deutschland GmbH, Frankfurt
OCT TissueTek	Sakura FineTek, Zoeterwoude, NL
Orange G	Fermentas, St. Leon-Rot
RedTaq Ready Mix	Sigma-Aldrich Chemie GmbH, Steinheim
RLT Buffer	Qiagen GmbH, Hilden
SuperScript II reverse transcriptase	Inivitrogen, Karlsruhe

Reagent	Source
SYBR® Green PCR Master Mix	Applied Biosystems, Darmstadt
TRIS	Carl Roth GmbH, Karlsruhe
Tween 20	Carl Roth GmbH, Karlsruhe

2.4. Kits

Kit	Source
RNeasy Mini	Qiagen GmbH, Hilden
Plasmid Mini, Midi, Maxi,	Qiagen GmbH, Hilden
Plasmid Mega EndoFree	Qiagen GmbH, Hilden
One-Cycle cDNA Synthesis-Kit	Affymetrix, Santa Clara, CA, USA
IVT Labeling Kit	Affymetrix, Santa Clara, CA, USA
3' IVT Express Kit	Affymetrix, Santa Clara, CA, USA
GeneChip® Sample Cleanup Module	Affymetrix, Santa Clara, CA, USA
Luciferase Assay System	Promega GmbH, Mannheim
TaqMan Reverse Transcription Kit	Applied Biosystems Inc., Foster City, CA, USA

2.5. Antibodies

Antibody	Source
Anti-TVA antiserum, made in rabbit	Genetic immunization by GENOVAC GmbH, Freiburg
Anti-CK-19 TROMAIII IgG, made in rat	Developmental Studies Hybridoma Bank, Iowa City, IA, USA
Anti-CD24 (M1/69) IgG, made in rat	Santa Cruz Biotechnology, Inc., Santa Cruz, CA, USA
Anti-CD44 IgG, made in rabbit	Abcam plc, Cambridge, UK
Anti-CD133 IgG, made in rabbit	Abcam plc, Cambridge, UK

Antibody	Source
Anti-Nestin IgG, made in rabbit	Abcam plc, Cambridge, UK
Anti-Oct-3/4 (C-20) IgG, made in goat	Santa Cruz Biotechnology, Inc., Santa Cruz, CA, USA
Biotinylated Anti-Rabbit IgG, made in goat	Vector Laboratories, Burlingame, CA, USA
Biotinylated Anti-Rat IgG, made in goat	Vector Laboratories, Burlingame, CA, USA
Biotinylated Anti-Goat IgG, made in rabbit	Vector Laboratories, Burlingame, CA, USA

2.6. Primers

All primers were synthesized by MWG.

Table 2-1 Primer sequences

Designation	Name	Sequence
TaqMan	TVA forward	5'-CTCTGCCAGCCAGGAATCAC-3'
	TVA reverse	5'-CATCTCACCAGCTCACAGCAA-3'
TaqMan	mCyclophilin forward	5'-ATGGTCAACCCCACCGTGT-3'
	mCyclophilin reverse	5'-TTCTGCTGTCTTTGGAACTTTGTC-3'
Genotyping K-Ras^{G12D}	Kras-UP1-WT	5'-CACCAGCTTCGGCTTCCTATT-3'
	Kras-LP-URP1	5'-AGCTAATGGCTCTCAAAGGAATGTA-3'
	Kras^{G12D}mut-UP	5'-CCATGGCTTGAGTAAGTCTGC-3'
Genotyping p53^{R172H}	Trp53^{R172H}-WT-UP2	5'-AGCCTTAGACATAACACACGAACT-3'
	Trp53^{R172H}-URP-LP	5'-CTTGGAGACATAGCCACACTG-3'
	p53^{R172H}-mut UP4	5'-GCCACCATGGCTTGAGTAA-3'
Genotyping p53 ^{R172H} deleted stop	p53^{R172H}-LoxUP	5'-AGCCTGCCTAGCTTCCTCAGG-3'
	p53^{R172H}-LoxLP	5'-CTTGGAGACATAGCCACACTG-3'
Genotyping	R26-Tva-GT-UP	5'-AAAGTCGCTCTGAGTTGTTAT-3'

Designation	Name	Sequence
TVA	R26-Tva-GT-SA-mut-LP	5'-GCGAAGAGTTTGTCCTCAACC-3'
	R26-Tva-GT-WT-LP	5'-GGAGCGGGAGAAATGGATATG-3'
Genotyping TVA deleted stop	R26-Tva-GT-UP	5'-AAAGTCGCTCTGAGTTGTTAT-3'
	Tva LP 353	5'-CATCTCACCAGCTCACAGCAA-3'
Genotyping p48 Cre	p48-Cre-GT-LP-URP	5'-CCTCGAAGGCGTCGTTGATGGACTGCA-3'
	p48-Cre-GT-wt-UP	5'-CCACGGATCACTCACAAAGCGT-3'
	p48-Cre-GT-mut-UP-neu	5'-GCCACCAGCCAGCTATCAA-3'

2.7. Plasmids

Plasmid	Source
pIRES	Clontech Laboratories, Inc., Mountain View, CA, USA
pEGFP	Clontech Laboratories, Inc., Mountain View, CA, USA
pRosa26-ATG-LSL-Tva	Generated in our laboratory (see Figure 3-1)
pCR®II-TOPO® (backbone vector for TaqMan standard curves of Cyclophilin and TVA)	Inivitrogen, Karlsruhe

2.8. Buffers and solutions

Buffer	
PBS	20 mM Na_2HPO_4
	50 mM NaCl
	pH 7.4
KCM Buffer	500 mM KCl

Buffer	
50 x TAE-Buffer	150 mM $CaCl_2$ 250 mM $MgCl_2$ 2 M TRIS 100 mM EDTA 5.71% (v/v) Acetic acid (100%) pH 8.5
Loading Buffer Orange G (6 x)	60 % (v/v) Glycerin 60 mM EDTA 0.24 % (w/v) Orange G 0.12 % (w/v) SDS
Gitschier's Buffer (GB) (10 x)	670 mM Tris pH 8.8 166 mM $(NH_4)_2SO_4$ 67 mM $MgCl_2$ MilliQ H_2O
PCR Lysis Buffer	0.5 % Triton X-100 1 % β-Mercaptoethanol 10 % 10 x GB MilliQ H_2O 400 µg/ml Proteinase K (add just prior to use)

2.9. Histochemistry reagents and buffers

Reagent	Source
Avidin Biotin Block	Vector Laboratories, Burlingame, CA, USA
Donkey serum D9663	Sigma-Aldrich Chemie GmbH, Steinheim
Eosine	Waldeck GmbH, Münster
Goat serum G9023	Sigma-Aldrich Chemie GmbH, Steinheim
Haematoxylin	Merck KGaA, Darmstadt

Reagent	Source
Histoclear	Carl Roth GmbH, Karlsruhe
Histofix (4% Formalin)	Carl Roth GmbH, Karlsruhe
H_2O_2	Merck KGaA, Darmstadt
Nonidet NP-40	Sigma-Aldrich Chemie GmbH, Steinheim
Rabbit serum R9133	Sigma-Aldrich Chemie GmbH, Steinheim
Sucrose	Merck KGaA, Darmstadt
Unmasking Solution	Vector Laboratories, Burlingame, CA, USA
VECTASTAIN® Elite ABC solution	Vector Laboratories, Burlingame, CA, USA
X-gal	Sigma-Aldrich Chemie GmbH, Steinheim

Buffers	
TRIS based unmasking solution	10 mM TRIS-Base, pH 10
	0.05 % Tween20
LacZ wash buffer	2 mM $MgCl_2$
	0.01 % (w/v) sodium deoxycholate ($C_{24}H_{39}NaO_4$)
	0.02 % (w/v) Nonidet P-40
	PBS
LacZ staining buffer	5 mM Potassium ferrocyanide ($K_4Fe(CN)_6$)
	5 mM Potassium ferricyanide ($K_3Fe(CN)_6$)
	0.1 % X-gal
	LacZ wash buffer

2.10. Cell culture

Cells	Source
DF-1 cells	American Type Culture Collection
HEK-293 FT tva cells modified from HEK-293	American Type Culture Collection

2.10.1 Cell culture reagents and media

Reagent	Source
Collagenase 1	Worthington Biochemical Corporation, Lakewood, NJ, USA
EDTA	Invitrogen GmbH, Karlsruhe
FBS	Biochrom AG, Berlin
Geniticin	Biochrom AG, Berlin
Hygromycin	Merck KGaA, Darmstadt
MEM Non essential amino acids (100x)	Invitrogen GmbH, Karlsruhe
PAN-FBS	PAN-Biotech GmbH, Aidenbach
PBS	Invitrogen GmbH, Karlsruhe
Penicillin-Streptomycin	Invitrogen GmbH, Karlsruhe
D-MEM	Invitrogen GmbH, Karlsruhe
Trypsin-EDTA	Invitrogen GmbH, Karlsruhe

Media	
DF-1 Medium	D-MEM 10 % PAN-FBS 1 % Penicillin-Streptomycin 1 % MEM Non essential amino acids
Tumour cell medium	D-MEM 10 % FBS 1 % Penicillin-Streptomycin
HEK-293 FT tva cell medium	D-MEM 10 % FBS 1 % Penicillin-Streptomycin 1 % Non essential amino acids 500 µg/ml Geniticin

Media	
	100 µg/ml Hygromycin

3 Methods

3.1. Animal Experiments

To conduct the animal experiments a conditional Cre-loxP system was applied. Mice with a lox-stop-lox (LSL) cassette knock-in can be interbred with mouse strains expressing the *Cre* gene under control of tissue-specific promoter to allow conditional deletion of the LSL cassette and expression of the target genes.
All animal studies were conducted meeting the requirements of the European guidelines for the care and use of laboratory animals and were approved by the local authorities.

3.1.1 Mouse Strains and Tumour Models

To obtain mice which express the TVA receptor ubiquitously I interbred the *LSL-R26*$^{Tva\text{-}lacZ/+}$ mouse strain generated in our lab with the general deleter strain *Prm-Cre/+* (The Jackson Laboratory). Furthermore, to obtain mice which express the TVA receptor specifically in the pancreas and therefore in developing mPanIN lesions and PDAC these strains were interbred with *LSL-Kras*^{G12D} (Hingorani et al., 2003), *LSL-TP53*$^{R172H/+}$ (Hingorani et al., 2005) and *Ptf1a/p48*$^{Cre/+}$ (Nakhai et al., 2007).

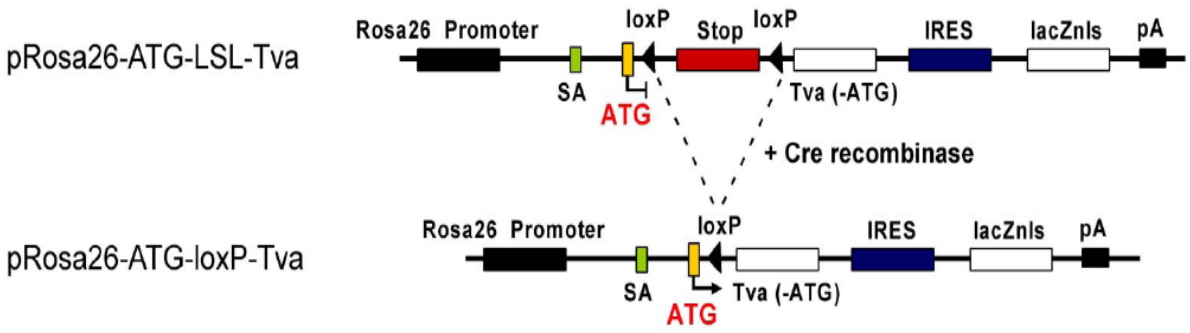

Figure 3-1 Knock-in construct for the *LSL-R26*$^{Tva\text{-}lacZ/+}$ mouse strain
Schematic representation and partial sequence of pRosa26-ATG-LSL-Tva -IRES-lacZnls expression plasmid under the control of the Rosa26 promoter. The LSL cassette disrupts the open reading frame of *Tva*. After Cre-mediated recombination of pRosa26-ATG-LSL-Tva the N-terminally mutated TVA receptor is expressed.

LSL-Kras^{G12D} and *LSL-TP53*$^{R172H/+}$ mouse strains were kindly provided by Dr. T. Jacks (Massachusetts Institute of Technology, Cambridge, MA) and *Ptf1a/p48*$^{Cre/+}$ mice were kindly provided by Dr. H. Nakhai (Klinikum rechts der Isar, TU Munich).

3.1.2 Dissection of tumour mice and isolation of cells from tissues and the circulation

Mice were anesthetised prior to cervical dislocation. They were disinfected with 70 % ethanol and further dissection was carried out in as sterile conditions as possible. To collect circulating tumour cells the thorax was opened, the *vena cava inferior* was cut and blood was collected in an Eppendorf reaction tube containing sterile EDTA to prevent coagulation. The sample was centrifuged for five minutes at 1000 rpm, the supernatant discarded and the cell pellet was cultured in a cell culture flask. Next the pancreatic tumour was measured and samples for RNA, protein, cryo- and paraffin-histochemistry analysis and for isolation and culturing of tumour cells were collected. Furthermore, liver, lung and lymph nodes were screened for macroscopic metastases and processed as the primary tumour. RNA samples were collected in tubes containing TissueTek (Sakura Finetek) and stored in liquid nitrogen. Protein samples were stored at -80 °C. Samples for histochemistry were treated as described in chapter 3.2.1. Samples for cell isolation and culture were transferred to sterile PBS until further handling. Next, the tissue samples were sliced into small pieces and incubated in medium containing 0.56 mg/ml collagenase for up to 36 h. By the time the small pieces of tissue were digested completely they were centrifuged for five minutes at 1000 g, the supernatant was discarded and the pellet was cultured in a cell culture flask. At passages three to seven cells were seeded to collect RNA, DNA and protein samples.

3.1.3 Orthotopic Implantation of tumour cells

20 minutes prior to operation nude mice were analgised with Novalgin (1:25 in isotonic NaCl-solution) and then constantly anaesthetised with isofluorane during the operation. The abdomen was disinfected on the left and a small incision was made in the skin and the peritoneum. The pancreas was carefully fetched and 20 µl of serum free medium containg 5000 tumour cells were injected orthotopically into the pancreas with a microlitre syringe with a 27-gauge needle (Hamilton Syringes). The peritoneum was sutured with an ethilon 5-0 (Ethicon) and the skin was sealed with wound clips. Post operationally the mouse was subcutaneously analgised with 1.5 µg/g Metacam (Boehringer Ingelheim).

3.1.4 *Ex Vivo* Fluorescence Imaging

EGFP expression of whole organs was assessed by fluorescence stereomicroscopy (Stemi 11, Carl Zeiss). Mice were sacrificed and the abdomen opened up. Emitted fluorescence was detected on a Zeiss colour charge-coupled device camera system (AxioCam MRc). Highresolution images were processed with Axio- Vision 4.3 software (Carl Zeiss).

3.2. Histological experiments and stainings

3.2.1 Cryo- and Paraffinsections

Samples for cryohistochemistry were fixed in Histofix (Roth) for four hours, dehydrated in a sucrose series (15 % for 4 h and 30 % overnight), embedded in TissueTek and stored long term at -80 °C. Cryosections were serially cut 7 µm thick on a cryostat and left to dry for one hour. Samples for paraffin-histochemistry were fixed in Roti-Histofix for 16 h, dehydrated using the ASP300 Tissue Processor (Leica) and embedded in paraffin. Liver and lung were sliced such that each lobe was separated and spread next to each other in the paraffin block. Thus it was possible to cut each lobe simultaneously. For metastatic screening 6 x 3 µm thick serial sections were cut followed by a 100 µm gap before the next series. For each organ tested six of these serial sections were done.

EGFP expression in cryosections was visualised by fluorescence microscopy (Axiovert 200 M) after counterstaining with DAPI (Vector Laboratories) to identify nuclei.

3.2.2 Haematoxylin and Eosin (HE) staining of tissue sections

At first, paraffin-embedded tissue sections were dewaxed and rehydrated in Roti-Histol (Roth) and a decreasing alcohol series (2 x 99 %, 2 x 96 % and 2 x 80 % ethanol). Second, cryosections and dewaxed paraffin-embedded sections were stained in haematoxylin for five sec and in eosin for 20 sec. Next, the sections were dehydrated again in an ethanol series (2 x 80 %, 2 x 96 % and 2 x 99 % ethanol) and Roti-Histol (Roth) before embedding them in Pertex (Medite GmbH).

3.2.3 Immunohistochemistry

Sections for all immunohistochemistry stainings were dewaxed and rehydrated as described in chapter 3.2.2. Antigen retrieval was performed for ten minutes in a microwave at 900 watt until boiling followed by 360 watt with Unmasking Solution (Vector Labs) if not stated differently. Endogenous peroxidase was blocked by incubation in 3 % H_2O_2 for 20 min. Unspecific binding of the antibodies was blocked with 5 % serum of the respective species in which the secondary antibody was generated and with Avidin/Biotin Block (Vector Labs). Incubation with primary antibodies is stated below. Biotinylated secondary antibodies were diluted 1:500. After incubation with VECTASTAIN® Elite ABC solution (Vector Labs) the sections were incubated with 3.3'- diaminobenzidine tetrahydrochloride (DAB, Vector Labs) until emergence of brown coloration according to the manufacturer's protocol. Hematoxylin was used for nuclear and eosin for cytoplasmatic counterstaining. Then the slides were permanently mounted as described in chapter 3.2.2.

Table 3-1 Condtions for primary antibodies applied in immunohistochemistry

Primary Antibodies/-sera	Dilution	Incubation	Special features
TVA	1:100	1 h at RT	Cryosections
CK-19	1:100	1 h at RT	-
CD24	1:100	1 h at RT	-
CD44	1:100	1 h at RT	Blocking solution 5 % serum and 10 % BSA
CD133	1:100	1 h at RT	-
Nestin	1:300	1h RT	Blocking solution 5 % serum and 10 % BSA
Oct 3/4	1:50	2 h at RT	Unmasking in TRIS, pH 10

3.2.4 Detection of β-Galactosidase Activity in whole organs and cryosections

Whole organs of *LSL-R26*$^{Tva\text{-}lacZ/+}$, *LSL-R26*$^{Tva\text{-}lacZ/+}$*/Ptf1a/P48*$^{Cre/+}$, *LSL-R26*$^{Tva\text{-}lacZ/+}$*/Prm*$^{Cre/+}$ and wildtype mice were incubated in 4 % PFA at 4 °C for two hours prior to washing three times in LacZ wash buffer and incubation in LacZ staining solution overnight. The blue colouration was examined regularly to avoid excess staining. For

histological analysis organs were subsequently dehydrated in 15 % sucrose for four hours followed by 30 % sucrose overnight. Afterwards, they were first incubated in TissueTek for 24 hours, second frozen on dry ice and finally stored at -80 °C until cryosection. 7µm thick cryosections were mounted on glass slides, air-dried at room temperature for 16 hours and postfixed in 0.2 % glutaraldehyde in PBS. After LacZ staining for 24 h at 37 °C with LacZ staining solution they were counterstained with eosine.

3.3. Cell Culture

3.3.1 Culture conditions and cryopreservation

DF-1 cells were cultured at 39 °C and 5 % CO_2.

Isolated tumour cells from pancreatic primary tumours, metastases and the circulation were cultured at 37 °C and 5 % CO_2. To split the cells they were washed with PBS, incubated with trypsin (Invitrogen) for three to five minutes and taken up in fresh medium. For cryopreservation trypsination of early passages were stopped with FBS containing medium, centrifuged for five minutes at 1000 g after and taken up in freezing medium (Invitrogen). Initially they were gradually cooled to -80 °C and subsequently they were stored in liquid nitrogen.

3.3.2 Virus Preparation and Infection

RCASBP(A) viruses were generated practically as described previously (Du et al., 2006). Briefly, DF-1 cells were transfected with 2.5 µg of the respective plasmid with Superfect. After one week cells were checked for high expression of the reporter gene. Before infection of experimental animals, virus titres were determined via limiting dilution. For this purpose the supernatant of the DF-1 cells was centrifuged for ten minutes at 3000 g, filtered through 0.45 µm pores to avoid contamination from detached DF-1 producer cells and a series of 10-fold dilutions of the viral supernatant (from 10^o to 10^9) in growth medium was prepared. DF-1 cells and HEK cells stably expressing the TVA receptor were then infected with the different dilutions. After four to seven days transduction efficiency was assessed via fluorescence microscopy.

For infection of experimental three weeks old mice 10^7 virus producing DF-1 cells were harvested and taken up in 30 µl of DMEM. To ensure a high infection efficiency

of the pancreas the cells were implanted into the pancreas as described in chapter 3.1.3.

3.4. Molecular techniques

3.4.1 Cloning of the viral plasmid RCASBP(A)-EGFP

RCASBP(A) plasmid for construction of further viruses was kindly provided by S. Hughes from the National Cancer Institute, Frederick, MD. The coding sequence of EGFP was subcloned from pEGFP (Clontech) into the blunted ClaI restriction site of RCASBP(A) in our laboratory. Integrity of the sequence was verified by automated DNA sequencing by GATC.

3.4.2 Generation of Polyclonal TVA Antibody

To generate an antibody against mutated TVA genetic immunization was applied as described previously (Bates et al., 2006). In summary, the pRosa26- ATG-LSL-Tva construct generated in our laboratory (see Figure 3-1) was used as the starting construct. First, the LSL element was removed by incubation with Cre-recombinase (Novagen) and the ATG-loxP-Tva cassette was subcloned into pIRES resulting in pIRES-ATG-loxP-Tva. In addition, to eliminate dispensable sequences of the construct and to enhance expression of the TVA receptor, the neo cassette of the plasmid, the IRES sequence and a possible expression-diminishing GC rich sequence was removed by enzymatic restriction digest. Transformation was done as described below. Plasmid isolaton was performed using the EndoFree Plasmid Mega Kit (Qiagen). Injection of the plasmid into rabbits and reception of a polyclonal antiserum was executed by Genovac (Freiburg, Germany).

3.4.3 Transformation of competent cells and isolation of plasmid DNA

Competent cells were transformed with the KCM method (Walhout et al., 2000). Briefly, KCM, 200 ng DNA and H_20 up to a total volume of 100 µl was mixed with an equal amount of E. coli strains Stbl3 or TOP10 (Invitrogen) competent cells, kept on ice for 20 minutes followed by ten minutes at room temperature. SOC medium was added and incubated at 25 °C or 37 °C for one or two hours according to the optimal growth temperature and velocity of the competent cells. Bacteria were streaked onto selective agar plates in various amounts and grown overnight at 25 °C or 37 °C,

respectively. To amplify the plasmids, selective growth medium was inoculated with a colony and grown for at least 12 h.

Depending on the amount needed plasmid DNA for production of virus or antibodies was isolated with Plasmid Mini-, Midi- or Maxi Kits from Qiagen. Isolation was completed according to the manufacturer's protocol employing buffers and solutions supplied with the kits.

For long-term stocks 400 µl bacteria was mixed with 500 µl glycerin and stored at -80 °C.

3.4.4 PCR

3.4.4.1 Genotyping

Genotyping of the mice was carried out by genomic PCR. For this purpose up to 2 mm of mouse tail was incubated in PCR Lysis Buffer (Kogan et al., 1987) for 90 minutes at 55 °C, heat inactivated for 20 minutes at 95 °C, vortexed and subsequently centrifuged for ten minutes at 14000 g. 1 µl of supernatant was used per PCR reaction.

Primers for PCR amplification were designed so that the amplified gene fragments of wildtype and mutated or knocked in DNA exhibited different molecular weight (see Table 3-2).

In addition, all isolated cells from tumours, metastases and the circulation were re-examined for recombination of the stop cassette upstream of $Kras^{G12D}$ to ensure that the cells actually originated from the tumours and not from different cell types. In these cell-based PCRs the mutated PCR band appears only 30 basepairs bigger than the wildtype band resulting from the excised LSL element with one loxP site remaining.

Table 3-2 PCR conditions for genotyping

Type of PCR	Denaturation	Annealing	Extension	Band size (bp)
LSL-K-Ras^{G12D}	95 °C 45 sec	55 °C 1 min	72 °C 1 min 30 sec	170 (mut mt) 270 (WT) 300 (deleted stop cassette, ic)
LSL-p53^{R172H}	95 °C 30 sec	60 °C 30 sec	72 °C 1 min	270(mut) 570 (WT)
p53^{R172H} stop	95 °C 45 sec	55 °C 1 min	72 °C 1 min 30 sec	290 (WT) 330 (deleted stop)
LSL-TVA	95 °C 45 sec	62 °C 1 min	72 °C 1 min 30 sec	310 (mut) 600 (WT)
TVA stop	95 °C 45 sec	53 °C 1 min	72 °C 1 min 30 sec	900 (deleted stop cassette)
p48 Cre	95 °C 45 sec	60 °C 1 min	72 °C 1 min 30 sec	400 (mut) 600 (WT)

mt=mouse tail PCR, ic=isolated cells PCR, mut=mutated, WT=wildtype

40 cycles were conducted for all PCRs. Results were analysed on agarose gels (Saiki et al., 1988) containing ethidium bromide. Separation of the PCR products was carried out on 1 % to 2 % agarose gels according to the size of the expected PCR bands at a voltage of 5 V/cm and detected on a gel doc XR+ documentation system (BioRad).

3.4.5 RNA Isolation and Quantitative Real-Time RT-PCR:

For expression analysis of *tva* small sections of pancreas, spleen, stomach, intestine, liver, kidney, lung, heart and brain were collected from mice and immediately homogenised in RLT buffer (Qiagen) and frozen in liquid nitrogen. The samples were stored at -80 °C until further analysis. Total RNA was isolated using RNeasy Mini Kit (Qiagen) and treated with DNAseI (Qiagen) according to the manufacturer's protocol. Five micrograms were reverse transcribed by using random hexamers and the TaqMan Reverse Transcription Kit (Applied Biosystems) as described (Saur et al.,

2002). Expression of *tva* was analysed by TaqMan PCR using the SYBR® Green PCR Master Mix (Applied Biosystems) using 100 ng total RNA with the following reaction conditions: 1 PCR cycle: 50°C, 2 minutes, 95°C, 10 minutes followed by 40 PCR cycles: 60°C, 1 minute, 95°C, 15 seconds.

TaqMan primers and probes were designed using Primer Express software (Applied Biosystems) according to the manufacturer's guidelines and synthesized from MWG.

For quantification standard curves were established with gene specific plasmid dilution series: 5×10^5, 1×10^5, 2×10^4, 4×10^3, 8×10^2, and 1.6×10^2 plasmid copies.

All RNA samples were normalised based on TaqMan PCR assays for the housekeeping gene cyclophilin as described (Saur et al., 2005). All reactions were performed in triplicate.

3.4.6 Reporter Gene Assays

To assess the transduction efficiency of the RCAS-TVA system *LSL-R26*$^{Tva\text{-}lacZ/+}$/ *Prm*$^{Cre/+}$ mice were injected i. p. with DF1 cells producing RCAS virus containing firefly luciferase (fluc) at day 2 in our laboratory. After seven months I sacrificed them together with a wildtype mouse and a *LSL-PCNA*$^{Ires\text{-}fluc/+}$ mouse expressing *fluc* under control of the PCNA promoter. All organs were removed, homogenised in passive lysis buffer (Promega) and centrifuged for 15 minutes at 14000 g. The supernatant was collected for further analysis. Firefly luciferase activity was determined with a Luciferase Reporter Assay System (Promega) and a luminometer according to the manufacturers protocol. Firefly luciferase activity was normalised to total protein content. Data are presented as relative light units of firefly luciferase per µg of protein.

3.4.7 Microarray Analysis

To analyse differential expressed genes and to determine potential gene signatures, underlying signalling pathways or indications for metastasis models 44 primary samples and 25 isolated cell lines were subjected to microarray analysis. Preparation of primary tumour and primary metastasis samples was carried out as follows: Tissues were collected from tumour mice (3.1.1), transferred to TissueTek containing tubes and immediately stored in liquid nitrogen until further handling. Next, samples were cryosectioned. The first and the last section were mounted on glass slides and

histologically analysed to confirm that samples contained at least 70 % tumour or metastasis tissue. Samples including normal pancreatic tissue or lymph nodes were excluded. In between these sections 10 x 30 µm thick sections were cut and homogenised in RLT buffer instantly.

RNA was isolated with the RNeasy Mini Kit (Qiagen). Quality and purity of RNA was assessed on an agarose gel and on a photometer at a wave length of 260 nm. Purity was deduced from the optical density ratio at wavelengths 260/280 nm which had to be above 1.8. Only samples with no detectable degradation and contamination were further processed using the Affymetrix One-Cycle cDNA Synthesis-Kit followed by the IVT Labeling Kit or the 3' IVT Express Kit according to the manufacturer's protocol. To be able to exclude differences in detection of these kits one sample was processed with both alternatives. In summary, RNA was reverse transcribed in cDNA which then itself was transcribed into biotin labelled cRNA. Fragmentation and processing with GeneChip Mouse Genome 430 2.0 Arrays which encompass over 39000 transcripts was performed by the team of PD Dr. Reinhard Hoffmann at the Institute for Medical Microbiology, Immunology and Hygiene, TU Munich. After hybridisation of the fragmented cRNA to the DNA oligonucleotides a streptavidin phycoerythrin conjugate binds and stains the chip dependant on the amount of transcript which is detected with the GeneArray Scanner. From the amount of light emitted at 570 nm the amount of target gene expression can be computed.

3.5. Statistical Analysis

Graphical depiction was conducted with "Sigma Plot" (Jandel Scientific, Corte Madera, USA). Data are presented as arithmetic mean ± standard deviation. To evidence statistical significance of differences between particular groups various tests were employed (e.g. Student's t-test, Fisher’s exact test, Wilcoxon signed-rank test, Log rank test). The following significance levels were applied: Error probability $p < 0.05$ (*), $p < 0.01$ (**) and $p < 0.001$ (***).

Microarray data analysis was performed by the team of Dr. Pagel at the "Lehrstuhl für Genomorientierte Bioinformatik" of the TU Munich. To determine genes that change their expression levels significantly across predefined groups of samples (contrasts) limma (an R Bioconductor package) was used. In order to find differentially expressed genes (DEGs), limma fits a linear model for each gene. As multiple testing could influence the significance of the results – Benjamini and Hochberg’s method

was used for controlling the false discovery rate (FDR) (Hochberg, 1995). Thus, FDR was corrected in all tests to 5%, which was also set as the significance threshold.

An approach that was developed to go beyond the analysis of patterns on a gene-by-gene basis, known as gene set enrichment analysis (GSEA), uses statistical measures of enrichment of annotated gene sets within expression profiles. For this analysis a collection of gene sets from the Molecular Signatures Database was employed. This collection contains 5066 gene sets and consists of curated sets (based on expert knowledge and PubMed-IDs), genes that share a regulatory motif (e.g. transcription factors), gene sets with the same gene ontology annotation and cancer modules identified in a large expression meta-study (Segal et al., 2004).

The implementation that was used applies a parametric gene set enrichment analysis (Volsky, 2005) that at first fits the expression values of a gene set to a parametric model and determines the deviation of this distribution from the global average as enrichment for a specific sample. Subsequently, these enrichments are fitted to a linear model in the same procedure that is also applied to expression values of genes. This way, gene sets with expression value distributions that are significantly different across two groups of samples can be determined.

As microarray chip differences and batch effects have a significant impact on the outcome of a predictive gene expression signature (Shi et al., 2006) these effects were modelled in the analyses so that these effects were negligible.

4 Results

4.1. Characterization of *LSL-R26$^{Tva\text{-}lacZ}$* knock-in mice

In our laboratory the novel *LSL-R26$^{Tva\text{-}lacZ}$* mouse strain has been generated. In my thesis I set out to characterize this mouse model which is to serve as a potent tool for cancer research and beyond.

4.1.1 Conditional Cre-Regulated TVA and LacZnls Expression *in vivo*

TVA in the *LSL-R26$^{Tva\text{-}lacZ/+}$* mouse model is expressed only in Cre recombinated organs as the open reading frame is interrupted by the stop cassette. To verify this I analyzed *LSL-R26$^{Tva\text{-}lacZ/+}$/Prm-Cre*, *LSL-R26$^{Tva\text{-}lacZ/+}$/Ptf1a/P48$^{Cre/+}$* and *LSL-R26$^{Tva\text{-}lacZ/+}$* mice. *Prm-Cre* mice express the Cre-recombinase under the control of the ubiquitously active *protamin* promoter which leads to general deletion of the stop cassette. *Ptf1a/P48$^{Cre/+}$* is a knock-in mouse line where Cre expression is restricted to pancreatic ducts, exocrine and endocrine cells in the pancreas and neurons of the retina, cerebellum, and dorsal neural tube (Kawaguchi et al., 2002; Nakhai et al.,

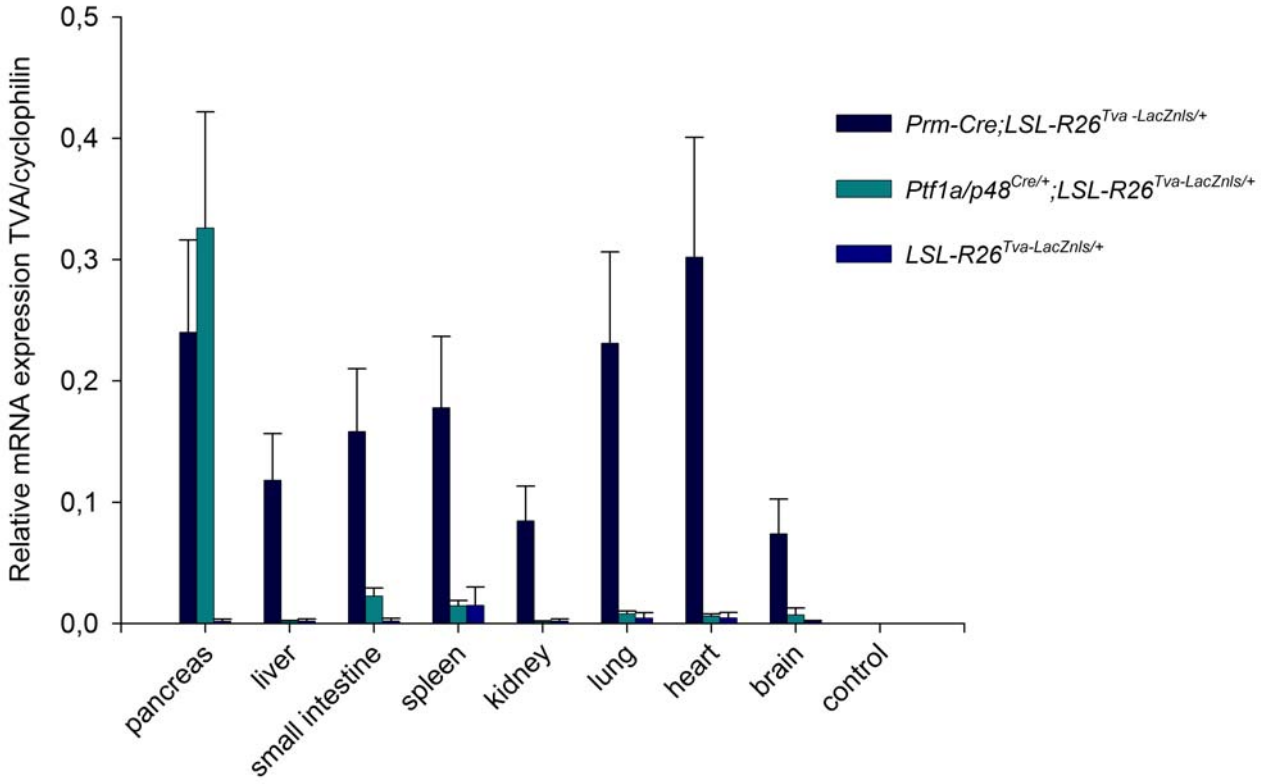

Figure 4-1 Relative mRNA Expression of TVA in the indicated organs of *LSL-R26$^{Tva\text{-}lacZ/+}$/Prm-Cre*, *LSL-R26$^{Tva\text{-}lacZ/+}$/Ptf1a/P48$^{Cre/+}$* and *LSL-R26$^{Tva\text{-}lacZ/+}$* mice Relative amounts of TVA transcripts were calculated by using standard curves and normalized against the globally expressed cyclophilin housekeeping gene measured in the same RNA preparation.

2007).

To investigate the transcriptional level of the TVA receptor I performed real-time TaqMan PCR. Results were normalised to transcription levels of the housekeeping gene cyclophilin.

The TVA receptor was expressed in every organ of the *LSL-R26*$^{Tva\text{-}lacZ/+}$*/Prm-Cre* mice (Figure 4-1). In contrast, only marginal transcription could be detected in the *LSL-R26*$^{Tva\text{-}lacZ/+}$ mice. However, as expected the TVA receptor was solely expressed in the pancreas of *LSL-R26*$^{Tva\text{-}lacZ/+}$*/Ptf1a/P48*$^{Cre/+}$ mice.

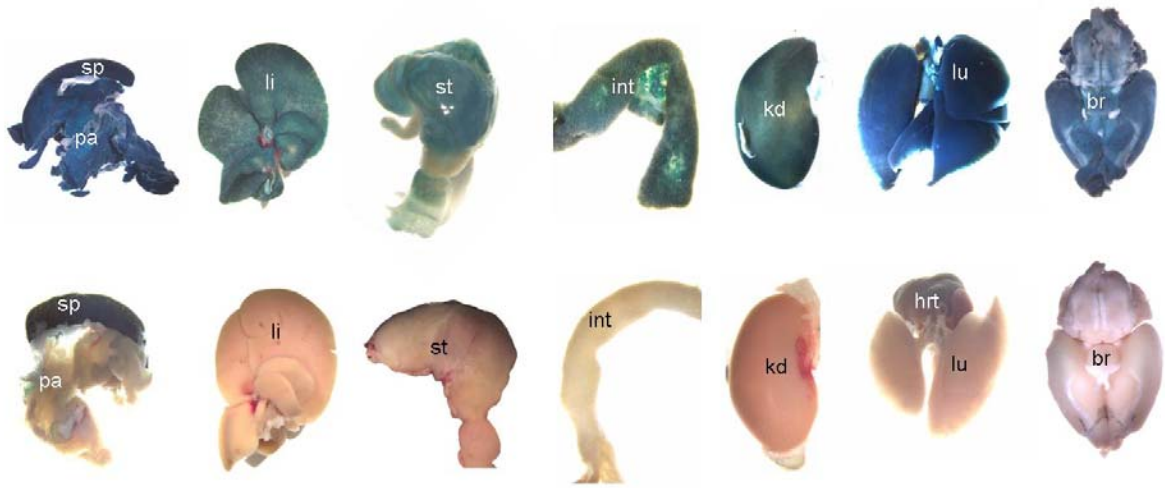

Figure 4-2 β-Galactosidase staining of organs of adult *LSL-R26*$^{Tva\text{-}lacZ/+}$*;Prm-Cre* (top row) and *LSL-R26*$^{Tva\text{-}lacZ/+}$ mice (bottom row) Blue staining is evident in all organs from mice expressing the TVA receptor ubiquitiously but in none with floxed TVA. sp=spleen, pa=pancreas, li=liver, st=stomach, int=intestine, kd=kidney, lu=lung, hrt=heart, br=brain

To verify these findings the expression level and pattern of the TVA receptor in *LSL-R26*$^{Tva\text{-}lacZ/+}$*/Prm-Cre*, *LSL-R26*$^{Tva\text{-}lacZ/+}$*/Ptf1a/P48*$^{Cre/+}$ and *LSL-R26*$^{Tva\text{-}lacZ/+}$ mice were monitored indirectly through β-Galactosidase staining in whole organs (Figure 4-2) and cryosections of organs (Figure 4-3).

For whole organs I compared adult organs of *LSL-R26*$^{Tva\text{-}lacZ/+}$*/Prm-Cre* mice with *LSL-R26*$^{Tva\text{-}lacZ/+}$*/Ptf1a/P48*$^{Cre/+}$ and *LSL-R26*$^{Tva\text{-}lacZ/+}$*/Prm-Cre* with *LSL-R26*$^{Tva\text{-}lacZ/+}$ mice, respectively. A strong staining and thus expression of the TVA receptor could be proved in every organ tested of the *LSL-R26*$^{Tva\text{-}lacZ/+}$*/Prm-Cre* mouse strain but in none of the organs of the *LSL-R26*$^{Tva\text{-}lacZ/+}$ mouse. This confirms that expression is strictly dependent on Cre-mediated excision of the loxP flanked stop cassette and that after Cre-mediated recombination nuclear LacZ and therefore TVA are expressed in all cells. This is in line with previous studies in which the Rosa26 promoter was found to be active throughout and from embryonic development on (Soriano, 1999).

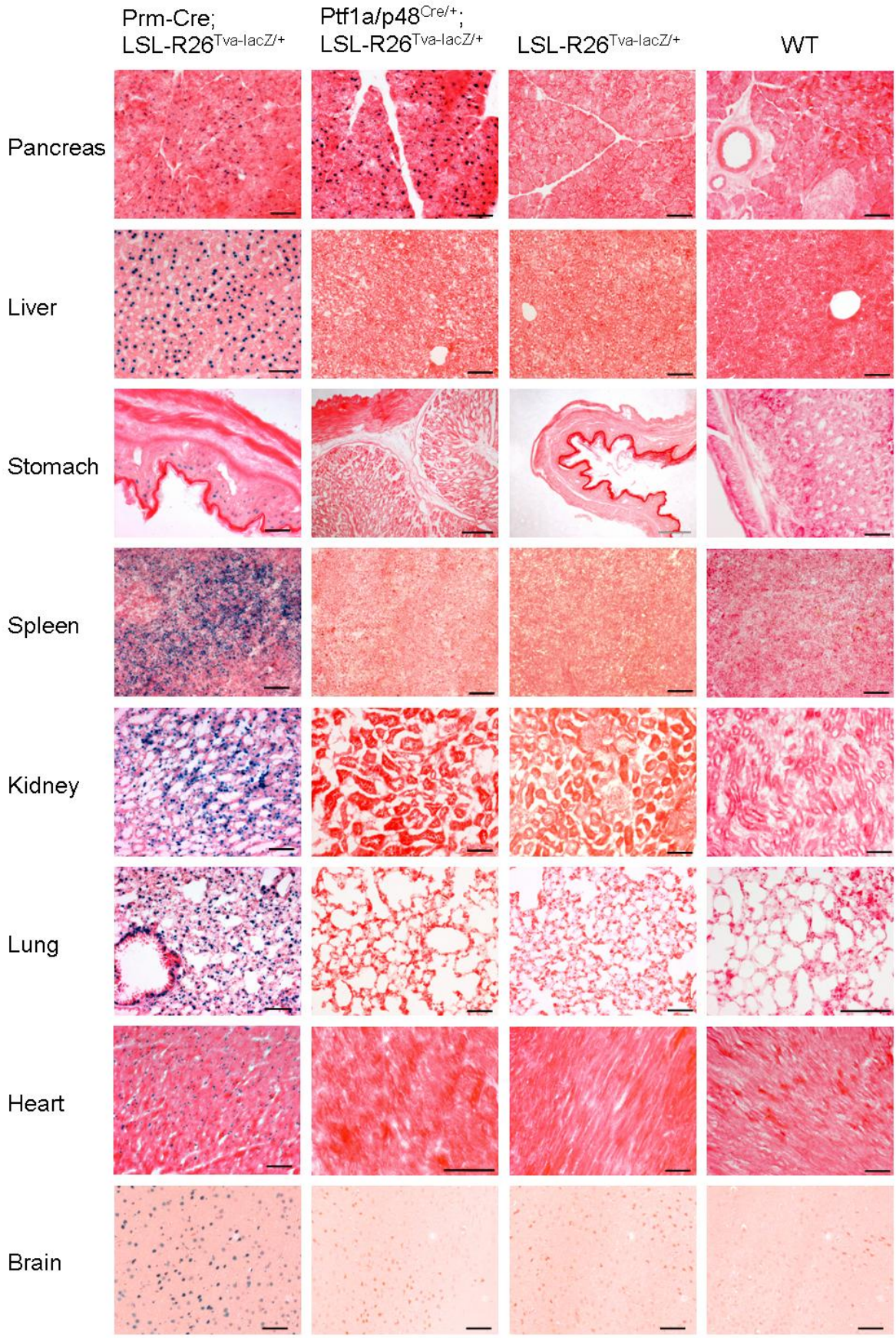

Figure 4-3 β-Galactosidase staining of cryosections of organs of adult *LSL-R26$^{Tva\text{-}lacZ/+}$/Prm-Cre, LSL-R26$^{Tva\text{-}lacZ/+}$/Ptf1a/p48$^{Cre/+}$, LSL-R26$^{Tva\text{-}lacZ/+}$* and WT mice

LacZ activity is visible in nuclei of the tissue sections. All organs of *LSL-R26$^{Tva\text{-}lacZ/+}$;Prm-Cre* but only pancreas of *LSL-R26$^{Tva\text{-}lacZ/+}$; Ptf1a/p48$^{Cre/+}$* displays blue staining. Tissue sections from floxed mice are equivalent to WT mice. Black bars represent 2 µm, grey bar represents 50 µm.

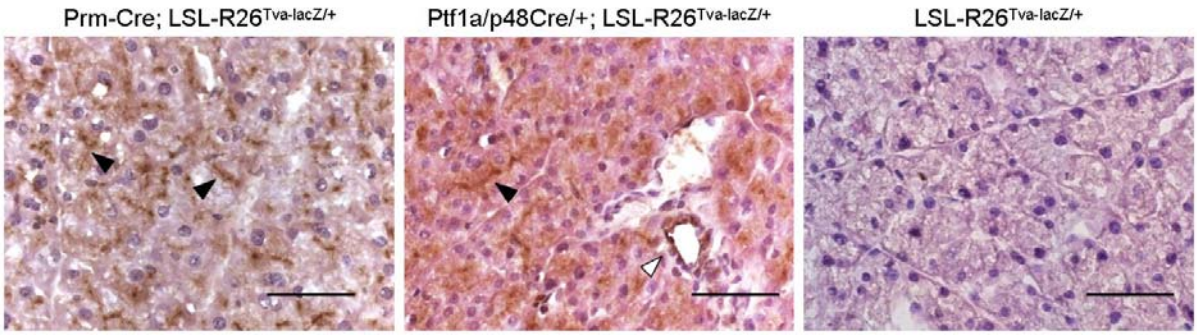

Figure 4-4 TVA Immunohistochemistry stain of pancreata of *LSL-R26$^{Tva\text{-}lacZ/+}$/Prm-Cre*, *LSL-R26$^{Tva\text{-}lacZ/+}$/Ptf1a/P48$^{Cre/+}$* and *LSL-R26$^{Tva\text{-}lacZ/+}$* mice Expression of the TVA receptor is localized to the cell surface (arrow heads). Bars represent 50µm.

Consistently, LacZ-stained cryosections of every organ tested showed LacZ expression in the *LSL-R26$^{Tva\text{-}lacZ/+}$/Prm-Cre* mice. However, cryosections of the *LSL-R26$^{Tva\text{-}lacZ/+}$* mice displayed no LacZ gene expression. Importantly, staining of whole organs (data not shown) and cryosections of *LSL-R26$^{Tva\text{-}lacZ/+}$/Ptf1a/P48$^{Cre/+}$* mice

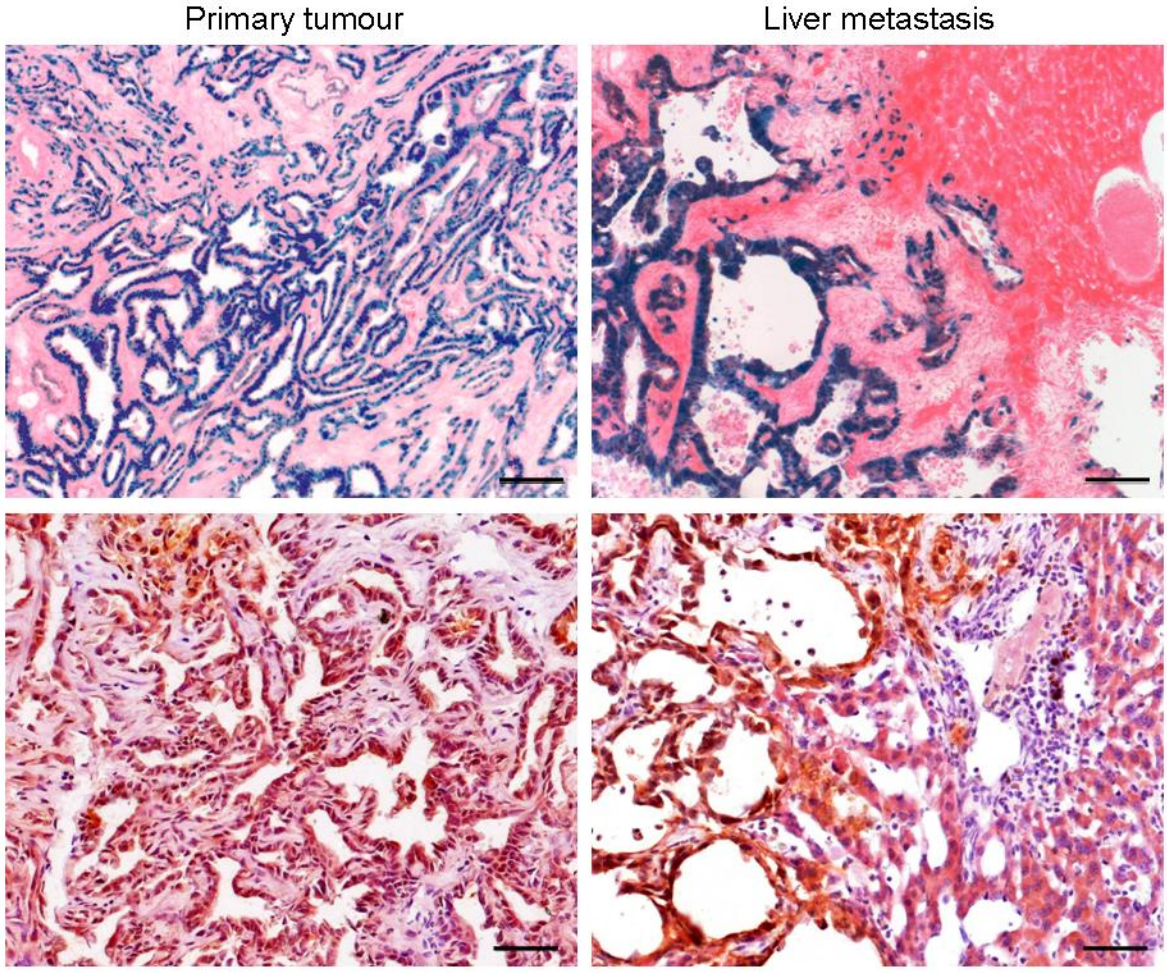

Figure 4-5 LacZ activity (upper row) and TVA immunohistochemical staining (lower row) of PDAC and corresponding liver metastases Both LacZ activity and TVA expression are restricted to the ducts in PDAC and liver metastasis of *Ptf1a/p48$^{Cre/+}$;LSL-R26$^{Tva\text{-}lacZ/+}$; LSL-Kras$^{G12D/+}$;LSL-TP53$^{R172H/+}$* mice. Neither desmoplastic stroma nor the adjacent liver tissue express TVA. Bars represent 50 µm.

displayed a LacZ staining only in the pancreas thus confirming the model of Cre-dependent recombination and organ-specific expression of the TVA receptor.

Furthermore, direct evidence of TVA receptor expression could be supplied by a TVA-IHC staining of pancreas of *LSL-R26*$^{Tva\text{-}lacZ/+}$*/Prm-Cre* and *LSL-R26*$^{Tva\text{-}lacZ/+}$*/ Ptf1a/P48*$^{Cre/+}$ mice. As depicted in Figure 4-4 expression of TVA is expressed in islets (data not shown), ducts (white arrowhead) and acini. It is localized to the cell surface of *LSL-R26*$^{Tva\text{-}lacZ/+}$*/Prm-Cre* and *LSL-R26*$^{Tva\text{-}lacZ/+}$*/Ptf1a/P48*$^{Cre/+}$ mice (black arrowheads) but there is no expression in the control mice.

To test whether the *Rosa26* locus is also active in PDAC of mice with endogenous expression of oncogenic *Kras*^{G12D} or simultaneous expression of *Kras*^{G12D} and mutant *TP53*^{R172H} and therefore if this model is applicable for cancer research I crossed *LSL-R26*$^{Tva\text{-}lacZ/+}$ mice with *Ptf1a/p48*$^{Cre/+}$*;LSL-Kras*$^{G12D/+}$ and *Ptf1a/p48*$^{Cre/+}$*;LSLKras*$^{G12D/+}$*;TP53*$^{R172H/+}$ animals, respectively.

I observed that expression of TVA both detected indirectly through LacZ activity or directly through TVA immunohistochemistry staining was exclusively localized in the ducts of PDAC or in metastases (Figure 4-5). Stroma or surrounding tissue of liver or other sites of metastasis (data not shown) did not exhibit TVA expression.

Taken together the TVA receptor can be conditionally expressed in any desired organ in which tissue specific promoters allow the specific Cre-loxP recombination.

4.1.2 RCASBP(A)-Mediated Retroviral Gene Transfer in Vivo

Having proven that with our mouse model TVA can be expressed conditionally in particular tissues it remained to be verified that these tissues can be infected with the RCASBP(A) retrovirus as has been shown in previous studies in different systems. As I am interested in development of metastasis and therefore in introducing genes

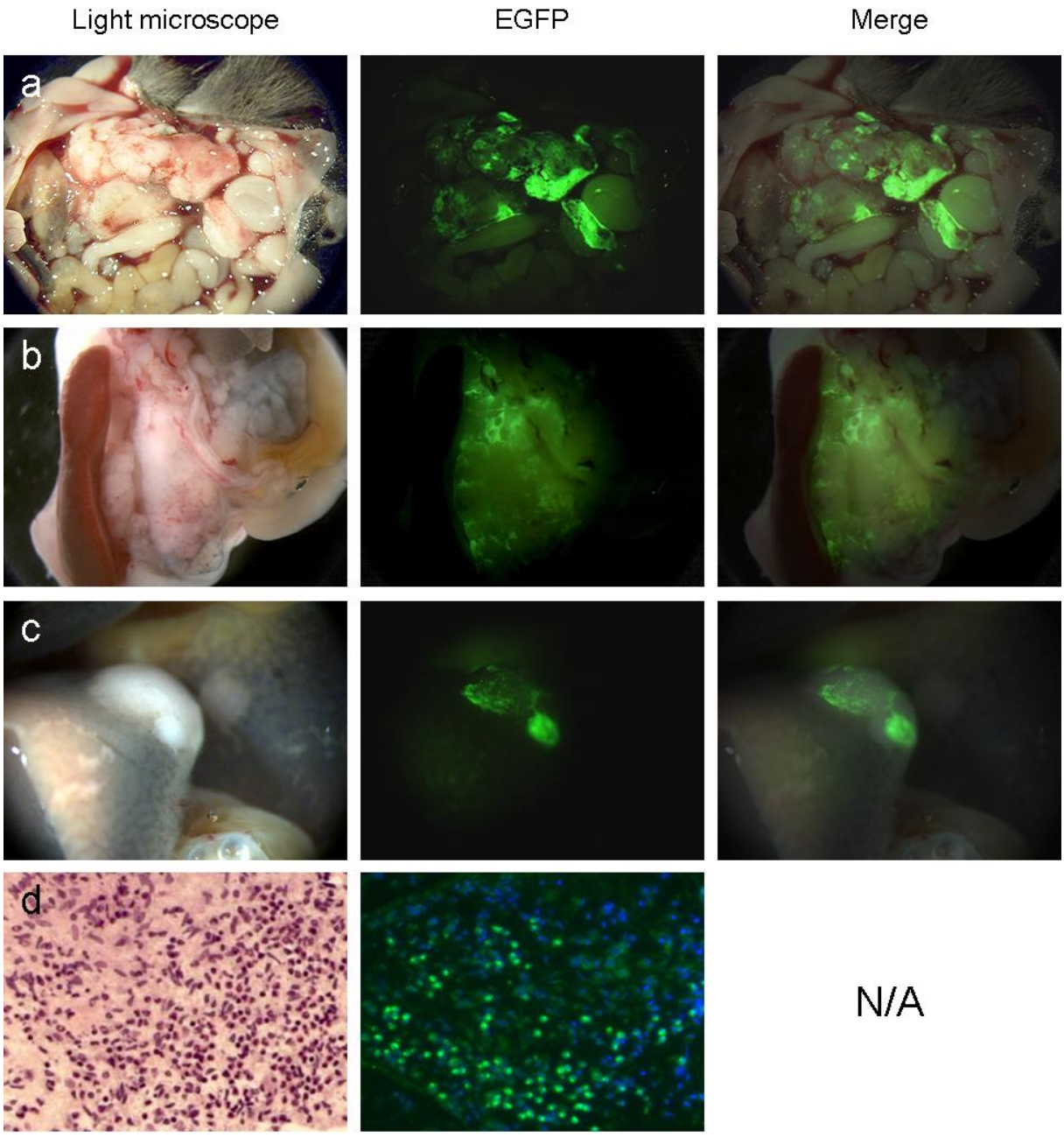

Figure 4-6 Retroviral transduction of PDAC *in vivo* by injection of DF-1 RCASBP(A)-EGFP cells into the pancreata of mice Macroscopic view of RCASBP(A)-EGFP infected *Ptf1a/p48$^{Cre/+}$; LSL-R26$^{Tva\text{-}lacZ/+}$;LSL-Kras$^{G12D/+}$;LSL-TP53$^{R172H/+}$* mouse with metastatic PDAC. EGFP expression of PDAC was visualized by fluorescence stereomicroscopy. Fluorescent and corresponding white-light images of primary PDAC (*a*-*b*) and liver metastases (*c*).
Microscopic white-light and fluorescent images of H&E and DAPI (*d*) stained serial cryosections of primary PDAC of RCASBP(A)-EGFP infected *Ptf1a/p48$^{Cre/+}$;LSL-R26$^{Tva\text{-}lacZ/+}$;LSL-Kras$^{G12D/+}$;LSL-TP53$^{R172H/+}$* mice.

into the developing cancer to accelerate metastasis formation I explored the retroviral transduction of PDAC with RCASBP(A). I injected 10^7 DF-1 cells transfected with RCASBP(A)-EGFP orthotopically into the pancreas of three weeks old *LSL-R26*$^{Tva\text{-}lacZ/+}$*;Ptf1a/p48*$^{Cre/+}$ mice. As cell proliferation is needed for retroviral transduction (Du et al., 2007; Fisher et al., 1999; Orsulic, 2002) mainly the proliferating ductal lesions of PanINs are infected with the virus. Of note, no immune response was observed in animals injected with DF-1 cells.

As shown in Figure 4-6, primary PDAC (*a*-*b*), and liver metastases (c) were EGFP-positive (pictures kindly taken by D. Saur). I therefore conclude that TVA expression renders proliferating neoplastic cells susceptible to RCASBP(A)-mediated somatic gene transfer *in vivo*.

4.2. Metastasis does not correlate with tumour size, phenotype of isolated tumour cells or loss of heterozygosity of wild type *Kras*

To classify all tumour mice correctly I screened mice with no overt metastasis for micrometastases in liver, lung and lymph nodes (Figure 4-7).

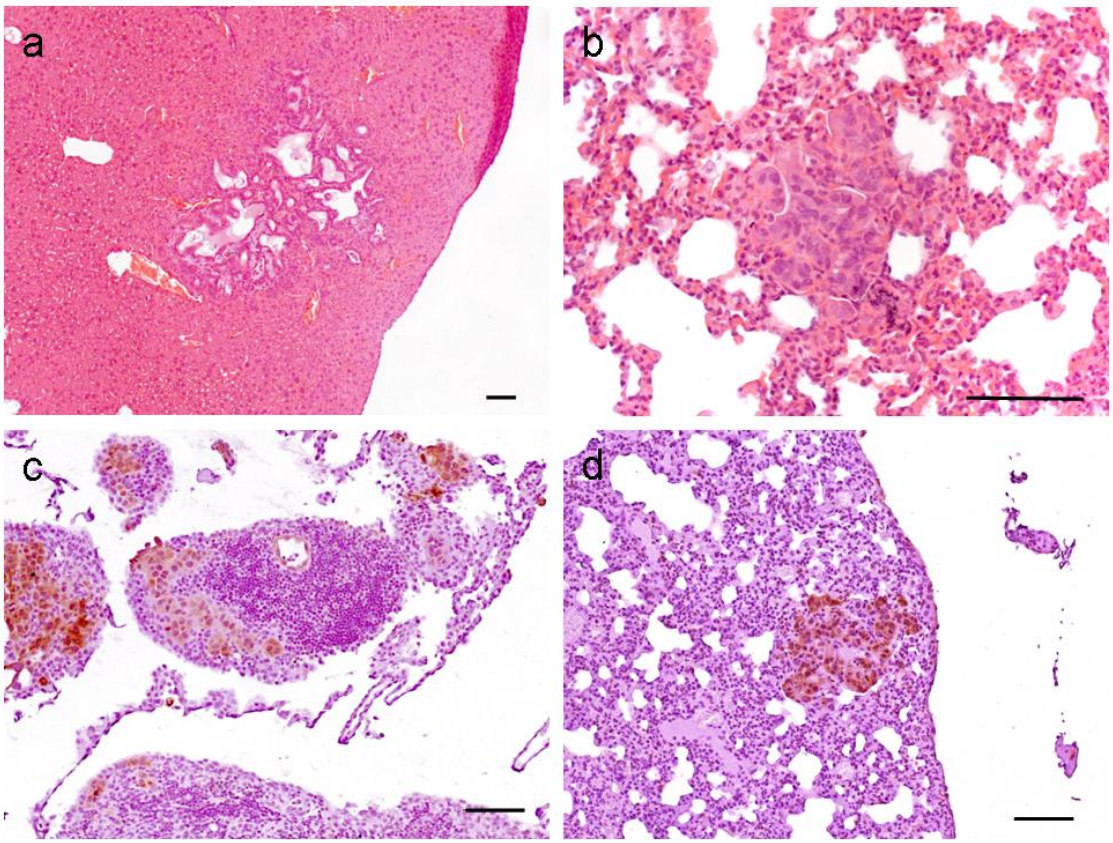

Figure 4-7 Screen for micrometastases in tumour mice in liver (a), lung (b) and (d) and lymph nodes (c). If histological evaluation alone was not sufficient for definite classification an immuno-histological staing was performed using a CK-19 antibody as an epithelial marker (c) and (d).

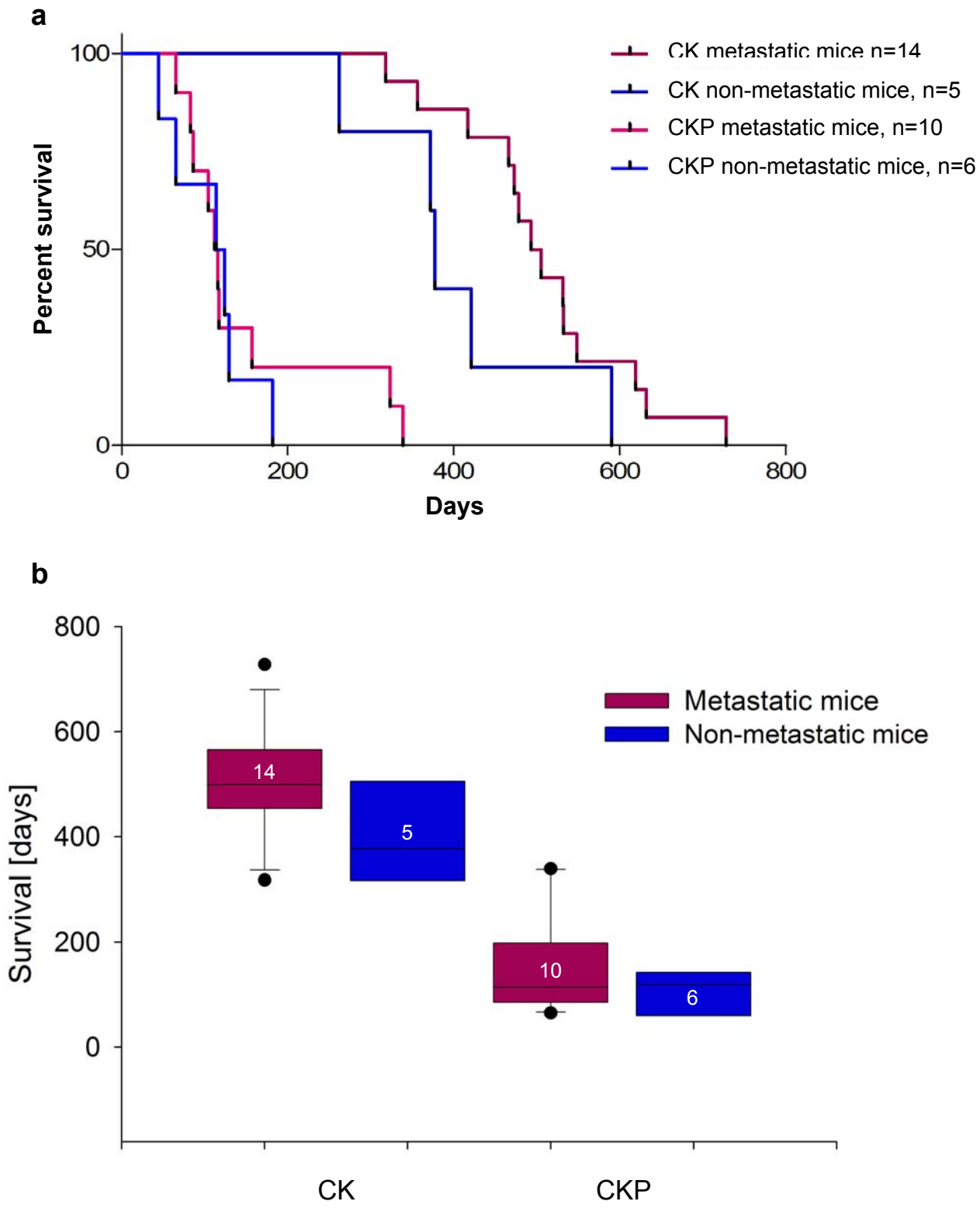

Figure 4-8 Survival of metastatic mice versus non-metastatic mice depicted in a) Kaplan-Meier-Curves and b) boxplots. For both genotypes there is no significant difference of survival between mice with metastatic and non-metastatic disease (log Rank test, p=0.13 (CK) and p=0.65 (CKP)). CK=*Ptf1a/p48*$^{Cre/+}$*/LSL-Kras*^{G12D}, CKP=*Ptf1a/p48*$^{Cre/+}$*/ LSL-Kras*^{G12D}*/LSL-TP53*$^{R172H/+}$, white numbers equal n.

All mice were sacrificed shortly before a natural death occurred due to tumour or metastatic burden. Thus, I could exclude the possibility that tumours with the

potential to metastasize did not reach that stage due to the artefact of preterm decease and might therefore be grouped wrongly. Since amongst other factors age, tumour size and histological tumour type are prognostic and predictive factors relied upon in clinical practice I assessed tumour size and phenotype of isolated tumour cells with regard to metastasis.

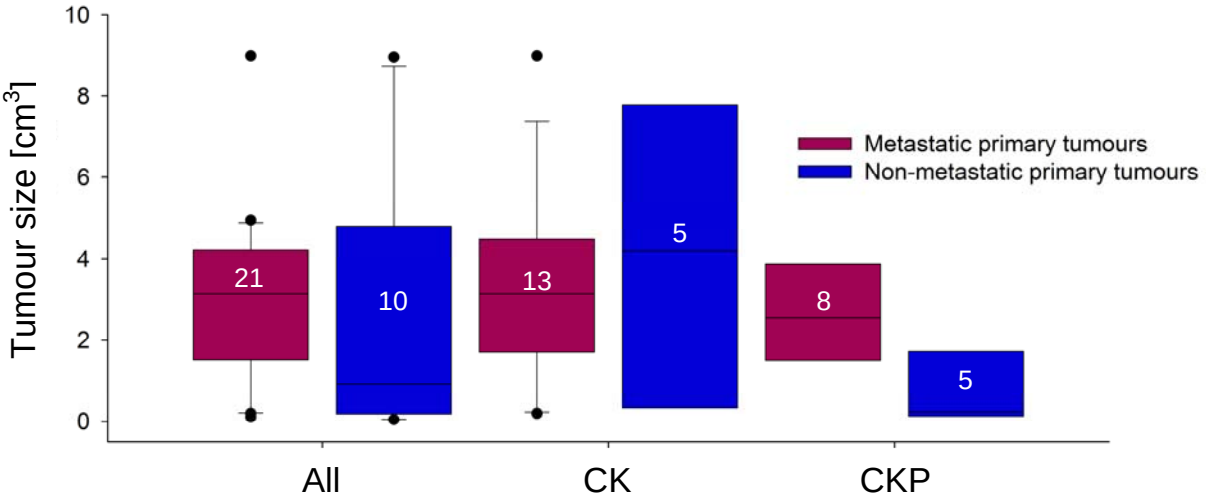

Figure 4-9 Tumour size of metastatic versus non-metastatic primary tumours No significant differences could be observed (Student's t-test). CK=Ptf1a/p48$^{Cre/+}$/LSL-Kras^{G12D}, CKP=Ptf1a/p48$^{Cre/+}$/ LSL-Kras^{G12D}/LSL-TP53$^{R172H/+}$, white numbers equal n.

Tumour size for both genotypes *Ptf1a/p48$^{Cre/+}$/LSL-Kras^{G12D}* and *Ptf1a/p48$^{Cre/+}$/ LSL-Kras^{G12D}/LSL-TP53$^{R172H/+}$* did not show significant difference between mice with metastases and mice without (Figure 4-9). Moreover, metastatic and non-metastatic mice of both groups survived about the same period of time (Figure 4-8). Even though in the Kaplan-Meier-Curves metastatic mice seemed to live somewhat longer no statistical significance could substantiate this. Thus, tumours with following metastasis had an equally long time to develop as tumours without metastasis.

Next, I investigated if well or poorly differentiated primary tumour histology correlated with metastastis as epithelial to mesenchymal transition (EMT) is known to be supportive of metastasis (Batlle et al., 2000; Cano et al., 2000; Thiery and Sleeman, 2006; Tse and Kalluri, 2007; Zavadil and Bottinger, 2005). As illustrated in Figure 4-10 this could not be proved for either primary tumours from mice with endogenous tumours nor for primary tumours from nude mice with orthotopically implanted tumour cells (p=0.5 and p=0.99, respectively, Fisher's Exact Test).

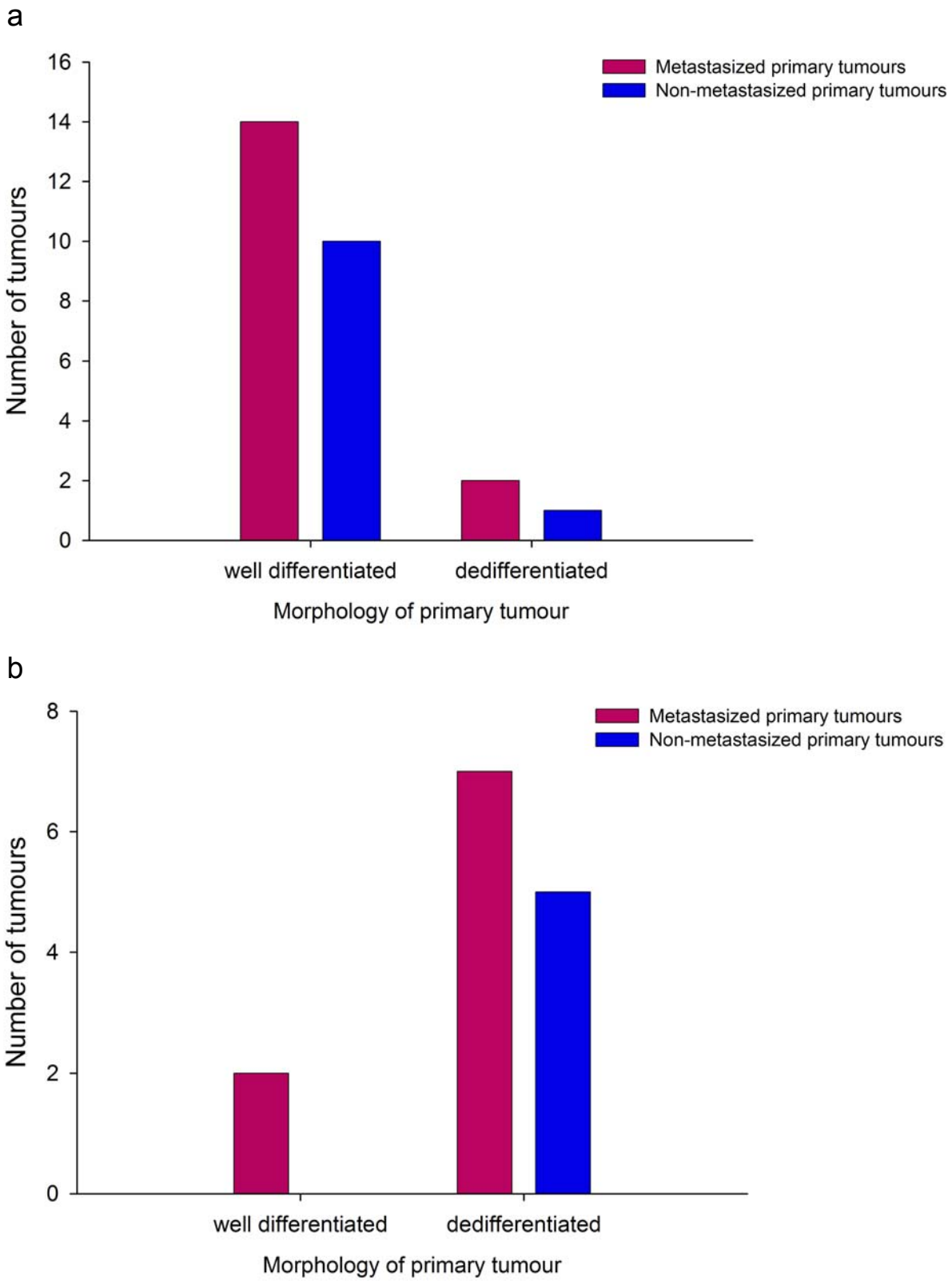

Figure 4-10 Morphology of primary tumours of a) tumour mice with endogenous tumours and b) nude mice with orthotopically implanted tumour cells Tumour morphology is not correlated with metastasis ((a) p=0.5 and (b) p=0.99, respectively, Fisher's Exact Test)

Analogously, I examined if mesenchymal phenotype of isolated cells was associated with metastasis. As depicted in Figure 4-11 no significance was observed here either, neither for cell lines grouped according to the metastatatic status of the organ they were isolated from nor for grouping according to the metastatic status after orthotopic implantation. The phenotype of cells isolated from primary tumours did mostly match the phenotype of the endogenous tumour they originated, however not in all cases. Cells isolated from the same mouse but from different sources such as primary

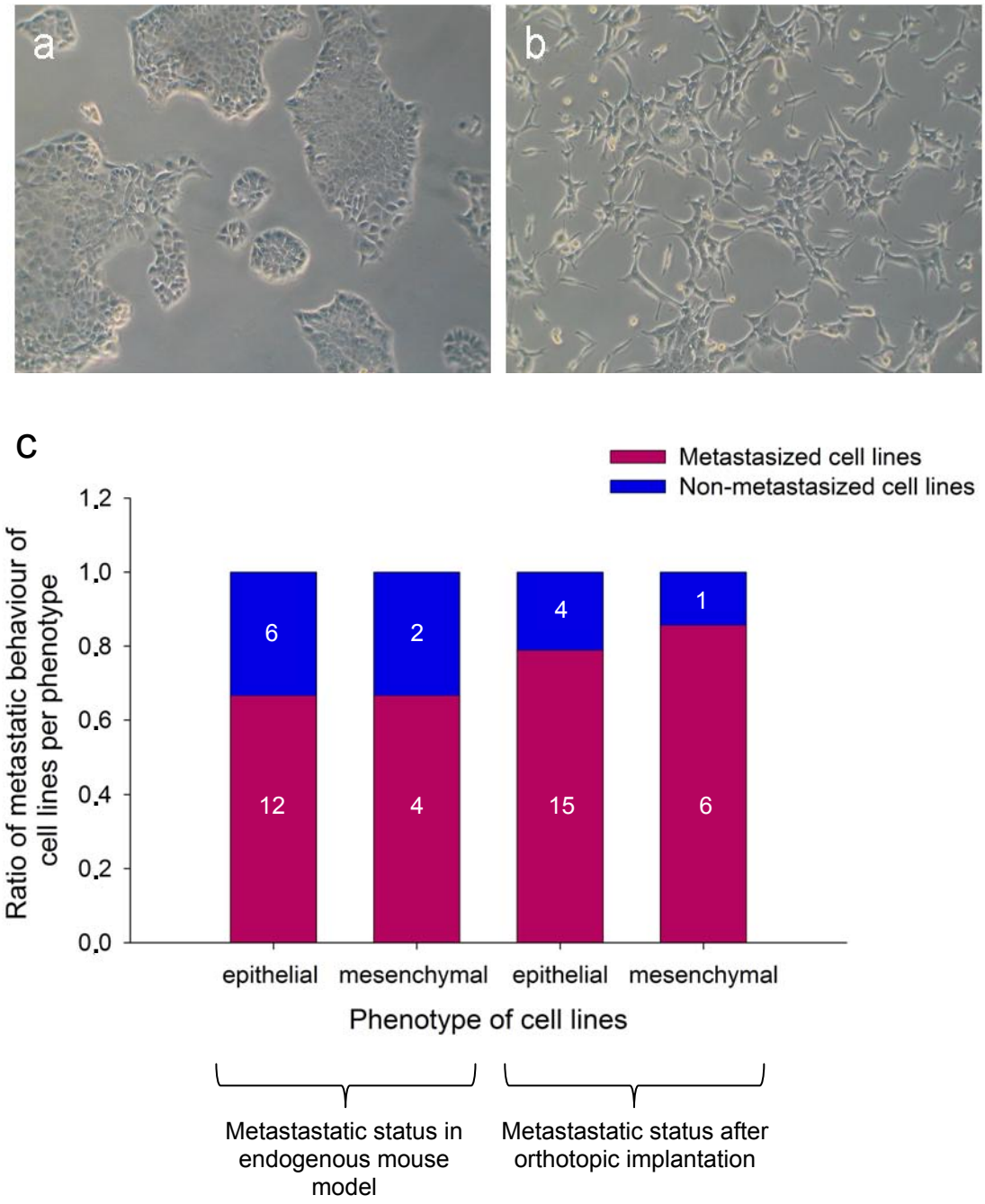

Figure 4-11 Correlation of metastasis and phenotype of isolated tumour cells with a) epithelial and b) mesenchymal phenotype. c) No significant difference in metastatic behaviour of these cells could be determined (Fisher's exact test). White numbers equal n.

tumour and corresponding metastases mostly exhibited the same phenotype.

This is true for all *Ptf1a/p48*$^{Cre/+}$*/LSL-Kras*^{G12D} cells, some of them having a particularly high metastatic potential.

That K-Ras exhibits oncogenic functions when constitutively activated is commonly accepted. However, some studies suggest that wild type K-Ras can function as a tumour suppressor. Zhang et al. (Zhang et al., 2001) investigated lung cancer that causes *Kras* activating mutations and found that tumours in mice expressing only activated and therefore oncogenic *Kras* were more abundant, larger, and were predominantly undifferentiated malignant adenocarcinomas, whereas tumours with heterozygous oncogenic and wild type *Kras* were smaller adenomas. In another study *Kras* was knocked out completely in a murine model for teratoma. This led to enhanced growth with higher proportions of undifferentiated embryonal carcinoma-like cells comparable to oncogenic *Kras* mice (James et al., 2003) also leading to the conclusion that *Kras* functions as a tumour suppressor.

To investigate if wild type status has an impact on metastasis in pancreatic cancer, I determined if loss of wild type *Kras* and therefore loss of heterozygosity (LOH) in all

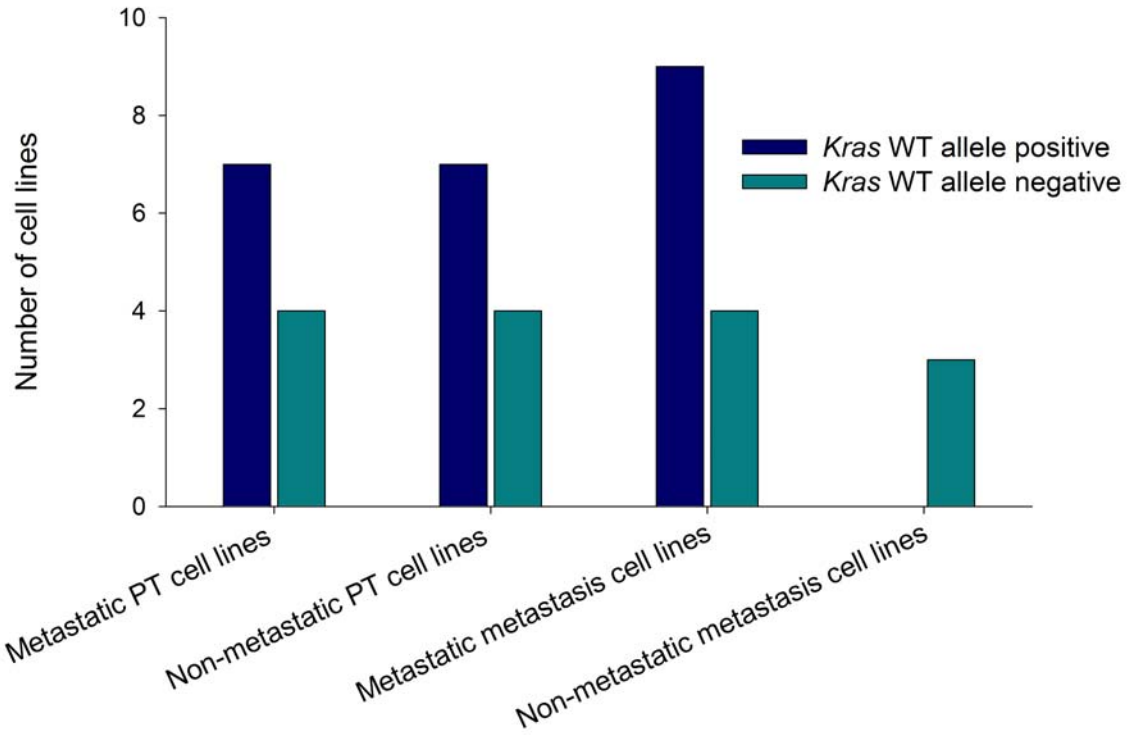

Figure 4-12 Correlation of metastasis with loss of heterozygosity of *Kras*
Loss of the *K-Ras* wild type allele does not result in an enhancement of metastatic potential for neither primary tumour cell lines nor for metastasis cell lines grouped for metastatic status after orthotopic implantation (p=0.67 and p=1, respectively, one sided Fisher's exact test).

isolated tumour cells was evident and subsequently tested for association with metastasis. I could not detect any correlation between loss of wild type *Kras* allele and metastasis for neither primary tumour cell lines nor for metastasis cell lines grouped according to their metastatic behaviour after orthotopic implantation (see Figure 4-12). Notably, metastatic cells with wild type *Kras* allele constitute the majority of cell lines. Thus, the wild type status of K-Ras does not account for diminished metastatic potential.

4.3. Metastasis of pancreatic tumour cells is not organ-specific

To analyze the metastatic behaviour of isolated tumour cells of both *Ptf1a/p48$^{Cre/+}$/LSL-Kras^{G12D}* and *Ptf1a/p48$^{Cre/+}$/LSL-Kras^{G12D}/LSL-TP53$^{R172H/+}$* genotypes in more detail I performed a comprehensive screen of the exact sites of metastasis after orthotopic implantation in comparison to the original sites of metastasis in the mouse model developing tumours endogenously. Intriguingly, metastasis of *Ptf1a/p48$^{Cre/+}$/LSL-Kras^{G12D}* primary tumour cells after orthotopic

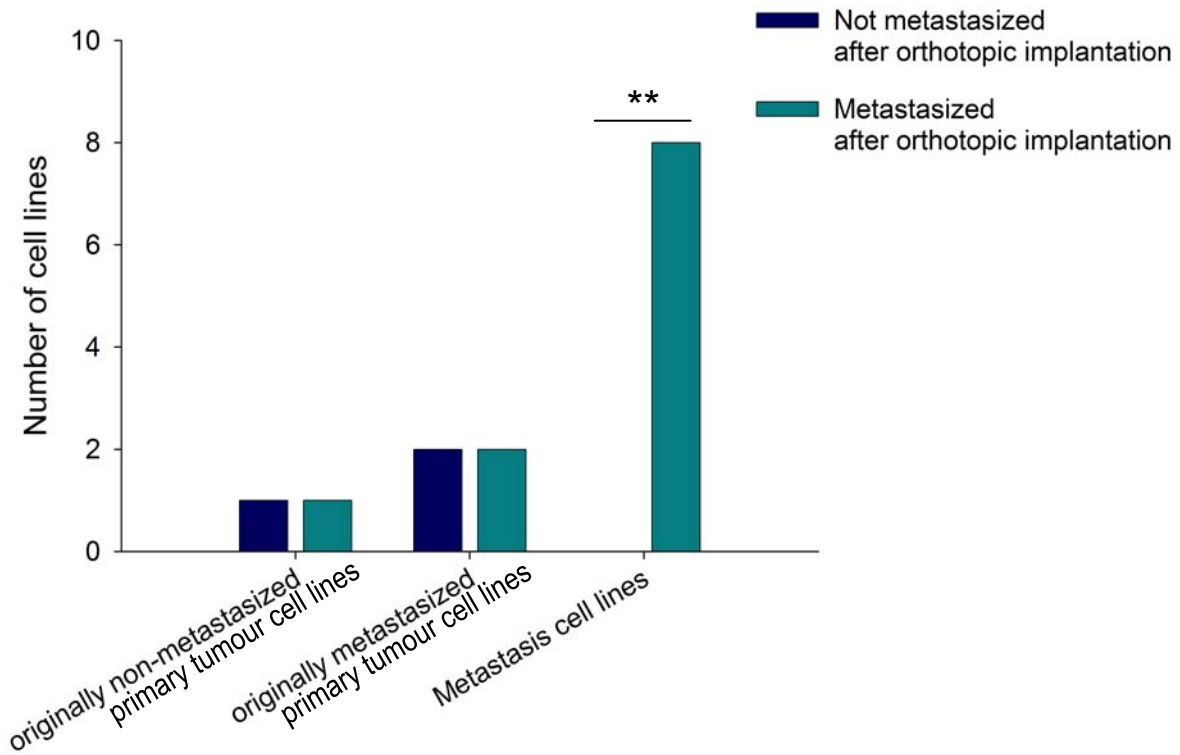

Figure 4-13 Metastatic behaviour of all *Ptf1a/p48$^{Cre/+}$/LSL-Kras^{G12D}* cell lines showing no deviation particularly for cells isolated from primary tumours. Conversely, all cells isolated from metastases did metastasize after orthopic implantation into the pancreas of nude mice whereas not one metastatis cell line did not metastasize after orthotopic implantation (p=0.0078, Wilcoxon signed-rank test)

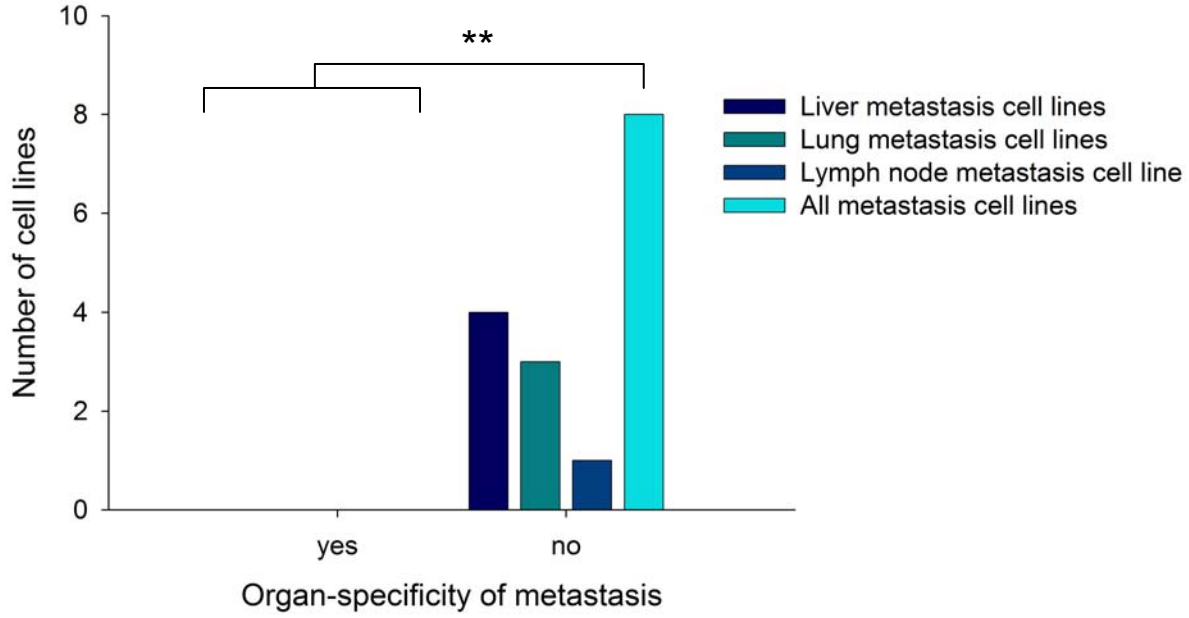

Figure 4-14 Organ-specificity of cells isolated from metastases of Ptf1a/p48$^{Cre/+}$/LSL-Kras^{G12D} mice None of the metastatic cell lines metastasized solely to the organ where it was isolated from. (p=0.0078, Wilcoxon signed-rank test)

implantation proved to be not predictable based on the metastatic status determined in the endogenous mouse model (Figure 4-13). Conversely, all cells isolated from metastases from this genotype did metastasize again after implantation which was confirmed to be highly significant (p=0.0078, Wilcoxon signed-rank test). As already mentioned Kang and colleagues performed functional metastasis assays to single out cell clones with an increased level of metastasis to the bone in breast cancer of mice (Kang et al., 2003). Their hypothesis of organ specific metastasis was supported by further studies of Vicent et al. who discovered a gene-expression signature specific for metastasis to the bone in a murine mouse model for lung cancer (Vicent et al., 2008).

In contrast, none of the investigated metastasis cell lines could prove this concept in our model system (Figure 4-14). None of the cell lines did metastasize solely to the distant organ they were originally isolated from (p=0.0078, Wilcoxon signed-rank test). Furthermore, some of them did not home to their original site at all whereas others did so in combination with metastasizing to additional sites.

Table 4-1 Homing of metastases of metastasis cell lines after orthotopic implantation

Organ of distant metastasis	Cell line ID	Not metastasized	Liver	Lung	Lymph node
Livermetastasis cell lines	53631 Liver II		no	no	yes
	53631 Liver I		no	yes	yes
	15272 Liver I		yes	yes	yes
	5123 Liver		yes	yes	yes
Lungmetastasis cell lines	53631 Lung III		yes	yes	no
	53631 Lung II		no	yes	yes
	15272 Lung		yes	yes	yes
Lymph node metastasis cell lines	3139 LK	*	no	yes	no
	5486 LK mdst	yes *	no	no	no
	15272 LK I		no	yes	yes

Each row represents one cell line, asterisk indicates *Ptf1a/p48$^{Cre/+}$/LSL-Kras^{G12D}/LSL TP53$^{R172H/+}$* genotype, other cell lines were of *Ptf1a/p48$^{Cre/+}$/LSL-Kras^{G12D}*genotype

In contrast to *Ptf1a/p48$^{Cre/+}$/LSL-Kras^{G12D}* cells, neither cells isolated from primary tumours nor from metastases of *Ptf1a/p48$^{Cre/+}$/LSL-Kras^{G12D}/LSL-TP53$^{R172H/+}$* tumour mice did metastasize according to their original metastasis status in the endogenous mouse model (Figure 4-15).

All of the originally not metastasized primary tumour cells did metastasize after implantation and 50 % of cells from originally metastasized samples did not.

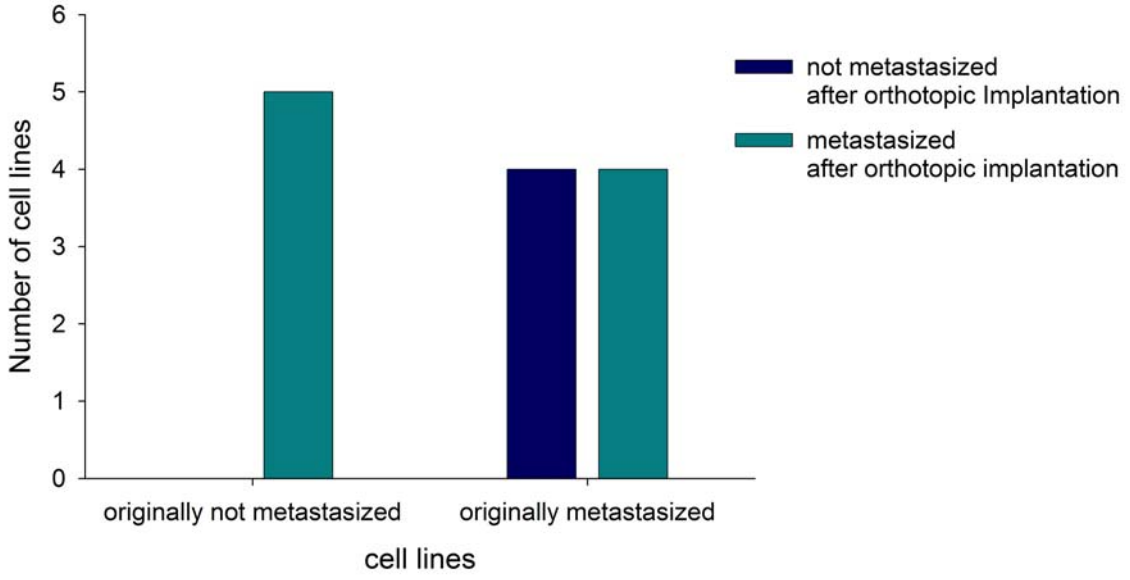

Figure 4-15 Metastatic behaviour of cells isolated from Ptf1a/p48$^{Cre/+}$/ LSL-Kras^{G12D}/LSL-TP53$^{R172H/+}$ mice is not consistent with regard to their original metastatic status in the endogenous mouse model after orthotopic implantation into nude mice (p=1, One-sided Fisher's exact test).

4.4. Differentially expressed genes in metastasis of pancreatic cancer

Several groups have conducted expression profiling of PDAC cell lines as well as primary tumours but none of them have focused on metastasis. Here, I set out to identify genes which predict metastasis in pancreatic cancer which might represent new drug targets. To achieve this I performed microarray analyses on both primary samples directly from tumour mice as well as on cells isolated from these samples. Through this approach it is possible to provide a link between these heterologous systems. A potential expression signature that is deducted from primary samples can be tested on the cell culture system or the other way round. Furthermore, overlapping gene sets for both systems can be determined possibly providing a more powerful prediction of which genes are linked to metastasis.

I was interested not only in differentially expressed genes but particularly in enriched gene sets. These provide insights into a wide array of genes underlying the same biological process, for example a specific signalling pathway, thus that the impact of that pathway can be assessed irrespective of how it might have been altered.

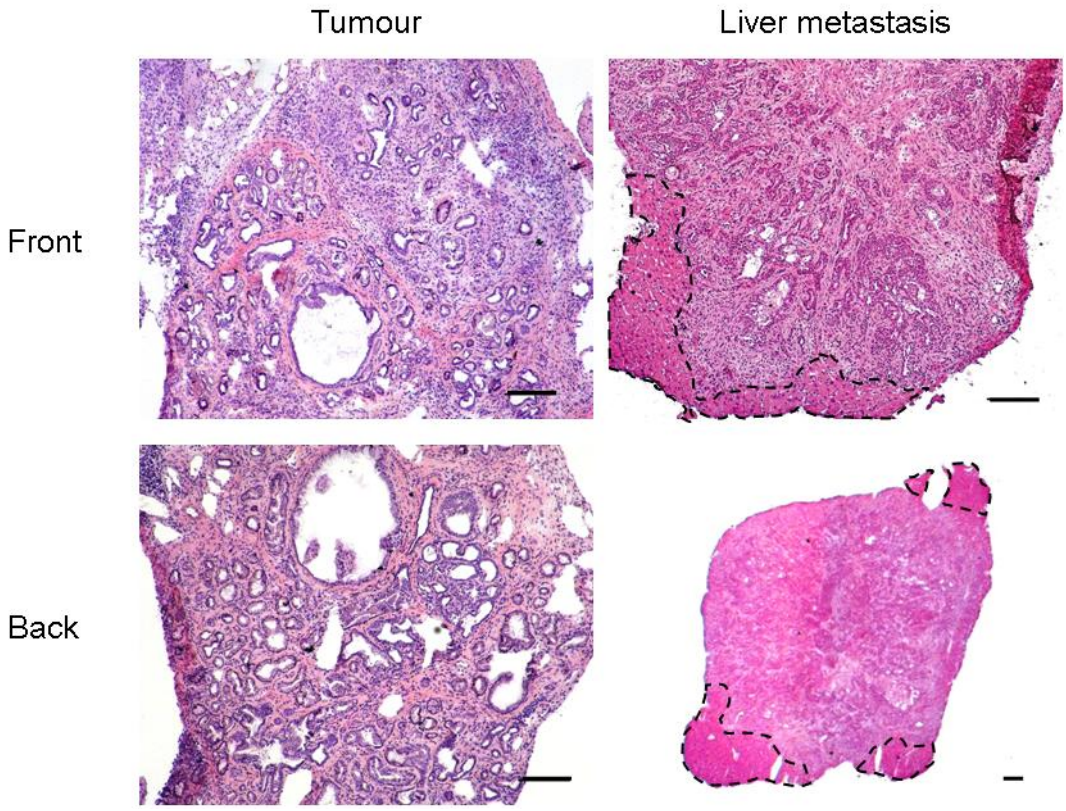

Figure 4-16 Histological verification of adequacy of samples used for microarray analysis I analyzed the first and the last cryosection histologically to determine the ratio of contaminating surrounding tissue. Dashed areas point out liver tissue in a metastasis sample that comprised at most 20 % to 25 % of tissue. Bars represent 200µm.

To confirm that primary samples used for microarray analysis actually consisted of tumour or metastasis rather than surrounding tissue, I screened all samples. For this purpose I cryosectioned the samples, keeping the first and the last section for H&E staining (Figure 4-16). Thus I proved on a histological basis that contamination of pancreas, lung or liver tissue was at most 25 %.

First of all, primary samples and isolated cells were analyzed together so that genes deregulated in both groups could be identified. However, the different methods to extract RNA from frozen tissue and from cultured cells proved to influence outcome in an extent that direct comparison was impossible (see Figure 4-17). Too high variation in the expression values across both groups made the samples from both approaches incomparable to each other. This means that in this comparison there is more difference between the type of sample like primary isolate and cell line than between biological meaningful groups like metastases and primary tumours. Thus, samples were normalized in two groups according to their specific background with the goal to identify intersecting groups of genes and gene sets between the two groups that were deregulated in the same manner. All analyses performed are listed in Table 4-2.

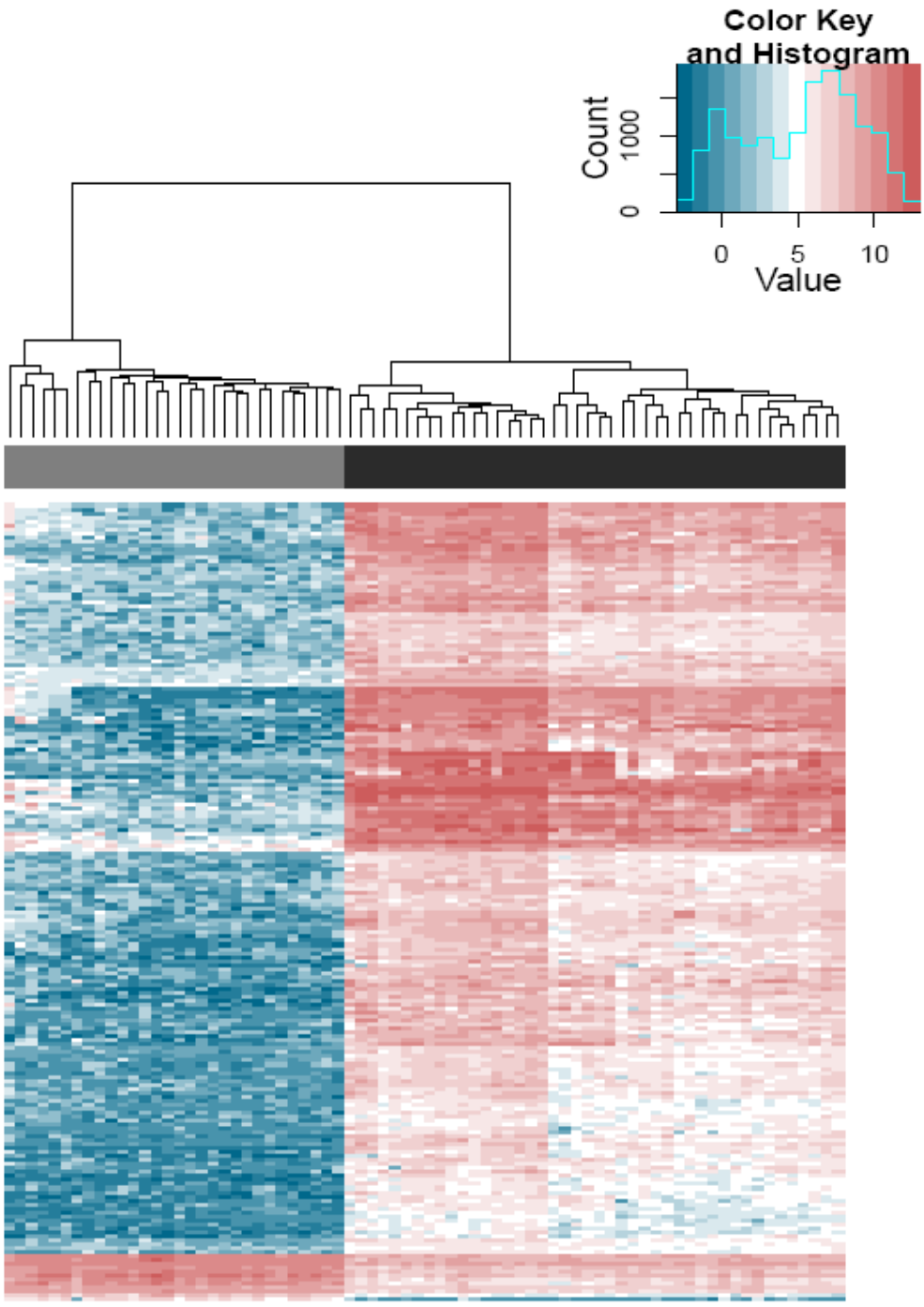

Figure 4-17 Microarray analysis of primary samples and isolated cells in one approach
The different methodology of isolating RNA caused clustering according to the method of RNA isolation producing incompatible results for both groups and proved to cover detection of differentially expressed genes. The grey bar indicates isolated cell samples, the black bar indicates primary samples from tumours and metastases. The colour key indicates relative expression value after normalisation.

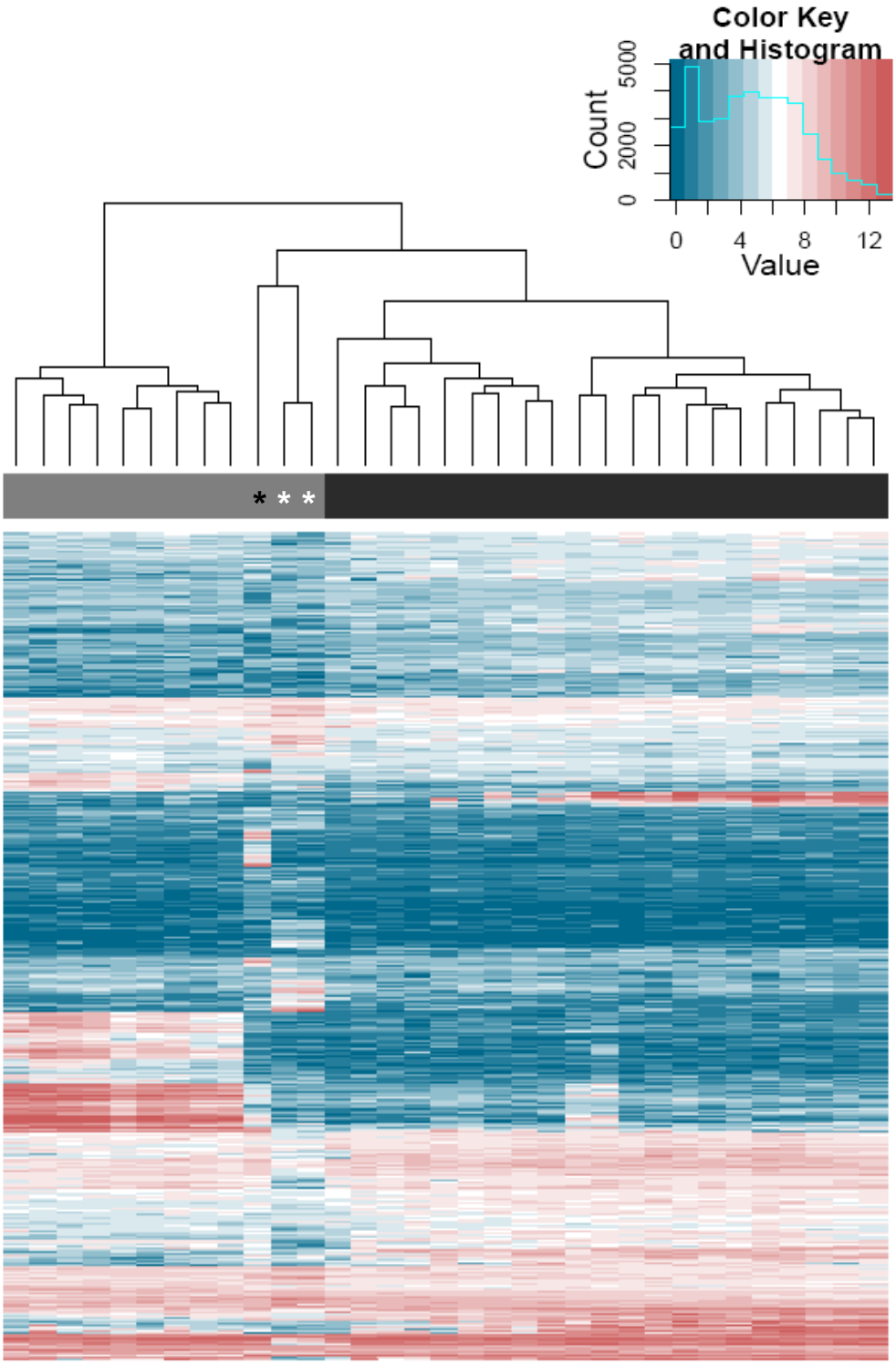

Figure 4-18 Microarray analysis of primary samples of metastasized primary tumours compared to metastasis samples
Metastasis samples (marked by grey bar) differ in gene expression from primary tumours samples (marked by black bar). Genes deregulated by organ tissue surrounding metastases can not be discerned in this comparison. Grey samples without asterisk mark liver metastases, grey samples with white asterisk mark lung metastases, grey sample with black asterisk marks diaphragm metastasis. The colour key indicates relative expression value after normalisation.

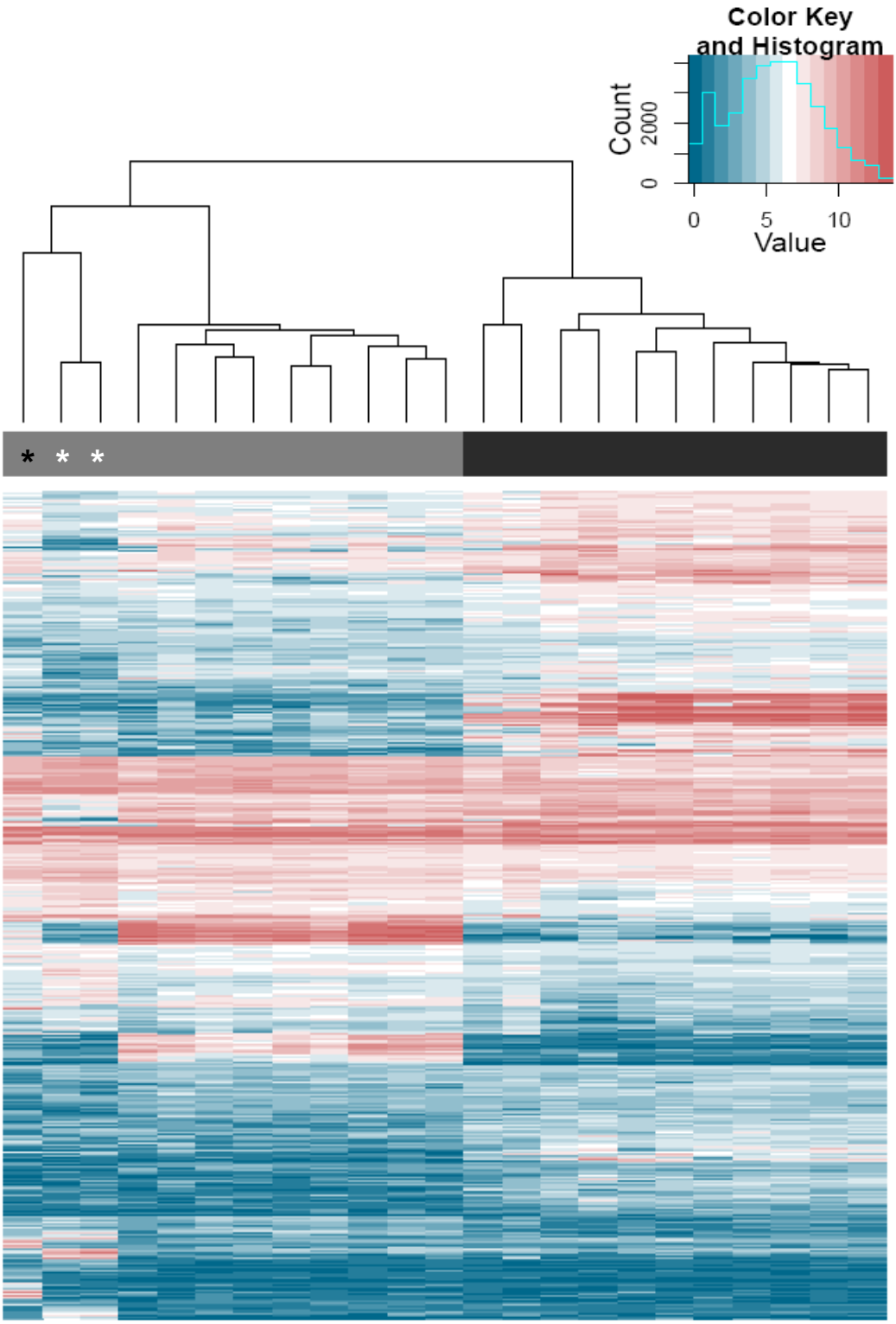

Figure 4-19 Microarray analysis of primary samples of non-metastasized primary tumours compared to metastasis samples
Metastasis samples (marked by grey bar) differ in gene expression from primary tumours samples (marked by black bar). Genes deregulated by organ tissue surrounding metastases can not be discerned in this comparison. Grey samples without asterisk mark liver metastases, grey samples with white asterisk mark lung metastases, and grey sample with black asterisk marks diaphragm metastasis. The colour key indicates relative expression value after normalisation.

Table 4-2 Overview of contrasts assessed by microarray analysis
Non-metPT = non-metatasized primary tumour, metPT = metastasized primary tumour, Met = metastasis, OI = orthotopic implantation, CTC = circulating tumour cells, LN-Met = lymph node metastasis

Contrast	Genotype	Number of significantly deregulated genes	Depicted in Figure or Table
Analysis of primary samples			
non-metPT vs. met PT	*Ptf1a/p48$^{Cre/+}$/LSL-Kras^{G12D}* ; *Ptf1a/p48$^{Cre/+}$/LSL-Kras^{G12D}/ LSL-TP53$^{R172H/+}$*	0	
non-metPT vs. met PT	*Ptf1a/p48$^{Cre/+}$/LSL-Kras^{G12D}*	0	
non-metPT vs. met PT	*Ptf1a/p48$^{Cre/+}$/LSL-Kras^{G12D}/ LSL-TP53$^{R172H/+}$*	0	
metPT vs. Met	*Ptf1a/p48$^{Cre/+}$/LSL-Kras^{G12D}* and *Ptf1a/p48$^{Cre/+}$/LSL-Kras^{G12D}/ LSL-TP53$^{R172H/+}$*	1173	Figure 4-18
non-metPT vs. Met	*Ptf1a/p48$^{Cre/+}$/LSL-Kras^{G12D}* and *Ptf1a/p48$^{Cre/+}$/LSL-Kras^{G12D}/ LSL-TP53$^{R172H/+}$*	3983	Figure 4-19
Analysis of isolated cell samples			
non-metPT cells vs. metPT cells	*Ptf1a/p48$^{Cre/+}$/LSL-Kras^{G12D}* ; *Ptf1a/p48$^{Cre/+}$/LSL-Kras^{G12D}/ LSL-TP53$^{R172H/+}$*	0	
metPT cells vs. Met cells	*Ptf1a/p48$^{Cre/+}$/LSL-Kras^{G12D}* ; *Ptf1a/p48$^{Cre/+}$/LSL-Kras^{G12D}/ LSL-TP53$^{R172H/+}$*	2	
Non-metPT and metPT cells vs. Met cells	*Ptf1a/p48$^{Cre/+}$/LSL-Kras^{G12D}* ; *Ptf1a/p48$^{Cre/+}$/LSL-Kras^{G12D}/ LSL-TP53$^{R172H/+}$*	8	Table 4-3
Non-metastasized cells (OI) vs. metastasized cells (OI)	*Ptf1a/p48$^{Cre/+}$/LSL-Kras^{G12D}/ LSL-TP53$^{R172H/+}$*	11	Table 4-4

Contrast	Genotype	Number of significantly deregulated genes	Depicted in Figure or Table
Non-metPT cells vs. metPT cells	*Ptf1a/p48$^{Cre/+}$/LSL-Kras^{G12D}*	0	
Non-metPT cells vs. Met cells	*Ptf1a/p48$^{Cre/+}$/LSL-Kras^{G12D}*	372 (out of these 23 genes are also deregulated in the contrast of non-metastasized primary tumour samples and metastases of primary tumour samples of both *Ptf1a/p48$^{Cre/+}$/LSL-Kras^{G12D}* and *Ptf1a/p48$^{Cre/+}$/LSL-Kras^{G12D}/LSL-TP53$^{R172H/+}$* genotypes)	Figure 4-21, (23 intersecting genes: Table 4-5)
metPT cells vs. Met cells	*Ptf1a/p48$^{Cre/+}$/LSL-Kras^{G12D}*	9 (out of these 2 genes were also deregulated in the contrast metastasized primary tumours vs. metastases of the primary tissue samples)	Figure 4-23
Non-metPT and metPT cells vs. CTC	*Ptf1a/p48$^{Cre/+}$/LSL-Kras^{G12D}* ; *Ptf1a/p48$^{Cre/+}$/LSL-Kras^{G12D}/LSL-TP53$^{R172H/+}$*	5	Table 4-6
CTC vs Met cells	*Ptf1a/p48$^{Cre/+}$/LSL-Kras^{G12D}* ; *Ptf1a/p48$^{Cre/+}$/LSL-Kras^{G12D}/LSL-TP53$^{R172H/+}$*	3	
MetPT cells vs. CTC	*Ptf1a/p48$^{Cre/+}$/LSL-Kras^{G12D}*	0	
CTC vs Met cells	*Ptf1a/p48$^{Cre/+}$/LSL-Kras^{G12D}*	10	Figure 4-24
Liver metastasis cells vs. lung metastasis cells	*Ptf1a/p48$^{Cre/+}$/LSL-Kras^{G12D}* ; *Ptf1a/p48$^{Cre/+}$/LSL-Kras^{G12D}/LSL-TP53$^{R172H/+}$*	1	

Contrast	Genotype	Number of significantly deregulated genes	Depicted in Figure or Table
Liver-Met cells vs. LN-Met cells	*Ptf1a/p48$^{Cre/+}$/LSL-Kras^{G12D}* ; *Ptf1a/p48$^{Cre/+}$/LSL-Kras^{G12D}/ LSL-TP53$^{R172H/+}$*	35 (out of these 19 genes were also deregulated in the contrast lung metastasis cells vs. lymph node metastasis cells)	Figure 4-26, (intersecting genes Table 4-7)
Lung-Met cells vs. LN-Met cells	*Ptf1a/p48$^{Cre/+}$/LSL-Kras^{G12D}* ; *Ptf1a/p48$^{Cre/+}$/LSL-Kras^{G12D}/ LSL-TP53$^{R172H/+}$*	31 (out of these 19 genes were also deregulated in the contrast liver metastasis cells vs. lymph node metastasis cells)	Figure 4-25, (intersecting genes Table 4-7)

Contrasting non-metastasized and metastasized primary tumour samples, I observed no significantly deregulated genes, neither in comparisons integrating both *Ptf1a/p48$^{Cre/+}$/LSL-Kras^{G12D}* and *Ptf1a/p48$^{Cre/+}$/LSL-Kras^{G12D}/LSL-TP53$^{R172H/+}$* genotypes nor for each of them alone. Conversely, both groups of non-metastasized primary tumour samples and metastasized primary tumour samples differed significantly from metastasis samples in a high number of genes (see Figure 4-18 and Figure 4-19). However, examining the gene set enrichment analyses for these contrasts (data not shown) I noticed that a number of gene sets identifying genes expressed specifically in liver tissue like "Hsiao Liver Specific Genes" and "Human Tissue Liver" were up-regulated in the metastasis group. This hindered the discrimination of genes deregulated between primary tumours and metastases or deregulation of genes caused by surrounding tissue. To circumvent this issue I focused on intersections of differentially expressed genes between contrasts of primary samples and isolated cells. These are validated by both methods and feature the following characteristics: Based on the analysis of primary samples directly from tissues the possibility of cell culture artefacts is excluded. On the other hand, based on analysis of dispersed and cultured cells the background of surrounding tissue of pancreas, liver, lung and lymph node is omitted. Thus, the resulting differentially expressed genes and gene sets can be considered highly interesting candidates.

Consequently, I analyzed the microarray data of cultured cells including both *Ptf1a/p48*$^{Cre/+}$*/LSL-Kras*^{G12D} and *Ptf1a/p48*$^{Cre/+}$*/LSL-Kras*^{G12D}*/LSL-TP53*$^{R172H/+}$ genotypes as a first step. Here non-metastasized and metastasized primary tumour

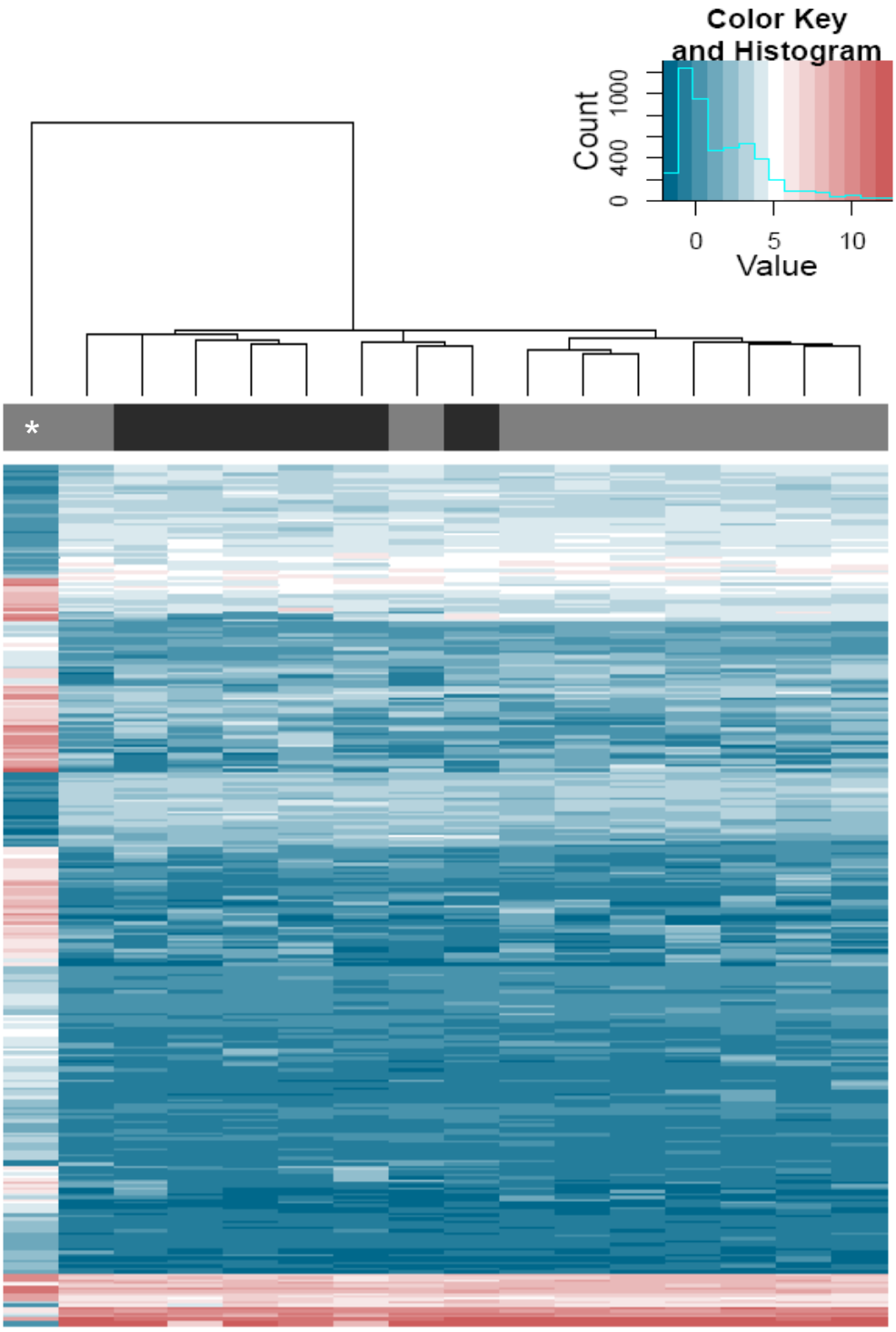

Figure 4-20 Microarray analysis of isolated cell samples of non-metastasized primary tumour cells compared to metastasis cells of both genotypes
Cells from metastasis samples (marked by grey bar) hardly differ in gene expression from cells from not metastasized primary tumours samples (marked by black bar). The lymph node metastasis cells outlier sample is marked by an asterisk. The colour key indicates relative expression value after normalisation.

cells did not differ significantly in expression of any gene. This confirms the results from primary samples. In addition, a significant distinction between metastasized primary tumour cells and metastasis cells could only be detected in two genes: *RIKEN cD E130215H24* gene and *Beta 1-like galactosidase*. In addition, I set out to compare non-metastasized primary tumour cells to metastasis cells. As depicted in Figure 4-20 most samples did not differ in a high amount of genes with the exception of an outlier metastasis cell sample. This sample was the only metastasis cell line that did not metastasize after orthotopic implantation into nude mice (*Ptf1a/p48$^{Cre/+}$/LSL-Kras^{G12D}/LSL-TP53$^{R172H/+}$* genotype). Therefore, I excluded it from analysis. This resulted in eight genes significantly deregulated between the two groups (see Table 4-3). However, none of them overlapped with genes identified from primary sample analysis.

Table 4-3 Differentially expressed genes in the contrast of non-metastasized primary tumour cells (n=6) versus metastasis cells (n=9) without outlier sample of isolated cells of both *Ptf1a/p48$^{Cre/+}$/ LSL-Kras^{G12D}* and *Ptf1a/p48$^{Cre/+}$/LSL-Kras^{G12D}/LSL-TP53$^{R172H/+}$* genotypes.

SYMBOL	GENENAME	Adjusted p-Value	Fold change
9330101J02Rik	RIKEN cD 9330101J02 gene	0.0019	5.4
Gata5	GATA binding protein 5	0.0308	$2.1x10^{-2}$
Dhh	desert hedgehog	0.0308	$5.9x10^{-2}$
Cnksr3	Cnksr family member 3	0.0308	2.6
Fam113b	family with sequence similarity 113, member B	0.0308	7.5
Porcn	porcupine homolog (Drosophila)	0.0455	$1.7x10^{-1}$
Myh10	myosin, heavy polypeptide 10, non-muscle	0.0455	48.9
Gata5	GATA binding protein 5	0.0455	$2.4x10^{-2}$
Eya2	eyes absent 2 homolog (Drosophila)	0.0455	$1.7x10^{-1}$

Fold change is referred to non-metastasized primary tumour cells compared to metastasis cells.

Furthermore, as I verified metastasizing behaviour of all isolated cell samples via orthotopic implantation into nude mice and detected that metastasizing behaviour of cells isolated from *Ptf1a/p48$^{Cre/+}$/LSL-Kras^{G12D}/LSL-TP53$^{R172H/+}$* mice in contrast to

cells isolated from *Ptf1a/p48$^{Cre/+}$/LSL-Kras^{G12D}* mice could not be predicted based on the original metastatic status of the sample (Figure 4-15) I subdivided the cell samples according to the respective genotype and analyzed them discretely. Due to their irregular behaviour *Ptf1a/p48$^{Cre/+}$/LSL-Kras^{G12D}/LSL-TP53$^{R172H/+}$* cell lines were grouped solely based on metastatic status after orthotopic implantation as opposed to their original source. No more than eleven genes depicted in Table 4-4 were significantly altered in this comparison. Moreover, only *Mcf2* was also identified in the analysis of primary samples (Figure 4-18 and Figure 4-19).

Table 4-4 Differentially expressed genes in the contrast of non-metastasized cells (n=4) versus metastasized cells (n=7) of isolated cells of *Ptf1a/p48$^{Cre/+}$/LSL-Kras^{G12D}/LSL-TP53$^{R172H/+}$* genotype grouped according to metastasis status after orthotopic implantation.

SYMBOL	GENENAME	Adjusted p-Value	Fold change
1439602_at	(no denotation)	0.0001	16.6
Nrarp	Notch-regulated ankyrin repeat protein	0.0053	$3.9x10^{-2}$
Mcf2	mcf.2 transforming sequence-like	0.014	$1.2x10^{-1}$
Accn2	amiloride-sensitive cation channel 2, neuronal	0.0243	8.5
Pabpc4l	poly(A) binding protein, cytoplasmic 4-like	0.0254	5.4
Clec4b1	C-type lectin domain family 4, member b1	0.0291	7.0
D730039F16Rik	RIKEN cD D730039F16 gene	0.0291	4.5
3110052M02Rik	RIKEN cD 3110052M02 gene	0.0341	$1.2x10^{-1}$
3110080O07Rik	RIKEN cD 3110080O07 gene	0.0411	3.9
1444115_at	(no denotation)	0.0411	$1.5\ x10^{-1}$

SYMBOL	GENENAME	Adjusted p-Value	Fold change
Mum1l1	melanoma associated antigen (mutated) 1-like 1	0.048	3.5

Fold change is referred to non-metastasized cells compared to metastasized cells. Only *Mcf2* was also identified in analysis of primary samples.

Next, I analyzed cells isolated solely from tissues of *Ptf1a/p48$^{Cre/+}$/LSL-Kras^{G12D}* mice. In line with results from primary samples, no significantly deregulated gene could be identified in the contrast of non-metastasized primary tumour cells versus metastasized primary tumour cells. Most differentially expressed genes were detected in the contrast of non-metastasized primary tumour cells compared with metastasis cell lines (see Figure 4-21). In Table 4-5 genes intersecting between this contrast of non-metastasized primary tumour cells compared with metastasis cell lines of the *Ptf1a/p48$^{Cre/+}$/LSL-Kras^{G12D}* genotype and the contrasts of non-metastasized primary tumour samples and metastases of primary tumour samples of both *Ptf1a/p48$^{Cre/+}$/LSL-Kras^{G12D}* and *Ptf1a/p48$^{Cre/+}$/LSL-Kras^{G12D}/LSL-TP53$^{R172H/+}$* genotypes are listed. Genes marked in yellow refer to overlapping genes with both contrasts of primary samples: non-metastasized primary tumours and metastasized primary tumours versus metastases, respectively. Moreover, gene set enrichment analysis (GSEA) underlines these findings (see Figure 4-22). Here, results are additionally emphasized by the fact that a number of genes belonging to the same set reflect the change in gene expression independently of how gene expression or which gene is altered. Interestingly, a number of gene sets reveal the importance of up-regulation of genes and pathways associated with cell cycle and cell division, cell cycle expression clusters, DNA damage response genes, nucleotide metabolism, M phase and signal transduction in metastasis samples. These clusters have been identified in a module map showing conditional expression in cancer by Segal and colleagues (Segal et al., 2004).

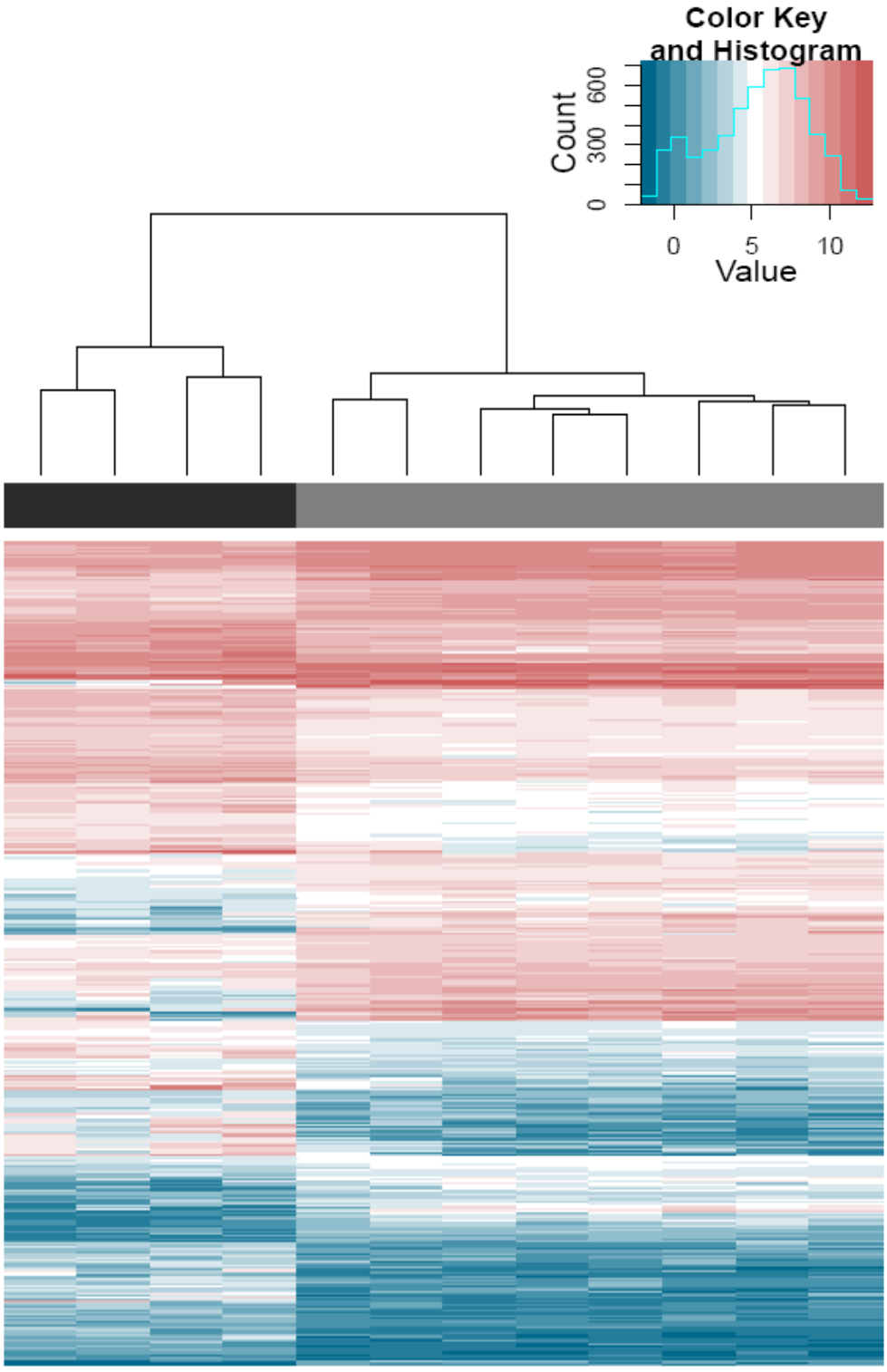

Figure 4-21 Microarray analysis of cell line samples of non-metastasized primary tumours compared to metastasis cell samples of Ptf1a/p48$^{Cre/+}$/LSL-Kras^{G12D} mice
Cells from metastasis samples (marked by grey bar) differ in gene expression from cells from non-metastasized primary tumours samples (marked by black bar). The colour key indicates relative expression value after normalisation.

Table 4-5 23 differentially expressed genes intersecting between the contrast of non-metastasized primary tumour cells (n=6) compared with metastasis cell lines (n=10) of the *Ptf1a/p48$^{Cre/+}$/LSL-Kras^{G12D}* genotype and the contrasts of non-metastasized primary tumour samples (n=11) and metastases (n=12) of primary tumour samples of both *Ptf1a/p48$^{Cre/+}$/LSL-Kras^{G12D}* and *Ptf1a/p48$^{Cre/+}$/LSL-Kras^{G12D}/LSL-TP53$^{R172H/+}$* genotypes

SYMBOL	GENENAME	Cells		Tissue samples	
		Adj. p-Value	Fold change	Adj. p-Value	Fold change
Ccl5	chemokine (C-C motif) ligand 5	0.0031	14.9	0.0469	4.3
Srd5a1	steroid 5 alpha-reductase 1	0.0055	$3.0x10^{-1}$	0.0313	$3.6x10^{-1}$
Osmr	oncostatin M receptor	0.0071	10.9	0.0256	2.0
Phyhd1	phytanoyl-CoA dioxygenase domain containing 1	0.0088	6.1	0.0058	1.8
Pcdhb7	protocadherin beta 7	0.0091	6.5	0.0009	2.6
Pbxip1	pre-B-cell leukemia transcription factor interacting protein 1	0.0109	3.0	0.048	1.4
Zfp521	zinc finger protein 521	0.0142	11.7	0.007	4.0
C1s	complement component 1, s subcomponent	0.0151	31.0	0.003	3.3
Kif23	kinesin family member 23	0.0154	$3.5x10^{-1}$	0.0218	$3.2x10^{-1}$
Txnrd3	thioredoxin reductase 3	0.0217	$4.7x10^{-1}$	0.0131	$5.4x10^{-1}$
Plat	plasminogen activator, tissue	0.0219	$2.1x10^{-1}$	0.0296	$5.2x10^{-1}$
Pde8a	phosphodiesterase 8A	0.0260	14.6	0.0253	1.7
Gstm2	glutathione S-transferase, mu 2	0.0268	4.2	0.0041	2.2
Mcm2	minichromosome maintenance deficient 2 mitotin (S. cerevisiae)	0.0278	$4.2x10^{-1}$	0.0126	$3.3x10^{-1}$
Cdca3	cell division cycle	0.0301	$3.8x10^{-1}$	0.0023	$2.4x10^{-1}$

SYMBOL	GENENAME	Cells		Tissue samples	
		Adj. p-Value	Fold change	Adj. p-Value	Fold change
	associated 3				
Foxm1	forkhead box M1	0.0322	$2.6x10^{-1}$	0.0013	$1.1x10^{-1}$
Nrp1	neuropilin 1	0.0379	7.4	0.0466	1.5
Galnt6	UDP-N-acetyl-alpha-D-galactosamine:polypeptide N-acetylgalactosaminyltransferase 6	0.0405	6.5	0.002	2.8
Tgfbr3	transforming growth factor, beta receptor III	0.0408	34.4	0.0128	2.4
Gns	glucosamine (N-acetyl)-6-sulfatase	0.0408	2.1	0.0181	1.5
Ssbp2	single-stranded D binding protein 2	0.0451	5.6	0.0301	3.1
Maf	avian musculoaponeurotic fibrosarcoma (v-maf) AS42 oncogene homolog	0.0477	5.0	0.0003	2.4
Casp12	caspase 12	0.0496	30.4	0.0248	1.7

Genes marked in yellow are also overlapping with primary tumour samples of the contrast of metastasized primary tumour samples versus metastases. Fold change is referred to non-metastasized primary tumour samples/cells compared to metastasis samples/cells of the isolated cells.

Further interesting enriched gene sets down-regulated in metastases are expression neighbourhood of *EI24*, a gene directly regulated by p53 which suppresses cell growth and induces cell death (Gu et al., 2000) or expression neighbourhood of *CTBP1*, which appears to modulate transformation, tumorigenesis, and metastasis negatively (Chen et al., 2008; Winklmeier et al., 2009). Next, I investigated gene expression alteration between metastasized primary tumour cells and metastasis cells. I revealed nine genes significantly altered of which two overlapped with the corresponding analysis on primary samples: *Odd-skipped related 2* (drosophila), a transcription factor important for development of the palate and cadherin 4, a

calcium-dependent cell-cell adhesion molecule important in cell-cell interaction (see Figure 4-23).

It is known that tumour cells can shed from the primary tumour, enter lymphatic and blood vessels, circulate through the bloodstream or the lymphatic system and

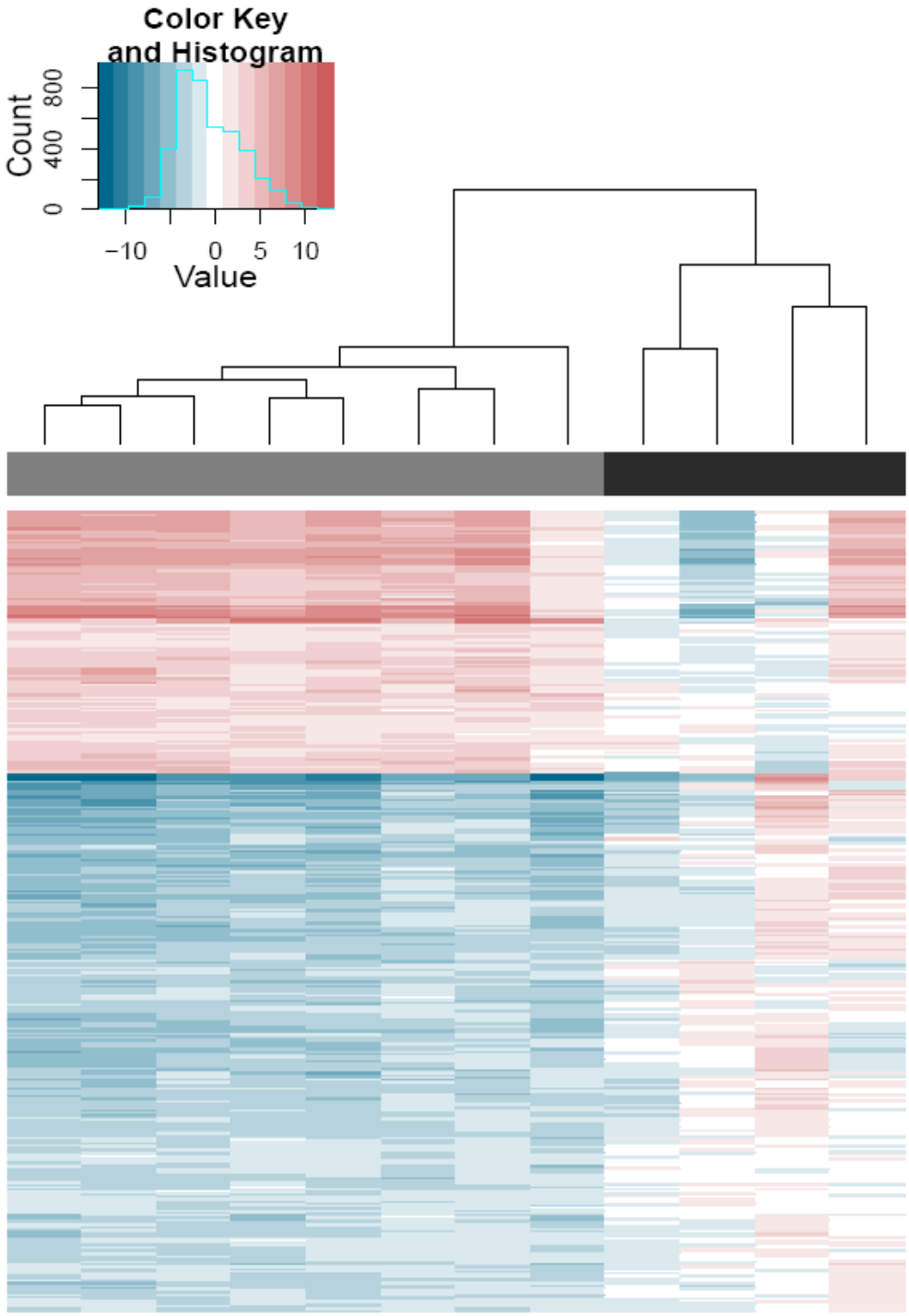

Figure 4-22 Gene set enrichment analysis of cell line samples of non-metastasized primary tumour cells compared to metastasis cells of Ptf1a/p48$^{Cre/+}$/LSL-Kras^{G12D} mice

Cells from metastasis samples (marked by grey bar) differ in gene expression from cells from non-metastasized primary tumours samples (marked by black bar). The colour key indicates relative expression value after normalisation.

colonize distant organs. (Kumar, 2005). To investigate if and how cells adopt an intermediate expression profile state in the circulation I evaluated the variance between circulating tumour cells and primary tumour cells or metastasis cells, respectively. I started out with comparing cell lines from both *Ptf1a/p48$^{Cre/+}$/LSL-Kras^{G12D}* and *Ptf1a/p48$^{Cre/+}$/LSL-Kras^{G12D}/LSL-TP53$^{R172H/+}$* genotypes. As I discovered that metastasized primary tumours can only be distinguished from metastases by two differentially expressed genes in the above enquiries I proceeded with comparing all primary tumour cell lines (metastasized and non-metastasized) with the circulating tumour cells. Five genes were found to be significantly altered (see Table 4-6).

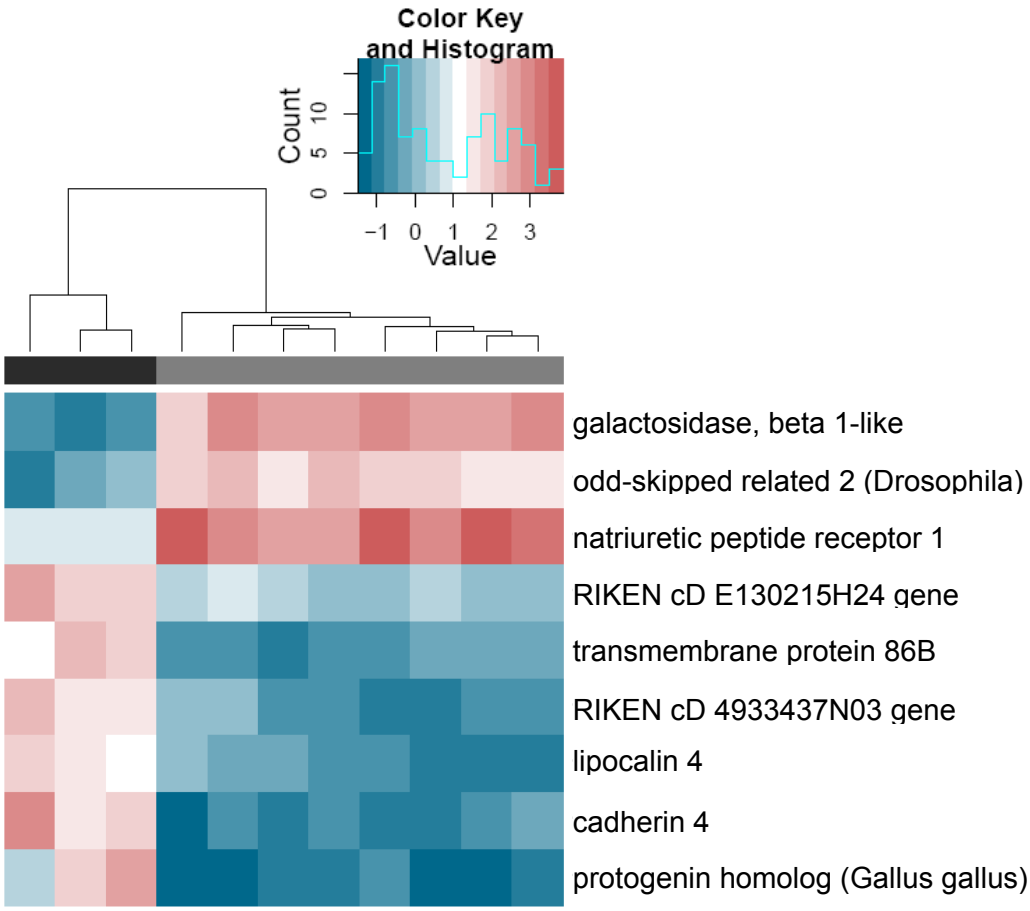

Figure 4-23 Microarray analysis of cell line samples of metastasized primary tumour cells compared to metastasis cells of Ptf1a/p48$^{Cre/+}$/LSL-Kras^{G12D} mice
Cells from metastasis samples (marked by grey bar) differ in nine genes in gene expression from cells from metastasized primary tumours samples (marked by black bar). Solely odd-skipped related 2 and cadherin 4 are in line with results from primary samples. The colour key indicates relative expression value after normalisation.

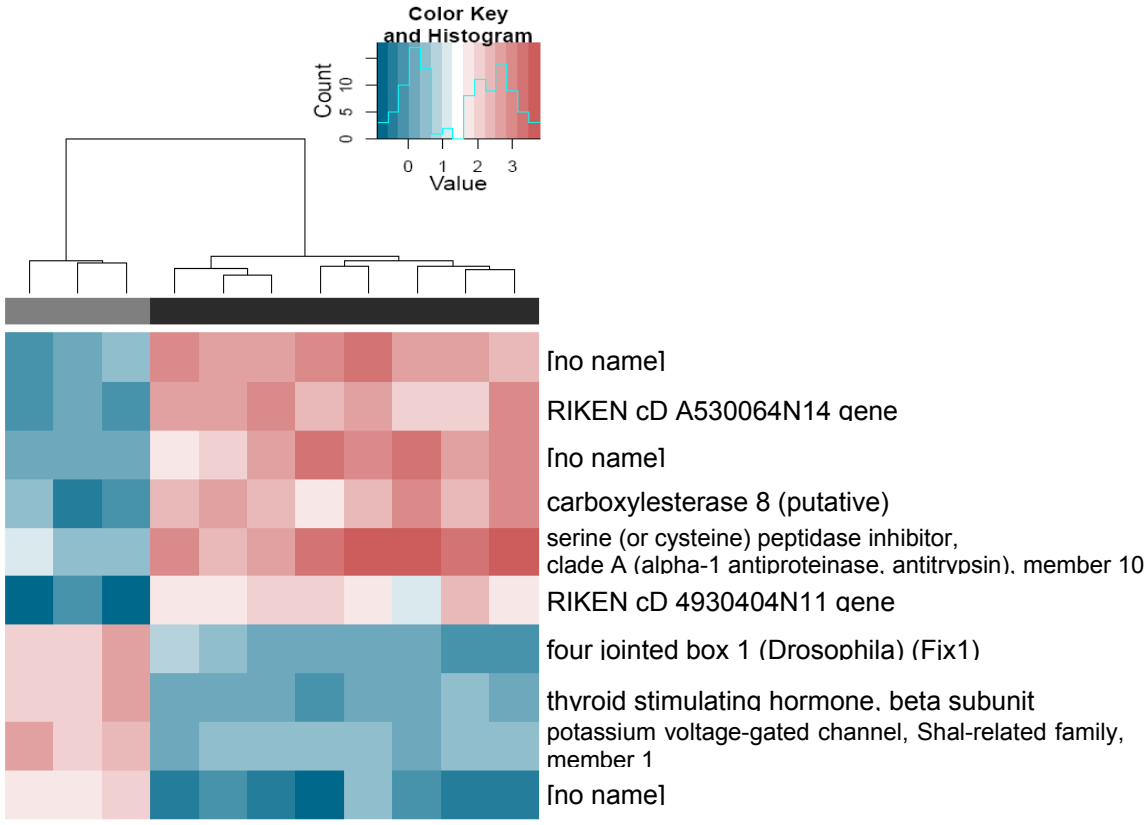

Figure 4-24 Microarray analysis of cell line samples of circulating tumour cells compared to metastasis cells of Ptf1a/p48$^{Cre/+}$/LSL-Kras^{G12D} mice
Circulating tumour cells (marked by grey bar) differ in ten genes in gene expression from metastasis cells (marked by black bar). The colour key indicates relative expression value after normalisation.

Table 4-6 Differentially expressed genes in the contrast of cells from primary tumours (n=32) versus circulating tumour cells (n=4) of both *Ptf1a/p48$^{Cre/+}$/LSL-Kras^{G12D}* and *Ptf1a/p48$^{Cre/+}$/LSL-Kras^{G12D}/ LSL-TP53$^{R172H/+}$* genotypes

SYMBOL	GENENAME	Adjusted p-Value	Fold change
Myh10	myosin, heavy polypeptide 10, non-muscle	0.0130	57.6
Gab1	growth factor receptor bound protein 2-associated protein 1	0.0254	7.3
2610524H06Rik	RIKEN cD 2610524H06 gene	0.0307	2.5
[1459612_at]	(no denotation)	0.0472	3.7
Twist2	twist homolog 2 (Drosophila)	0.0472	21.7

Fold change is referred to circulating cells compared to primary tumour cells.

Non-muscle myosin, heavy polypeptide 10 is required for communication between the microtubule cytoskeleton and the actin cytoskeleton and the cell membrane during cytokinesis (Straight et al., 2003). GAB1 is tyrosine phosphorylated upon stimulation in EGF- and insulin-receptor signalling and interacts with signaling

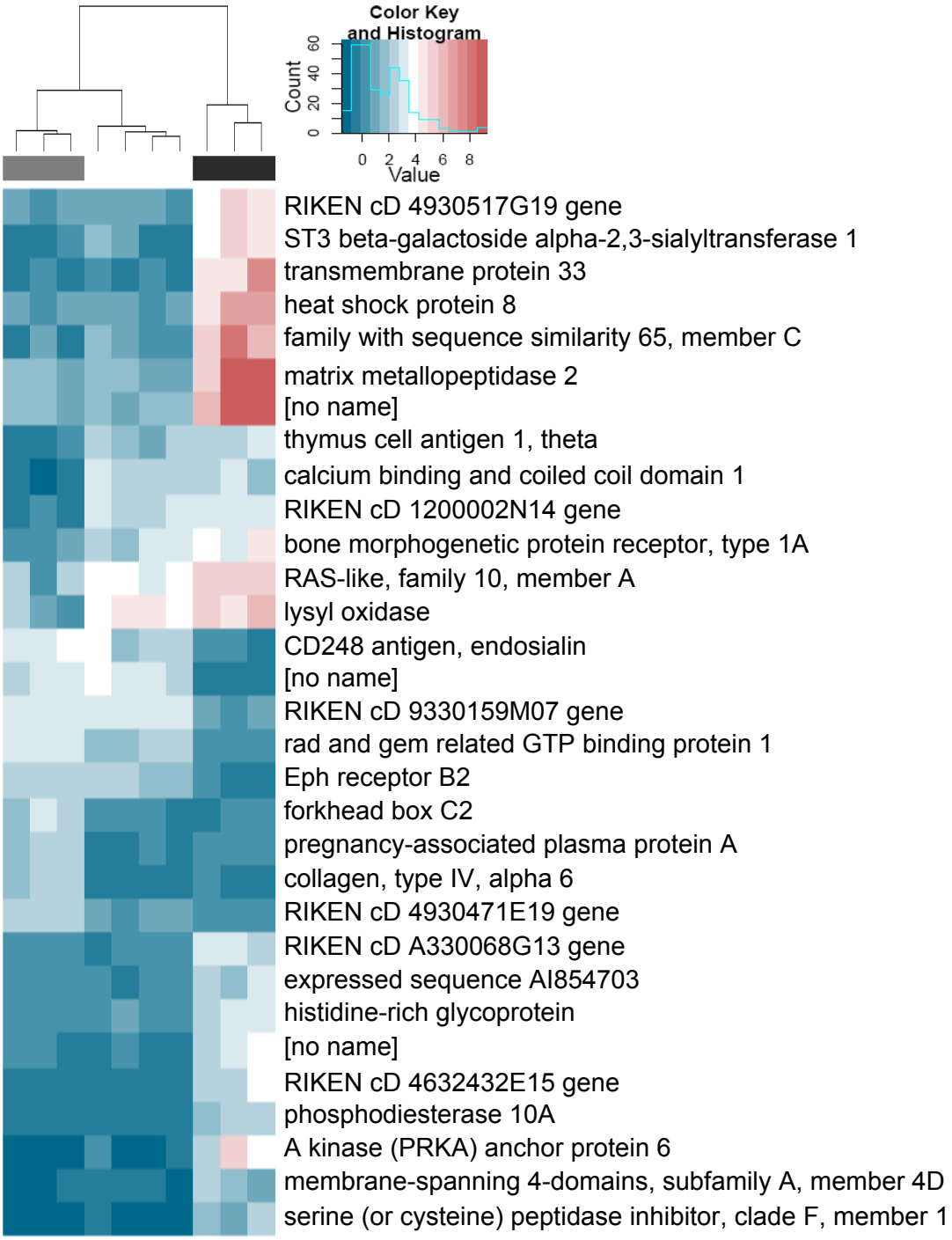

Figure 4-25 Contrast of lung metastasis cells compared to lymph node metastasis cells
Lung metastasis cells (marked by grey bar) differ significantly from lymph node metastasis cells (marked by black bar). Liver metastasis cells (marked by white bar) were not analyzed in this contrast, but were added and clustered with the lung metastasis cells. The colour key indicates relative expression value after normalisation.

molecules such as phosphatidylinositol 3-kinase (Holgado-Madruga et al., 1996; Holgado-Madruga et al., 1997). Particularly interesting is up-regulation of Twist homolog 2 in the circulating tumour cells, as twist is known to regulate epithelial-mesenchymal transition (EMT), which plays a role in the process of metastasis in cancer (Kalluri and Weinberg, 2009; Kang and Massague, 2004). Subsequently, I analyzed alterations in gene expression from circulating tumour cells towards metastasis cells.

Three genes could be detected: *Potassium voltage-gated channel, Shal-related family, member 1 (Kcnd1)*; *RIKEN cD 4921530L21* gene (*4921530L21Rik*); and one without denotation. None of these genes could be assigned to the metastatic process. Thus, to gain more insight, I repeated the same analyses for *Ptf1a/p48*$^{Cre/+}$*/LSL-Kras*^{G12D} cells only. Of note, no gene was found to be differentially expressed between the groups of metastasized primary tumour cells and circulating tumour cells. Conversely, as depicted in Figure 4-24 I determined ten genes which differed in expression between circulating tumour cells and metastasis cells, of which *Four jointed box 1* (*Fjx1*) was also discovered in the analysis of primary tissue samples. Remarkably, in microarrays of primary samples it was found to be up-regulated in metastases compared to primary tumours whereas in the cell lines it was up-regulated in circulating tumour cells compared to metastasis cells. Fjx1 is a target of Notch and plays a role in signalling that regulates growth, gene expression, and planar cell polarity (Ishikawa et al., 2008). Finally, to examine if metastasis of pancreatic cancer is organ-specific, I tested whether I could determine different gene expression profiles for cells isolated from different sites of metastasis. Remarkably, I could only identify one gene that differed between liver and lung metastasis cells: oxysterol binding protein-like 6. Surprisingly, however, the difference between liver and lymph node metastasis cells (Figure 4-26) and between lung and lymph node metastasis cells (Figure 4-25) exceeded that difference considerably. Metastasis to liver and lung occurs through the bloodstream whereas metastasis to the lymph nodes occurs through the lymphatic system. To identify if there were overlapping genes between these contrasts which distinguish these different routes of metastasis from one another, I screened for intersecting genes. In Table 4-7 these intersecting genes are listed. Moreover, several genes were also identified in the contrasts of primary samples between metastasized primary tumours and metastases and/or non-metastasized primary tumours and metastases.

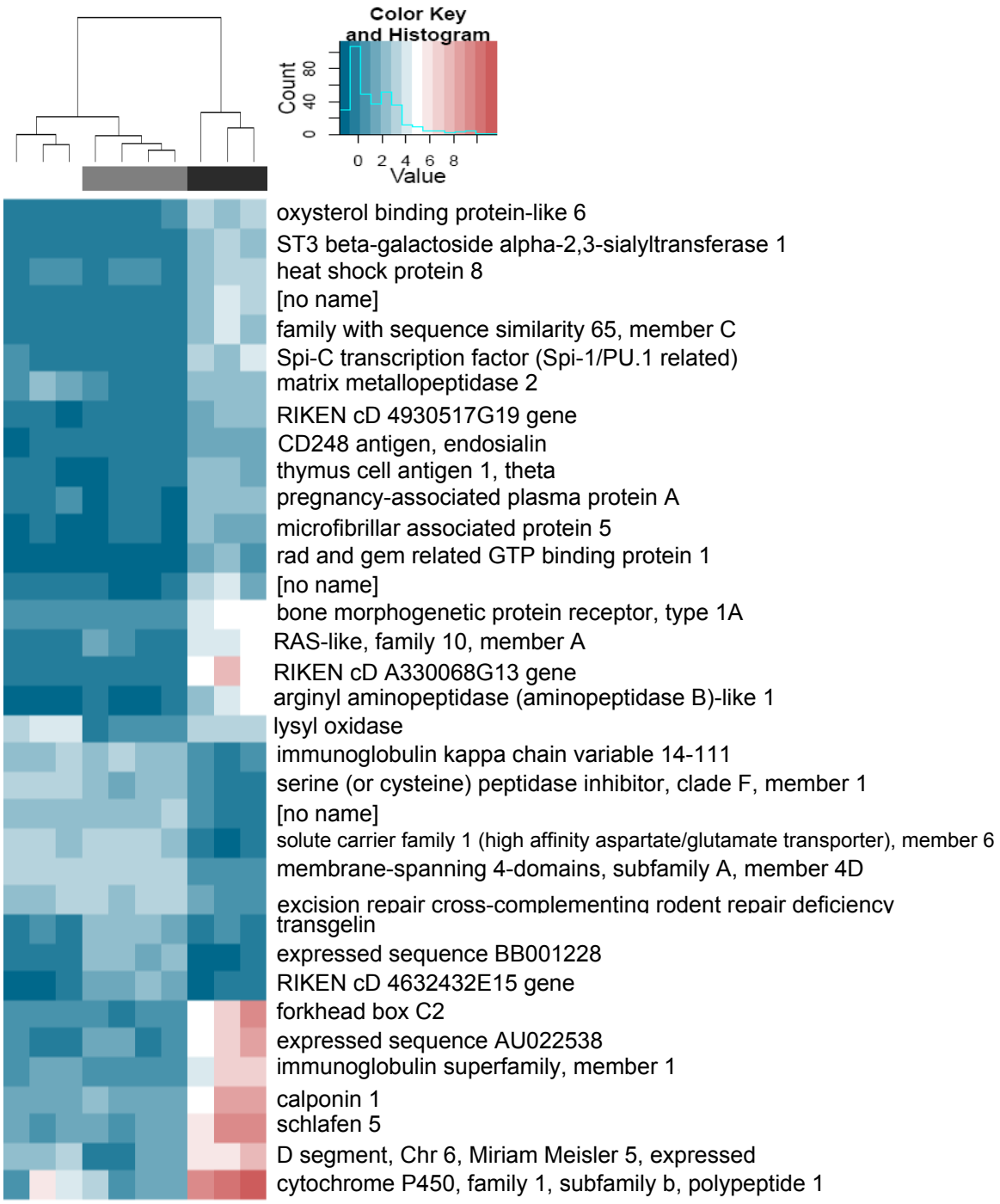

Figure 4-26 Contrast of liver metastasis cells compared to lymph node metastasis cells
Liver metastasis cells (marked by grey bar) differ significantly from lymph node metastasis cells (marked by black bar). Lung metastasis cells (marked by white bar) were not analyzed in this contrast, but were added and clustered with the liver metastasis cells. The colour key indicates relative expression value after normalisation.

Table 4-7 Differentially expressed genes overlapping between the contrasts of the groups liver metastasis cells versus lymph node metastasis cells or lung metastasis cells versus lymph node metastasis cells, respectively, of both *Ptf1a/p48$^{Cre/+}$/LSL-Kras^{G12D}* and *Ptf1a/p48$^{Cre/+}$/LSL-Kras^{G12D}/LSL-TP53$^{R172H/+}$* genotypes

SYMBOL	GENENAME	Adjusted p-Value [liver vs LN]	Fold change [liver vs LN]	Adjusted p-Value [lung vs LN]	Fold change [lung vs LN]
St3gal1	ST3 beta-galactoside alpha-2,3-sialyltransferase 1	0.0242	$1.6x10^{-1}$	0.0345	$1.5x10^{-1}$
Hspb8	heat shock protein 8	0.0242	$6.7x10^{-2}$	0.0345	$6.3x10^{-2}$
[1457079_at]	(no denotation)	0.0242	11.9	0.0402	10.5
Fam65c	family with sequence similarity 65, member C	0.0242	5.0	0.0402	5.0
Mmp2	matrix metallopeptidase 2	0.0242	$1. 9x10^{-2}$	0.0402	$1.7x10^{-2}$
4930517G19Rik	RIKEN cD 4930517G19 gene	0.0242	4.3	0.0285	7.4
Cd248	CD248 antigen, endosialin	0.0242	$2.2x10^{-2}$	0.0402	$2.8x10^{-2}$
Thy1	thymus cell antigen 1, theta	0.0242	$8.4x10^{-3}$	0.0402	$8.3x10^{-3}$
Pappa	pregnancy-associated plasma protein A	0.0300	$8.3x10^{-2}$	0.0402	$9.4x10^{-2}$
Rem1	rad and gem related GTP binding protein 1	0.0304	$1.9x10^{-1}$	0.0402	$1.9x10^{-1}$
Bmpr1a	bone morphogenetic protein receptor, type 1A	0.0304	$1.7x10^{-1}$	0.0402	$1.6x10^{-1}$
Rasl10a	RAS-like, family 10, member A	0.0334	$1.5x10^{-1}$	0.0402	$1. 4x10^{-1}$
A330068G13Rik	RIKEN cD A330068G13 gene	0.0385	$2.0x10^{-1}$	0.0402	$1.9x10^{-1}$

SYMBOL	GENENAME	Adjusted p-Value [liver vs LN]	Fold change [liver vs LN]	Adjusted p-Value [lung vs LN]	Fold change [lung vs LN]
Lox	lysyl oxidase	0.0386	$1.8x10^{-2}$	0.0402	$1.1x10^{-2}$
Serpinf1	serine (or cysteine) peptidase inhibitor, clade F, member 1	0.0386	$1.3x10^{-2}$	0.0454	$1.3x10^{-2}$
[1457743_at]	(no denotation)	0.0386	$1.4x10^{-1}$	0.0402	$1.3x10^{-1}$
Ms4a4d	membrane-spanning 4-domains, subfamily A, member 4D	0.0410	$3.9x10^{-2}$	0.0440	$3.4x10^{-2}$
4632432E15Rik	RIKEN cD 4632432E15 gene	0.0430	$1.2x10^{-1}$	0.0407	$1.0x10^{-1}$
Foxc2	forkhead box C2	0.0430	$5.6x10^{-2}$	0.0402	$3.9x10^{-2}$

Genes marked in yellow were also identified in the contrast of primary tissue samples between non-metastasized primary tumours and metastases. Furthermore, genes marked in orange were additionally identified in the contrast of metastasized primary tumours and metastases. Fold change is referred to liver or lung compared to lymph node.

4.5. Stem cells do not account for metastasis in pancreatic cancer

Various markers have already been tested for putative stem cells in pancreatic tumorigenesis. The most frequently and most controversial results have been discussed for CD133. Some groups proposed a role in metastasis for this marker (Hermann et al., 2007; Maeda et al., 2008) while others doubted its suitability as a stem cell marker (Immervoll et al., 2008; Welsch et al., 2009). Other markers which have been investigated and might distinguish pancreatic cancer stem cells include CD44, CD24 and ESA (Li et al., 2007a). Furthermore, in the pancreatic cancer model of the hamster, Oct4 has also been postulated to account for stemness (Iki and Pour, 2006). None of these markers, however, has been analyzed with regard to metastasis.

Another marker that so far has not been related to pancreatic cancer stem cells is the intermediate filament Nestin. It has, however, been characterised as a marker of pancreatic islet progenitors (Lumelsky et al., 2001) and of pancreatic exocrine progenitors that might represent the progenitor population in which PDAC arises (Carriere et al., 2007). According to the CSC model, cells disseminating from the primary tumour are stem cells which finally colonize a distant organ and build up metastases. To discover stem cells in the bulk of a tumour might equal to look for a needle in a haystack. On the contrary, in a smaller entity such as a micrometastasis it should be an unequally easier task. To reveal if the CSC model is applicable to pancreatic cancer I examined micrometastases that I found in the metastasis screen and tested for all of the above mentioned markers by immunohistochemistry.

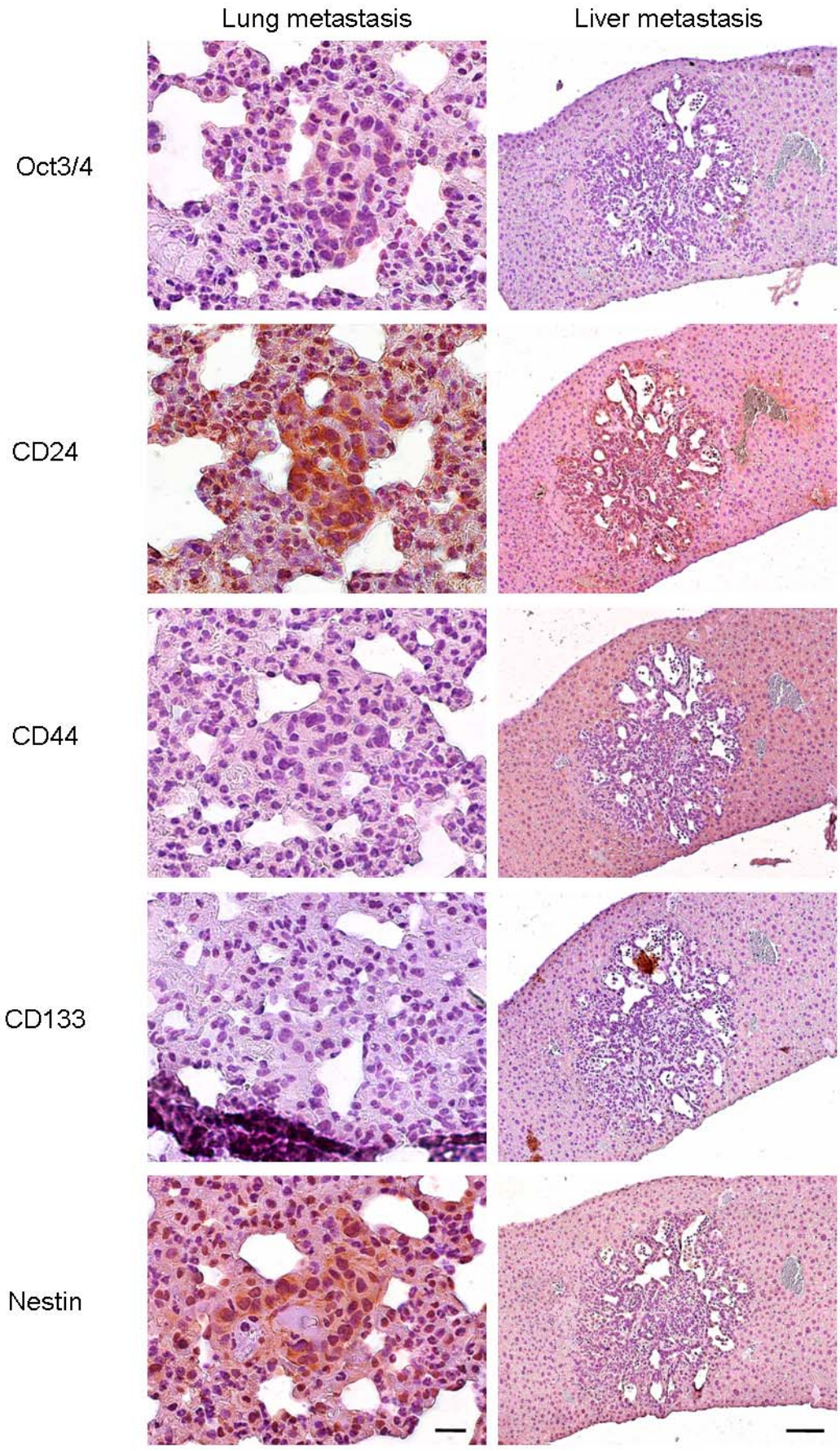

Figure 4-27 Stem cell markers in metastases of lung and liver of tumours grown from orthotopically implanted tumour cells in nude mice
Sections are depicted according to the sequence they were cut. Immunohistochemistry was performed and brown staining reflects the expression pattern of the indicated markers. In both lung and liver metastases either the whole micrometastasis is stained for the marker or no staining is visible. Cell line number 53631 Lungmet III was implanted here. Bars represent 20 µm for lung and 100 µm for liver samples.

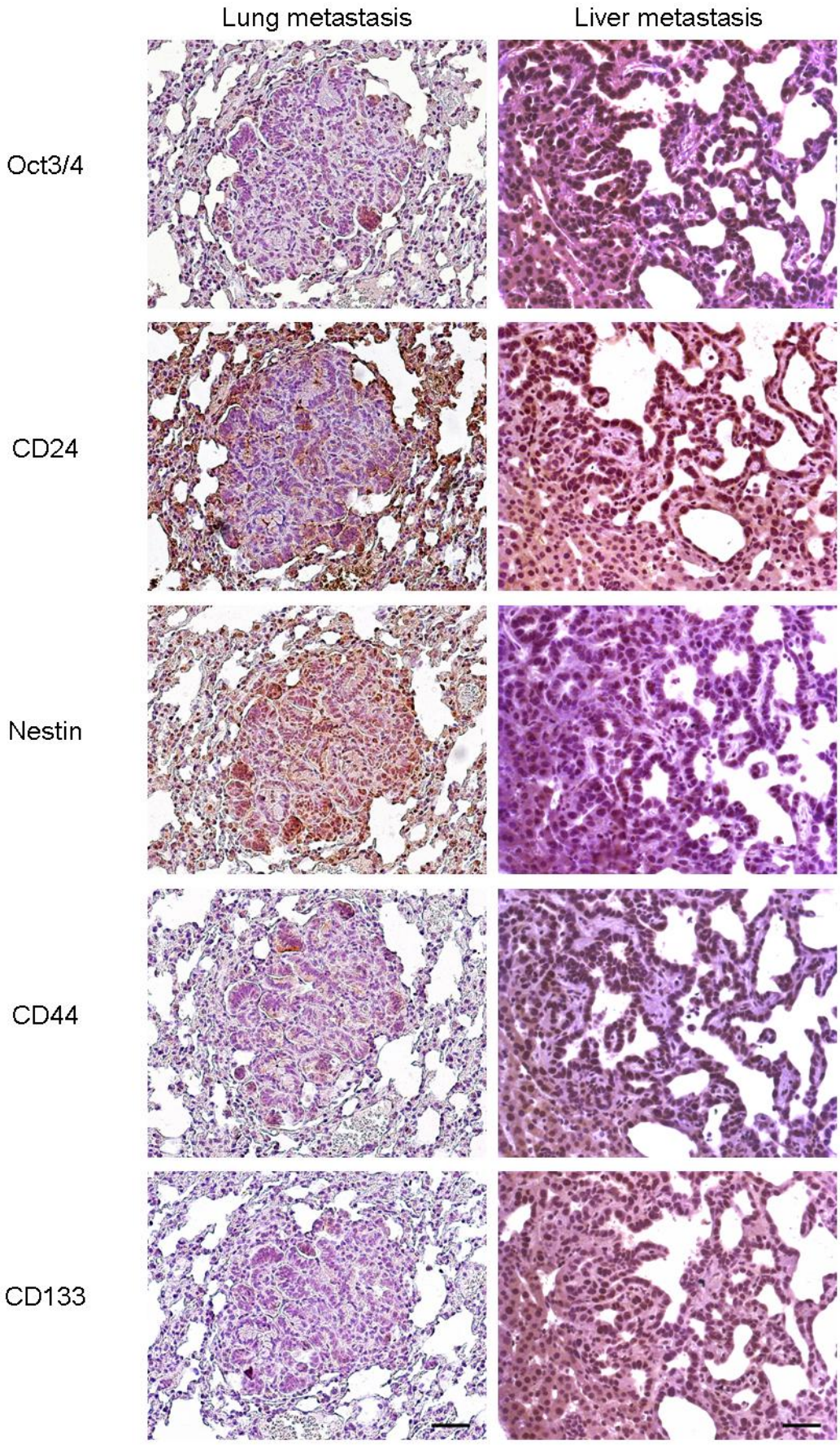

Figure 4-28 Stem cell markers in metastases of lung and liver of endogenously developed tumours
Sections are depicted according to the sequence they were cut. Immunohistochemistry was performed and brown staining reflects the expression pattern of the indicated markers. In lung metastases (mouse number 53646) mostly cell cohorts are stained whereas in liver metastases (mouse number 53631) all ducts express the markers. Bars represent 50 µm.

Table 4-8 None of the tested markers exhibits a uniform expression pattern in micrometastases of lung and liver in the endogenous and the implantation mouse model

	Oct3/4	CD24	CD44	CD133	Nestin
Endogenous Lung	+ Cell cohorts	+ Cell cohorts	+ Cell cohorts	+ Cell cohorts	+ Cell cohorts
	No staining	Weakly + All tumour cells	Weakly + Some tumour cells	No staining	No staining
Endogenous Liver	+ All tumour cells	+ All tumour cells	+ All tumour cells	+ All tumour cells	Weakly + 50% of tumour cells
	+ Many individual tumour cells/ cell cohorts	+ Some tumour cells	+ 50% of tumour cells	+ Many individual tumour cells/ cell cohorts	No staining
	No staining	No staining	No staining	No staining	No staining
Implantation Lung	Weakly + All tumour cells	++ All tumour cells	No staining	No staining	++ All tumour cells
	No staining	+ Approx. 30% of metastasis, Individual tumour cells	Weakly + All tumour cells	No staining	Weakly + 50% of tumour cells
	No staining	No staining	Weakly + Individual tumour cells	No staining	Weakly + 50% of undifferentiated cells
	No staining	No staining	Weakly + All tumour cells	No staining	No staining
Implantation Liver	No staining	++ All tumour cells	No staining	No staining	No staining
	No staining	No staining	+ Some tumour cells	Weakly + Some tumour cells	Weakly + Individual tumour cells

	Oct3/4	CD24	CD44	CD133	Nestin
	Weakly + Some tumour cells	No staining	Weakly + Individual tumour cells	No staining	No staining

Each cell represents staining of one metastasized lung or liver, respectively, in a distinct mouse.

In order to possibly identify cells with concurrent expression of more than one marker in the same cells I stained serial sections of micrometastases. In Figure 4-28 the expression pattern of all five markers in one series of sections for both liver and lung of the endogenous mouse model is depicted. Looking at one marker at a time lung sections display an expression pattern that would be expected for stem cells: only some cell cohorts express the respective marker. However, while all markers are expressed the cell cohorts expressing the markers differ evidently between the different serial sections.

On the contrary, in the micrometastasis of the liver all tumour cells are relatively uniformly stained for the markers. In Figure 4-27 the equivalent is illustrated for micrometastases of mice of the implantation model. In the micrometastasis of the lung only CD24 and Nestin are epressed strongly in the whole metastasis. Oct3/4 shows merely weak expression whereas CD44 and CD133 are not expressed at all. In the metastasis of the liver only CD24 is expressed, again in all tumour cells.

To get a better understanding of these expression patterns I repeated the stainings in a total of six micrometastases for each tissue. Results are presented in Table 4-8.

None of the markers shows a uniform expression pattern in all metastases. Surprisingly, it not only differs between expression status "expressed" and "not expressed", but also in the expression pattern. All markers vary between expression in individual cells, some tumour cells, all tumour cells and no expression. This indicates that the chosen markers are not representative of a possible stem cell compartment.

To underline these results, I checked the expression of these markers in the data of the microarray analyses. CD133, CD44 and Oct3/4 were not detected in any contrast. Nestin was down-regulated in metastases compared to non-metastasized primary tumours in the analysis of primary samples. Surprisingly, CD24 was up-regulated approximately five-fold in metastases compared to non-metastasized primary tumours in the same analysis. However, these results could not be confirmed in microarray analysis of isolated cells.

5 Discussion

5.1. Establishment of the *LSL-R26$^{Tva\text{-}lacZ/+}$* mouse strain for cancer research

Research on cancer biology has been facilitated enormously by retroviral gene transfer systems. Especially the site- and time-specific somatic gene transfer using the avian sarcoma-leukosis retrovirus RCASBP(A) has been shown to be a powerful tool to analyze gene function *in vivo*. It binds the avian TVA receptor and allows the retrovirus to integrate into the host genome. So far it has been necessary to generate a new mouse model with expression of the TVA receptor under control of the desired promoter to transduce mammalian cells.

To date a number of mouse models are available in which genes of interest are conditionally expressible due to a stop cassette flanked by loxP sites preceding the gene of interest which can be excised by the Cre recombinase. In addition, a number of mice expressing this Cre recombinase under different tissue specific promoters are available enabling the expression of the target gene specifically in many tissues (Feil, 2007). To take advantage of these existing mouse models and to combine them with the TVA-RCASBP(A) system and therefore to make headway in simplifying cancer research a novel mouse model has been generated in our lab. The *LSL-R26$^{Tva\text{-}lacZ/+}$* mouse strain can be coupled to other mice employing the Cre/lox system and allows Cre-inducible TVA expression and RCASBP(A)-mediated gene transfer in a wide range of different tissue types and cell populations. By means of this strategy the major limitations of existing mouse lines that use tissue-specific promoters for transgenic TVA expression (Du et al., 2007; Du et al., 2006; Dunn et al., 2000; Federspiel et al., 1994; Holland et al., 1998; Lewis et al., 2003; Orsulic et al., 2002) and the need for generation of a high number of new mouse lines can be overcome. In this thesis I set out to characterize and establish this mouse model for cancer research.

I report that functional TVA expression in this model is restricted to the tissues expressing Cre recombinase as demonstrated by quantitative RT-PCR analysis (Figure 4-1), nuclear LacZ staining (Figures 4-2, 4-3 and 4-5) and immunohistochemistry of TVA (Figure 4-4). This includes expression of TVA in the primary tumour and the corresponding metastases of a mouse model of pancreatic cancer (Figure 4-5). Furthermore, I prove that TVA expression renders proliferating

neoplastic cells susceptible to RCASBP(A) virus infection *in vivo* (Figure 4-6). In case of transduction with oncogenes or RNAi containing tumour suppressors presumably oligoclonal tumours would arise from cells independently infected with a single virus. This would be in line with the study of Du and colleagues demonstrating that RCASBP(A)-PyMT induced oligoclonal mammary tumours (Du et al., 2006). On the other hand it is also possible that one cell is transduced with multiple viruses integrating into different sites of the host genome leading to a monoclonal tumour. By proving that transduction with RCASBP(A) viruses is possible in our novel mouse model I establish this mouse model as capable of modelling cancer as has been confirmed to be achievable in previous studies using the TVA system (Du et al., 2006; Holland et al., 1998; Lewis et al., 2003; Orsulic et al., 2002). Particularly, this has been verified in our group using RCASBP(A)-Kras^{G12D} for tumour induction and RCASBP(A)-shTP53 for down-regulation of p53 in pancreatic tumours (Seidler et al., 2008). The observed spatiotemporal gene transfer and knockdown makes the system remarkably useful to model carcinogenesis and investigate the role of oncogenes and tumour suppressor genes for tumour initiation, progression and metastasis as has also been recommended by other groups (Du et al., 2006; Orsulic, 2002; Pao et al., 2003).

Furthermore, our model mimics human carcinogenesis accurately. It is widely accepted that sequential accumulation of mutations in oncogenes and tumour suppressors in single somatic cells lead to tumour formation in humans (Fearon and Vogelstein, 1990). Transduction of oncogenes or silencing tumour suppressors via the TVA- RCASBP(A) system also hits only a limited number of somatic cells in an intact microenvironment. This is a major advantage over knock-in or knock-out models where the whole tissue bears the mutations and a functionally intact interaction with the surrounding cells might be interrupted. To recapitulate the multistep process of human carcinogenesis even more closely the *LSL-R26*$^{Tva\text{-}lacZ/+}$ mouse strain can be used to introduce cooperating oncogenes or tumour suppressors sequentially or simultaneously. Orsulic et al. have reported that the delivery of target genes into the same somatic cells of a single mouse is feasible (Orsulic et al., 2002).

RCASBP(A)-mediated gene transfer allows for delivery of cDNA, regulatory RNA, shRNA, or miRNA of up to 2.5 kb *in vivo*. Sequences beyond that limit can not be packaged efficiently into the virus. Nonetheless they can still be transduced via the

TVA receptor. To this end other retroviruses such as lentiviral vectors can be pseudotyped with envA which is needed for interaction with TVA and entrance into the cell. This strategy has successfully been used for *in vitro* delivery of expression cassettes beyond 2.5 kb into TVA positive cells (Lewis et al., 2001).

Taken together, our novel mouse model opens up many possibilities for analysis of gene function in a time-controlled and tissue-specific fashion *in vivo*. Coupling to existing knock-in and knock-out mouse strains using the Cre/loxP system expands the applications of the TVA-RCAS system to a large extent. It enables the analysis of collaborating target genes in defined tissues and malignancies without the need to generate specific mouse lines for every gene of interest.

5.2. Metastasis of pancreatic cancer

5.2.1 Insights into the mechanism

Global gene expression profiling provides new prospects to address important questions, such as the mechanisms behind the process of cancer progression. Metastatic progression correlates with the deregulation of certain genes in the primary tumour. For certain types of cancer it has been shown that gene expression analyses allow discrimination between tumours with a good prognosis and those with a poor prognosis (Beer et al., 2002; Berchuck et al., 2005; Huang et al., 2003; Paik et al., 2004; Pittman et al., 2004; Potti et al., 2006; Ramaswamy et al., 2003; Shipp et al., 2002; Singh et al., 2002; van 't Veer et al., 2002; van de Vijver et al., 2002; West et al., 2001). So far, several groups have already performed analyses on pancreatic cancer expression profiles (Crnogorac-Jurcevic et al., 2002; Jones et al., 2008). However, these studies did not focus on pancreatic cancer metastasis but on initiation and progression. Beyond that two studies aimed at identifying genes linked to the metastatic process (Missiaglia et al., 2004; Nakamura et al., 2004) and found differentially expressed genes with a possible role in metastasis. Nonetheless, to date an integrative and comprehensive overview on metastasis of pancreatic cancer and the underlying mechanism is still missing. To this end, I set out to characterize and elucidate pancreatic cancer metastasis.

First, although it has been confirmed that the prominent features in the gene expression patterns of cell lines still reflect the molecular signature of the tissue from which the cells originated (Ross et al., 2000) the presented data proves that direct

comparisons between two different experimental setups such as microarrays on tissue sections and cell lines are not recommendable. The different methods exhibit differences that obscure the actual biological outcome. Furthermore, in this study analysis of gene expression profiles deduced from tissue sections alone revealed a list of genes and gene sets resulting from organ-specific background. To avoid this bias it is advisable to perform tissue specific arrays from the particular organs so that the respective genes can be subtracted from data analysis. To avoid this bias in my thesis, I focused on genes overlapping between analyses on the two different setups. Therefore, I could deduce significant conclusions for the models described in Figure 1-3. The data gathered for primary and cell line samples contradict the model in which metastatic potential can be predicted based on a poor-prognosis versus good-prognosis gene signature. The respective contrasts did not yield any significant DEGs or gene sets. Especially concerning the contrasts for cell lines one might argue that possibly this comparison lacks statistical power as the groups consist of only a few samples. However, this does not hold true for the contrast on primary samples which compares 11 to 21 samples. This indicates that there is no primary tumour signature on which basis metastatic status can be predicted. Moreover, the metastatic behaviour of the primary tumour cell lines implanted into nude mice did not accurately reflect the metastatic behaviour of the tumour they originated from. This supports the hypothesis that primary tumours cannot be grouped into the categories good and poor prognosis for pancreatic cancer.

According to the popular stem cell model for tumorigenesis dissemination is driven by cancer stem cells which are the only capable cells of reconstituting colonies at distant sites (see model d in Figure 1-3). Considering that cancer stem cells compose a minor fraction of tumours and corresponding metastases, no significant difference in gene expression should be detected. The high amount of variance observed between primary tumours and metastases disprove this hypothesis for pancreatic cancer. Arguing that in metastases the fraction of stem cells is high enough to justify such a difference in gene expression, the markers for stem cells should be easy to detect in such gene expression profiles. However, neither CD133 nor CD44, Nestin nor Oct3/4 could be detected in any contrast. This contrasts the results of various groups (Hermann et al., 2007; Li et al., 2007a; Maeda et al., 2008; Wang et al., 2009) who claim to have identified the first two as pancreatic stem cell markers. On the other hand, CD24 was the only marker that was up-regulated approximately five-fold in

metastases compared to primary tumours in primary samples. Still, the immunohistochemical stainings of micrometastases did not validate this marker as a stem cell marker. Expression was not consistent in all micrometastases. It rather exhibits a heterogenous expression pattern as in some metastases it was expressed in all ductal structures whereas in others it was not expressed at all or only in a fraction of cells. Thus, CD24 might play an important role in metastasis of pancreatic cancer, but whether it does account for stemness is still in question particularly because only one marker might hardly reflect that. Besides, the circulating tumour cells should clearly differ from all other samples, considering that they should comprise a high amount of cancer stem cells. As this does not correspond to the results gained from gene expression profiling of the tumour cells isolated from the circulation this does not provide evidence for the cancer stem cell theory. Yet, this could also be attributed to the small group size of samples or to cell culture artefacts due to changes in gene expression owing to the shift of contact free survival towards attachment to the cell culture dish in monolayer cultures.

Above all, the data support the early dissemination model. In this model dissemination occurs independently from tumour cells at the primary site. Therefore the expression profile of primary tumours and metastasis are different. This is conform with the metastasized primary tumours being indistinguishable from non-metastasized tumours and with metastases being different from primary tumours. This opens the question why the metastasized primary tumours can not be discriminated from their metastases. In the case of breast cancer Vecchi et al. argue that even though the primary tumours exhibit a gene signature predictive of metastasis the primary tumours are molecularly distinct from their metastases because they still progress on a molecular level (Vecchi et al., 2008). This might be conferrable to the primary tumours in this study. Cells with the potential to disseminate very early from the primary tumour might also have growth advantages over the primary tumour mass and might therefore expand to an extent that the primary tumour "matures" into an intermediate state between non-metastasizing tumours and metastases. Thus, the difference between these groups might not be measurable at a significant level. This could represent a deviant version of the 'clonal dominance' theory of metastasis which proposes that once metastatic subclones emerge within a primary tumour, the progeny of these subclones overgrow and dominate the tumour mass itself (Kerbel et al., 1988; Kerbel et al., 1987). Also,

findings of Schmidt-Kettler et al. and Hüsemann et al. who have revealed strong evidence in the direct analysis of disseminated cancer cells support the model that dissemination is a very early event in the genetic development of human breast cancer (Husemann et al., 2008; Schmidt-Kittler et al., 2003). In line with this Hezel et al. argue that often within an individual tumour, there is heterogeneity in histology, tumour grade, and degree of differentiation so that even the smallest primary lesions commonly exhibit perineural and lympho-vascular invasion. This would even enable cells of very early lesions to spread to distant sites (Hezel et al., 2006).

Furthermore, the hypothesis of early dissemination accompanied by molecular progression of the progeny of metastatic subclones in the primary tumour in pancreatic cancer matches the insignificance of tumour size for metastasis which I determined. This is substantiated by Weiss et al. who showed that large or small tumours showed no difference in their metastatic potential in mice, indicating that there is no apparent relationship between metastatic potential and tumour size (Weiss et al., 1983). Taking into account the similarity of survival time of metastatic and non-metastatic tumour mice, the primary tumour does not seem to need to grow extended time periods in order to become malignant. This indicates that proliferation time and speed are not crucial for development of metastasis.

Moreover, it agrees with the dissemination behaviour of the cell lines isolated from the tumours: I observed that primary tumour cells were unpredictable in their metastatic behaviour. On the other hand, nearly all cells isolated from metastases did metastasize again after functional in vivo validation.

Surprisingly, cells containing the gain of function mutation *TP53*$^{R172H/+}$ displayed very heterogeneous behaviour with regard to their original metastatic status and the matched *in vivo* validation. For this genotype the 'dynamic heterogeneity' model may hold true. This proposes that metastatic subpopulations are generated at high rates in a primary tumour, but that these variants are relatively unstable, resulting in a dynamic equilibrium between generation and loss of metastatic variants (Hill et al., 1984; Ling et al., 1985). An alternative feature of cell lines with the *Ptf1a/p48*$^{Cre/+}$/ *LSL-Kras*^{G12D}/*LSL-TP53*$^{R172H/+}$ genotype influencing metastatic behaviour could be the greater chromosomal instability compared to *Ptf1a/p48*$^{Cre/+}$/*LSL-Kras*^{G12D} cells isolated of pancreatic cancer. Carter and colleagues have developed an expression signature that reflects chromosomal instability in multiple human cancers (Carter et al., 2006). However, the signature was found to be elevated in metastatic specimens

compared with primary tumours, providing a means to measure the role of chromosomal instability in determining malignant potential. This is in conflict with my assessment of metastasized compared to non-metastasized tumour cells with only five significantly differentially expressed genes between the two groups. Therefore, I conclude that the 'dynamic heterogeneity' model is more probable.

Although I exclude the model of a gene signature distinguishing benign primary tumours from malignant ones and considering that metastasis likely occurs early in pancreatic cancer progression the question of organ-specificity of metastasis (model b in Figure 1-3) remains unanswered. Amongst other studies, for breast cancer organ-specific signatures for cells disseminating to the lung have been established (Minn et al., 2005a). In analogy to Missiaglia et al. (Missiaglia et al., 2004) I compared cells isolated from metastases of lung, liver and lymph nodes. Of note, I assured that only cells with low passage numbers were analyzed so that the cell culture artefacts that are common in conventional cell lines could be attenuated. Interestingly, I found hardly any difference between liver and lung metastasis cells. On the contrary, I found around 30 differentially expressed genes (but no enriched gene sets) for both contrasts against lymph nodes. This result may be attributed to the different routes of dissemination that are taken by tumour cells invading the lymphatic system opposed to the bloodstream. Access to the lymph might require the activity of other genes than dissemination to liver and lung. However, this could not be verified in the functional assessment of the metastatic characteristics of cell lines. Here, I established that cells isolated from a specific metastatic site did not metastasize exclusively to the same distant organ after orthotopic implantation. In fact no organ specificity could be detected for any cell line. Moreover, there was no apparent distinction between metastasis via the lymphatic system and the bloodstream. Thus, it remains disputable whether the difference in gene expression between metastasis cells from lymph nodes and liver or lung refers to the different route of metastasis.

In conclusion, the data did not support the theory that primary tumours developing metastases show different expression levels compared to non-metastasising primary tumours. The huge difference in expression levels that was observed comparing primary tumours to metastases renders the model of cancer stem cells mediating the progress of metastatic disease implausible. To this end the data most likely support

the model of early dissemination, stating that metastases develop independently from primary tumours.

Still, it is probable that multiple pathways and multiple routes exist by which transformed pancreatic cancer cells may disseminate and arrive at an apparently common phenotype.

5.2.2 Differentially expressed genes and gene sets

In addition to providing overall insight into the underlying general mechanism of pancreatic cancer metastasis, I discovered various interesting target genes that might elucidate the molecular processes essential for progression and dissemination of PDAC.

The collection of gene sets from the Molecular Signatures Database analyzed in this study stem from a large expression meta-study (Segal et al., 2004).

Generally, the gene sets mostly expose the importance of up-regulation of pathways and molecular processes associated with cell division and M phase, cell cycle expression clusters, DNA damage response, nucleotide metabolism and signal transduction in metastasis samples.

However, there are some gene sets that are closer related to the metastatic process itself. For instance the expression neighbourhood of *HMMR* is highly up-regulated in metastases. Antibodies directed against HMMR have been shown to block locomotion of cells induced by expression of a mutant H-ras (Hardwick et al., 1992).

An additional gene set related to movement also up-regulated in metastases is a set of genes annotated by the GO term "GO:0006974". These genes denote a change in state or activity of a cell or an organism – amongst others in terms of movement – as a result of a stimulus indicating damage to its DNA from environmental insults or errors during metabolism. These two gene sets might designate attractive targets for inhibition of metastasis.

Pro-proliferative stimuli and resistance to apoptosis may be conferred to metastases by down-regulation of the expression neighbourhood of *EI24*, a gene directly regulated by p53 which suppresses cell growth and induces cell death (Gu et al., 2000). Surprisingly, expression neighbourhood of *CTBP1*, which appears to modulate transformation, tumorigenesis, and metastasis negatively (Chen et al., 2008; Winklmeier et al., 2009), was down-regulated in metastases compared to primary tumours. This might indicate that once the disseminated cells reach the

distant organ and assemble colonies expression of these genes is no longer needed but rather genes that help the establishment of the metastasis in an alien microenvironment.

A third and very intriguing group of gene sets up-regulated in metastases compared to primary tumours comprise clusters of genes associated with poor survival and chemoresistance. This group includes first a set of genes which are up-regulated in gastric cancer cell lines resistant to doxorubicin compared to parent chemosensitive cell lines, second genes highly expressed in hepatocellular carcinoma with poor survival and third genes highly associated with medulloblastoma treatment failure. Knowledge of the up-regulation of these gene sets once they are confirmed in patient samples might enable an improved treatment and its management reducing the amount of futile therapies and therefore increasing quality of life for patients.

Finally, a vast range of genes with assigned promoter regions containing specific motifs is down-regulated in metastases. These motifs partly match known transcription factors such as c-fos serum response element-binding transcription factor, sterol regulatory element binding transcription factor 1, activating enhancer binding protein 4, heat shock transcription factor 2, neurofibromin 1, interferon regulatory factor 1 and 2 and GATA binding protein 3. Several other motifs could not be assigned to any known transcription factor. Investigation on all of them will be very informative and helpful in dissecting the metastatic process.

In addition to the acknowledged gene sets I also identified some remarkable single genes deregulated in pancreatic cancer metastasis.

In the contrast of metastasized primary tumour cells versus metastasis cells I discovered the transcription factor *Odd-skipped related 2*, which so far has been associated with development of the palate, the limb and kidney (Lan et al., 2001; Lan et al., 2004). As in cancer progression often developmental signalling pathways are switched on again and mediate tumour progression, including local invasion, spread through the circulation and, devastatingly, metastasis, this might be an interesting target to investigate further.

Another interesting DEG includes *Cadherin 4*, a calcium-dependent cell-cell adhesion molecule important in cell-cell interaction. Considering the role of the related E-cadherin – also a member of the cadherin family of cell surface glycoproteins – this might have implications for epithelial-mesenchymal-transition (EMT), which for instance plays a role in the process of metastasis in breast cancer (Kang and

Massague, 2004). Along these lines up-regulation of Twist homolog 2 in the circulating tumour cells is equally intriguing, as Twist is known to regulate EMT. However, EMT could not be confirmed in terms of morphologic phenotype of cells. Nearly all tumour cells isolated from primary tumours and their corresponding circulating tumour cells as well as metastasis cells displayed the same morphology. Still, the morphologic exhibition of EMT might only be transient and therefore not detectable in cell culture, or the molecular processes might influence metastasis but not be efficient enough to change the morphology of cells to a comprehensive EMT phenotype. *Four jointed box 1* is a second gene up-regulated in circulating tumour cells. It is a target of Notch which plays an important role in pancreatic cancer initiation (Mullendore et al., 2009; Nakhai et al., 2008).

Surprisingly, I could only identify very few genes to be differentially expressed for the duration of survival in the circulation. This could be an artefact obtained during cell culture or just as the metastasized primary tumour cell lines, the circulating tumour cells might represent an intermediate state that differs significantly neither from the primary tumour nor from the resulting metastases.

5.2.3 Outlook

Prevention of cancer metastasis is thought to provide the key to cancer treatment and therefore is one important goal in drug development. In my thesis, I report that primary tumour formation and metastasis are processes that probably follow a distinct route from very early on in tumorigenesis.

To develop the right therapeutic approach it will be necessary to extend the knowledge on the mechanisms by which the identified genes have been altered. To this end, it will be indispensable to assess whether decreased expression of gene neighbourhoods are due to loss of chromosomal fragments or methylation. Up-regulation might be due to amplification of DNA sequences or enhanced expression.

Further validation of the herein identified genes, gene sets and possibly signatures for the route of metastasis in patient samples will make use of independent samples that reflect the phenotype of interest but were not used in the initial identification.

The comparison of my results to the data obtained in different investigations will not be straightforward, as different microarray platforms or different methodology as well as mathematical algorithms will have been used. However, it has been shown that

different approaches might reveal different gene sets, but are actually reporting the same biological processes (Tan et al., 2003).

It might also be rewarding to expand the research on the analyzed samples even further. Recently it has become clear that the expression of microRNAs (miRNAs) can be used to identify cancer-relevant signatures (He et al., 2005; Iorio et al., 2005; Lu et al., 2005; Volinia et al., 2006; Yanaihara et al., 2006). This method is currently being optimized in our lab.

Moreover, our understanding of the metastatic process can also be broadened by using integrated genome comparison, which is a combination of comparative genomic hybridisation (CGH) arrays and microarrays. This methodology correlates genomic alterations with transcript levels. As published on a conference on invasion and metastasis this has yielded insights exceeding those gained by either method alone, and has produced a 'metastatic determinant signature' (Tapon and Ziebold, 2008).

Finally, having identified the key collaborating target genes for metastasis in pancreatic cancer, functional validation and investigation on them will be enabled and fascilitated by our newly developed mouse model.

6 Summary

Pancreatic ductal adenocarcinoma (PDAC) is the 4th most common cause for cancer associated death and has a poor 5-year survival rate below 5%. One major problem in treating the disease is its early metastatic dissemination. However, the genes involved in metastasis of PDAC remain mostly unknown.

To identify metastasis genes and to analyze the molecular mechanism of the metastatic process, we investigated gene expression profiles of primary tumours and their corresponding metastases in genetically engineered oncogenic *Kras*^{G12D} based mouse models of pancreatic ductal adenocarcinoma, which accurately recapitulate the human disease. We compared gene expression profiles of non-metastasized and metastasized primary tumours and their metastases in liver, lung and lymph nodes. Furthermore, to enhance understanding of the metastatic process I isolated tumour cells from primary tumours, disseminated tumour cells and metastases and tested their metastatic capacity via an orthotopic transplantation model *in vivo*. These isolated tumour cells were also analyzed in regard to their gene expression profiles using microarray analysis.

Intriguingly, we identified a high number of genes and gene sets significantly up- or down-regulated in metastases compared to primary tumours. Thus metastases display a distinct transcription profile in comparison to their corresponding primary tumours. In contrast, the expression profile of non-metastasized primary tumours did not differ from metastasized primary tumours indicating that gene-expression profiling of primary pancreatic tumours cannot predict metastasis risk.

Cells isolated from primary tumours did not reflect the metastatic capacity of their original primary tumour whereas cells isolated from metastases did so. Analysis of organ-speficity revealed that even though metastasis was not organ-specific there might be a signature for metastasis via the lymphatic system opposed to metastasis via the bloodstream.

In conclusion, I suggest that metastasis does not occur as progression from a premetastatic to a metastatic state of the primary tumour. Instead, my results support the model that metastatic cells arise from a small subset of rare, variant tumour cells that disseminate early during tumorigenesis.

To verify the relevance of these data and to functionally characterize the candidate genes in an endogenous genetically defined mouse model a knock-in mouse line termed *LSL-R26*$^{Tva\text{-}lacZ}$ with conditional expression of TVA has been generated in our

laboratory. TVA is a receptor for the avian sarcoma-leucosis retrovirus RCAS which transduces exclusively mammalian cells genetically engineered to express the avian retroviral receptor. In my thesis, I set out to characterize and establish this novel mouse model as a tool to functionally validate the identified genes relevant for metastasis in pancreatic cancer. TVA mediated infection of genetically engineered mice with endogenous expression of $Kras^{G12D}$ in pancreatic cancer cells using RCAS virus carrying the reporter gene EGFP proved that conditional expression of TVA enables spatio-temporal gene expression and knock-down in a small subset of somatic cells *in vivo*. This enables selective manipulation and investigation of candidate genes and the relevant signal transduction pathways in pancreatic cancer metastasis. Combined with the growing number of Cre expression models, RCAS-TVA based gene expression and knock-down systems open up promising perspectives for analysis of gene function in a time-controlled and tissue-specific fashion *in vivo*.

7 Appendix I: Mice

Mouse ID	Genotype	Survival time (days)	Tumour size (cm^3)	Histology	Validation of histology	Metastatic status					
						Liver		Lung		Lymph node	
						Macro-scopic	Microscopic	Macroscopic	Microscopic	Macroscopic	Microscopic
110	*Ptf1a/p48$^{Cre/+}$/ LSL-Kras^{G12D}*	590	6.6	cystic	IHC CK19	negative	negative	negative	negative	negative	negative
434	*Ptf1a/p48$^{Cre/+}$/ LSL-Kras^{G12D}/ LSL-TP53$^{R172H/+}$*	129	unknown	unknown	n.a.	negative	negative	negative	negative	negative	negative
1048	*Ptf1a/p48$^{Cre/+}$/ LSL-Kras^{G12D}/ LSL-TP53$^{R172H/+}$*	124	1.25	Ductal/ cystic	IHC CK19	negative	negative	negative	negative	negative	negative
1054	*Ptf1a/p48$^{Cre/+}$/ LSL-Kras^{G12D}/ LSL-TP53$^{R172H/+}$*	114	0.045	cystic	n.a.	negative	negative	negative	negative	negative	negative
1194	*Ptf1a/p48$^{Cre/+}$/ LSL-Kras^{G12D}/ LSL-TP53$^{R172H/+}$*	86	0.108	intermedi-ate	n.a.	negative	negative	negative	negative	negative	positive
1419	*Ptf1a/p48$^{Cre/+}$/ LSL-Kras^{G12D}/ LSL-TP53$^{R172H/+}$*	104	1.5	ductal	n.a.	negative	unknown	postive		unknown	Unknown
3014	*Ptf1a/p48$^{Cre/+}$/ LSL-Kras^{G12D}/ LSL-TP53$^{R172H/+}$*	112	unknown	cystic	n.a.	Unknown (diaphragm positive)		unknown		positive	
3040	*Ptf1a/p48$^{Cre/+}$/ LSL-Kras^{G12D}/ LSL-TP53$^{R172H/+}$*	118	unknown	unknown	n.a.	negative	unknown	negative	unknown	negative	unknown
3086	*Ptf1a/p48$^{Cre/+}$/ LSL-Kras^{G12D}/ LSL-TP53$^{R172H/+}$*	128	unknown	unknown	n.a.	negative	unknown	negative	unknown	negative	unknown

Mouse ID	Genotype	Survival time (days)	Tumour size (cm^3)	Histology	Validation of histology	Metastatic status					
						Liver		Lung		Lymph node	
						Macro-scopic	Microscopic	Macroscopic	Microscopic	Macroscopic	Microscopic
3107	*Ptf1a/p48$^{Cre/+}$/ LSL-Kras^{G12D}/ LSL-TP53$^{R172H/+}$*	65	4	unknown	n.a.	negative	negative	negative	negative	positive	
3108	*Ptf1a/p48$^{Cre/+}$/ LSL-Kras^{G12D}/ LSL-TP53$^{R172H/+}$*	65	unknown	dedifferen-tiated	IHC CK19	negative	negative	negative	negative	negative	negative
3139	*Ptf1a/p48$^{Cre/+}$/ LSL-Kras^{G12D}/ LSL-TP53$^{R172H/+}$*	157	1.701	ductal	n.a.	negative	unknown	negative	unknown	positive	
3150	*Ptf1a/p48$^{Cre/+}$/ LSL-Kras^{G12D}/ LSL-TP53$^{R172H/+}$*	83	unknown	unknown	IHC CK19	negative	negative	negative	negative	negative	positive
3251	*Ptf1a/p48$^{Cre/+}$/ LSL-Kras^{G12D}/ LSL-TP53$^{R172H/+}$*	67	unknown	unknown	n.a.	negative	unknown	negative	unknown	negative	unknown
3256	*PDX$^{Cre/+}$/ LSL-Kras^{G12D}/ LSL-TP53$^{R172H/+}$*	182	2.2	ductal	IHC CK19	negative	negative	negative	negative	negative	negative
5123	*Ptf1a/p48$^{Cre/+}$/ LSL-Kras^{G12D}*	356	3.136	intermedi-ate	n.a.	positive		positive		unknown	
5320	*Ptf1a/p48$^{Cre/+}$/ LSL-Kras^{G12D}*	466	4.5	dedifferen-tiated	n.a.	positive		positive		unknown	
5436	*Ptf1a/p48$^{Cre/+}$/ LSL-Kras^{G12D}/ LSL-TP53$^{R172H/+}$*	44	unknown	cystic	n.a.	negative	negative	negative	negative	negative	negative
5486	*Ptf1a/p48$^{Cre/+}$/ LSL-Kras^{G12D}/ LSL-TP53$^{R172H/+}$*	117	3.375	cystic	n.a.	negative	unknown	negative	positive	negative	positive

Mouse ID	Genotype	Survival time (days)	Tumour size (cm^3)	Histology	Validation of histology	Metastatic status					
						Liver		Lung		Lymph node	
						Macro-scopic	Microscopic	Macroscopic	Microscopic	Macroscopic	Microscopic
5671	*Ptf1a/p48$^{Cre/+}$/ LSL-Kras^{G12D}*	280	unknown	unknown	n.a.	negative	unknown	negative	unknown	negative	unknown
5748	*Ptf1a/p48$^{Cre/+}$/ LSL-Kras^{G12D}*	262	4.2	ductal	IHC CK19	negative	negative	negative	negative	negative	negative
5836	*Ptf1a/p48$^{Cre/+}$/ LSL-Kras^{G12D}/ LSL-TP53$^{R172H/+}$*	120	unknown	unknown	n.a.	negative	unknown	negative	unknown	negative	unknown
6021	*Ptf1a/p48$^{Cre/+}$/ LSL-Kras^{G12D}/ LSL-TP53$^{R172H/+}$*	136	unknown	unknown	IHC CK19	negative	negative	negative	negative	negative	negative
6034	*PDX$^{Cre/+}$/ LSL-Kras^{G12D}/ LSL-TP53$^{R172H/+}$*	323	4.62	ductal	n.a.	positive		positive		unknown	unknown
6051	*PDX$^{Cre/+}$/ LSL-Kras^{G12D}/ LSL-TP53$^{R172H/+}$*	339	3.51	intermedi-ate	n.a.	negative	unknown	positive		negative	unknown
6410	*Ptf1a/p48$^{Cre/+}$/ LSL-Kras^{G12D}/ LSL-TP53$^{R172H/+}$*	116	1.54	ductal	n.a.	positive		negative	unknown	negative	unknown
7801	*Ptf1a/p48$^{Cre/+}$/ LSL-Kras^{G12D}*	728	0.272	cystic	n.a.	negative	positive	negative	unknown	negative	unknown
12591	*Ptf1a/p48$^{Cre/+}$/ LSL-Kras^{G12D}*	493	1.944	cystic	n.a.	positive		positive		negative	unknown
15272	*Ptf1a/p48$^{Cre/+}$/ LSL-Kras^{G12D}*	417	4.95	cystic	n.a.	positive		positive		negative	unknown

Mouse ID	Genotype	Survival time (days)	Tumour size (cm^3)	Histology	Validation of histology	Metastatic status					
						Liver		Lung		Lymph node	
						Macro-scopic	Microscopic	Macroscopic	Microscopic	Macroscopic	Microscopic
16990	*Ptf1a/p48$^{Cre/+}$/ LSL-Kras^{G12D}*	377	0.084	cystic	IHC CK19	negative	negative	negative	negative	negative	negative
17728	*Ptf1a/p48$^{Cre/+}$/ LSL-Kras^{G12D}*	531	1.47	cystic	IHC CK19	negative	positive	negative	negative	negative	negative
18905	*Ptf1a/p48$^{Cre/+}$/ LSL-Kras^{G12D}/ LSL-TP53$^{R172H/+}$*	555	unknown	unknown	n.a.	negative	unknown	negative	unknown	negative	unknown
19073	*Ptf1a/p48$^{Cre/+}$/ LSL-Kras^{G12D}*	372	0.575	cystic	IHC CK19	negative	negative	negative	negative	negative	negative
51942	*Ptf1a/p48$^{Cre/+}$/ LSL-Kras^{G12D}*	318	9	cystic	IHC CK19	negative	negative	negative	negative	negative	positive
53266	*Ptf1a/p48$^{Cre/+}$/ LSL-Kras^{G12D}*	632	4.464	cystic	IHC CK19	negative	positive	negative	unknown	negative	unknown
53268	*Ptf1a/p48$^{Cre/+}$/ LSL-Kras^{G12D}*	619	3.6	dedifferen-tiated	n.a.	positive		positive		negative	unknown
53631	*Ptf1a/p48$^{Cre/+}$/ LSL-Kras^{G12D}*	478	unknown	cystic	n.a.	positive		positive		negative	unknown
53646	*Ptf1a/p48$^{Cre/+}$/ LSL-Kras^{G12D}*	505	3.388	cystic	n.a.	positive		negative	positive	negative	unknown
53704	*Ptf1a/p48$^{Cre/+}$/ LSL-Kras^{G12D}*	548	0.195	unknown	n.a.	positive		negative	unknown	negative	unknown
53909	*Ptf1a/p48$^{Cre/+}$/ LSL-Kras^{G12D}*	473	2	unknown	n.a.	positive		negative	unknown	negative	unknown
53913	*Ptf1a/p48$^{Cre/+}$/ LSL-Kras^{G12D}*	532	1.96	cystic	n.a.	negative	unknown	positive		negative	unknown

Mouse ID	Genotype	Survival time (days)	Tumour size (cm^3)	Histology	Validation of histology	Metastatic status					
						Liver		Lung		Lymph node	
						Macro-scopic	Microscopic	Macroscopic	Microscopic	Macroscopic	Microscopic
54050	*Ptf1a/p48$^{Cre/+}$/ LSL-Kras^{G12D}/ LSL-TP53$^{R172H/+}$*	128	unknown	unknown	n.a.	negative	unknown	negative	unknown	negative	unknown
54240	*PDX$^{Cre/+}$/ LSL-Kras^{G12D}*	421	8.97	cystic	IHC CK19	negative	negative	negative	negative	negative	negative
54394	*Ptf1a/p48$^{Cre/+}$/ LSL-Kras^{G12D}/ LSL-TP53$^{R172H/+}$*	49	unknown	Unknown	n.a.	negative	unknown	negative	unknown	negative	unknown
54716	*Ptf1a/p48$^{Cre/+}$/ LSL-Kras^{G12D}/ LSL-TP53$^{R172H/+}$*	72	unknown	Unknown	n.a.	negative	unknown	negative	unknown	negative	unknown

8 Appendix II: Cell lines

Cell line ID	Genotype	Phenotype	Source organ	Metastatized in endogenous mouse model (source)	Metastatisized after orthotopic implantation into mude mice	Kras WT Status
110 PPT	*Ptf1a/p48$^{Cre/+}$/ LSL-Kras^{G12D}*	Epithelial	Non-metastatic primary tumour	No	Lung	Unknown
434 PPT	*Ptf1a/p48$^{Cre/+}$/ LSL-Kras^{G12D}/ LSL-TP53$^{R172H/+}$*	Mesenchymal	Non-metastatic primary tumour	No	Lung, Lymph node	Positive
1048 PPT	*Ptf1a/p48$^{Cre/+}$/ LSL-Kras^{G12D}/ LSL-TP53$^{R172H/+}$*	Epithelial	Non-metastatic primary tumour	No	Lymph node	Unknown
1054 PPT	*Ptf1a/p48$^{Cre/+}$/ LSL-Kras^{G12D}/ LSL-TP53$^{R172H/+}$*	Unknown	Non-metastatic primary tumour	No	Lung	Unknown
1419 PPT	*Ptf1a/p48$^{Cre/+}$/ LSL-Kras^{G12D}/ LSL-TP53$^{R172H/+}$*	Both	Metastatic primary tumour	Yes	Not Implanted	Negative
3014 LK1	*Ptf1a/p48$^{Cre/+}$/ LSL-Kras^{G12D}/ LSL-TP53$^{R172H/+}$*	Epithelial	Lymph node metastasis	Yes	Lung	Negative
3014 LK2	*Ptf1a/p48$^{Cre/+}$/ LSL-Kras^{G12D}/ LSL-TP53$^{R172H/+}$*	Epithelial	Lymph node metastasis	Yes	Not Implanted	Positive
3014 LK3	*Ptf1a/p48$^{Cre/+}$/ LSL-Kras^{G12D}/ LSL-TP53$^{R172H/+}$*	Epithelial	Lymph node metastasis	Yes	Not Implanted	Negative
3014 LK4	*Ptf1a/p48$^{Cre/+}$/ LSL-Kras^{G12D}/ LSL-TP53$^{R172H/+}$*	Epithelial	Lymph node metastasis	Yes	Not Implanted	Negative

Cell line ID	Genotype	Phenotype	Source organ	Metastatized in endogenous mouse model (source)	Metastatisized after orthotopic implantation into mude mice	Kras WT Status
3014 LKS	*Ptf1a/p48$^{Cre/+}$/ LSL-Kras^{G12D}/ LSL-TP53$^{R172H/+}$*	Epithelial	Lymph node metastasis	Yes	Not Implanted	Positive
3107 LK	*Ptf1a/p48$^{Cre/+}$/ LSL-Kras^{G12D}/ LSL-TP53$^{R172H/+}$*	Epithelial	Lymph node metastasis	Yes	Unknown	Positive
3108 PPT	*Ptf1a/p48$^{Cre/+}$/ LSL-Kras^{G12D}/ LSL-TP53$^{R172H/+}$*	Both	Non-metastatic primary tumour	No	Lung	Unknown
3108 PPT K1	*Ptf1a/p48$^{Cre/+}$/ LSL-Kras^{G12D}/ LSL-TP53$^{R172H/+}$*	Epithelial	Non-metastatic primary tumour	No	Not Implanted	Positive
3108 PPT K4	*Ptf1a/p48$^{Cre/+}$/ LSL-Kras^{G12D}/ LSL-TP53$^{R172H/+}$*	Epithelial	Non-metastatic primary tumour	No	Lung	Positive
3108 PPT K5	*Ptf1a/p48$^{Cre/+}$/ LSL-Kras^{G12D}/ LSL-TP53$^{R172H/+}$*	Epithelial	Non-metastatic primary tumour	No	Lung	Positive
3108 PPT K7	*Ptf1a/p48$^{Cre/+}$/ LSL-Kras^{G12D}/ LSL-TP53$^{R172H/+}$*	Epithelial	Non-metastatic primary tumour	No	Unknown	Positive
3139 PPT	*Ptf1a/p48$^{Cre/+}$/ LSL-Kras^{G12D}/ LSL-TP53$^{R172H/+}$*	Epithelial	Metastatic primary tumour	Yes	No	Unknown
3139 LK ua Darn	*Ptf1a/p48$^{Cre/+}$/ LSL-Kras^{G12D}/ LSL-TP53$^{R172H/+}$*	Epithelial	Lymph node metastasis	Yes	Lung	Positive

Cell line ID	Genotype	Phenotype	Source organ	Metastatized in endogenous mouse model (source)	Metastatisized after orthotopic implan-tation into mude mice	Kras WT Status
3150 PPT	*Ptf1a/p48$^{Cre/+}$/ LSL-Kras^{G12D}/ LSL-TP53$^{R172H/+}$*	Unknown	Metastatic primary tumour	Yes	Lung, Lymph node	Positive
5123 PPT	*Ptf1a/p48$^{Cre/+}$/ LSL-Kras^{G12D}*	Mesenchymal	Metastatic primary tumour	Yes	No	Positive
5123 PPT II	*Ptf1a/p48$^{Cre/+}$/ LSL-Kras^{G12D}*	Mesenchymal	Metastatic primary tumour	Yes	Not Implanted	Positive
5123 Lebermet	*Ptf1a/p48$^{Cre/+}$/ LSL-Kras^{G12D}*	Epithelial	Liver metastasis	Yes	Liver, Lung, Lymph node	Positive
5123 VB	*Ptf1a/p48$^{Cre/+}$/ LSL-Kras^{G12D}*	Unknown	Circulation	Yes	Liver, Lung, Lymph node	Positive
5193 PPT	*Ptf1a/p48$^{Cre/+}$/ LSL-Kras^{G12D}/ LSL-TP53$^{R172H/+}$*	Unknown	Metastatic primary tumour	Yes	Not Implanted	Positive
5193 Aszites	*Ptf1a/p48$^{Cre/+}$/ LSL-Kras^{G12D}/ LSL-TP53$^{R172H/+}$*	Unknown	Ascites	Yes	Not Implanted	Negative
5288 PPT	*Ptf1a/p48$^{Cre/+}$/ LSL-Kras^{G12D+}*	Unknown	Metastatic primary tumour	Yes	Unknown	Positive
5288 Leb1	*Ptf1a/p48$^{Cre/+}$/ LSL-Kras^{G12D+}*	Unknown	Liver metastasis	Yes	Unknown	Positive
5288 Leb2	*Ptf1a/p48$^{Cre/+}$/ LSL-Kras^{G12D+}*	Unknown	Liver metastasis	Yes	Not Implanted	Positive
5288 Lunge3	*Ptf1a/p48$^{Cre/+}$/ LSL-Kras^{G12D+}*	Unknown	Lung metastasis	Yes	Unknown	Positive
5288 Lunge4	*Ptf1a/p48$^{Cre/+}$/ LSL-Kras^{G12D+}*	Unknown	Lung metastasis	Yes	Not Implanted	Positive

Cell line ID	Genotype	Phenotype	Source organ	Metastatized in endogenous mouse model (source)	Metastatisized after orthotopic implan-tation into mude mice	Kras WT Status
5320 Leb3	*Ptf1a/p48$^{Cre/+}$/ LSL-Kras^{G12D+}*	Mesenchymal	Liver metastasis	Yes	Not Implanted	Negative
5436 PPT	*Ptf1a/p48$^{Cre/+}$/ LSL-Kras^{G12D}/ LSL-TP53$^{R172H/+}$*	Epithelial	Non-metastatic primary tumour	No	Lung	Unknown
5486 PPT	*Ptf1a/p48$^{Cre/+}$/ LSL-Kras^{G12D}/ LSL-TP53$^{R172H/+}$*	Mesenchymal	Metastatic primary tumour	Yes	Lung	Positive
5486 LK mdst	*Ptf1a/p48$^{Cre/+}$/ LSL-Kras^{G12D}/ LSL-TP53$^{R172H/+}$*	Both	Lymph node me-tastasis	Yes	No	Negative
5486 VB	*Ptf1a/p48$^{Cre/+}$/ LSL-Kras^{G12D}/ LSL-TP53$^{R172H/+}$*	Both	Circulation	Yes	No	Negative
5671 PPT	*Ptf1a/p48$^{Cre/+}$/ LSL-Kras^{G12D}*	Epithelial	Non-metastatic primary tumour	No	No	Positive
5748 PPT	*Ptf1a/p48$^{Cre/+}$/ LSL-Kras^{G12D}*	Epithelial	Non-metastatic primary tumour	No	No	Positive
6051 PPT	*Ptf1a/p48$^{Cre/+}$/ LSL-Kras^{G12D}/ LSL-TP53$^{R172H/+}$*	Epithelial	Metastatic primary tumour	Yes	No	Unknown
6051 Aszites	*PDX$^{Cre/+}$/ LSL-Kras^{G12D}/ LSL-TP53$^{R172H/+}$*	Epithelial	Ascites	Yes	Not Implanted	Positive
6410 PPT	*Ptf1a/p48$^{Cre/+}$/ LSL-Kras^{G12D}/ LSL-TP53$^{R172H/+}$*	Epithelial	Metastatic primary tumour	Yes	Not Implanted	Positive

Cell line ID	Genotype	Phenotype	Source organ	Metastatized in endogenous mouse model (source)	Metastatisized after orthotopic implantation into mude mice	Kras WT Status
6410 Aszites	*Ptf1a/p48$^{Cre/+}$/ LSL-Kras^{G12D}/ LSL-TP53$^{R172H/+}$*	Mesenchymal	Ascites	Yes	Not Implanted	Negative
12591 Leber	*Ptf1a/p48$^{Cre/+}$/ LSL-Kras^{G12}*	Unknown	Liver metastasis	Yes	Not Implanted	Negative
12591 Lunge1	*Ptf1a/p48$^{Cre/+}$/ LSL-Kras^{G12}*	Mesenchymal	Lung metastasis	Yes	Not Implanted	Negative
12591 Lunge2	*Ptf1a/p48$^{Cre/+}$/ LSL-Kras^{G12}*	Mesenchymal	Lung metastasis	Yes	Not Implanted	Negative
15272 PPT	*Ptf1a/p48$^{Cre/+}$/ LSL-Kras^{G12D}*	Epithelial	Metastatic primary tumour	Yes	Liver, Lung	Positive
15272 Lebermet 1	*Ptf1a/p48$^{Cre/+}$/ LSL-Kras^{G12D}*	Epithelial	Liver metastasis	Yes	Liver, Lung, Lymph node	Unknown
15272 Leb Met 3	*Ptf1a/p48$^{Cre/+}$/ LSL-Kras^{G12}*	Epithelial	Liver metastasis	Yes	Not Implanted	Positive
15272 Lungenmet	*Ptf1a/p48$^{Cre/+}$/ LSL-Kras^{G12}*	Epithelial	Lung metastasis	Yes	Liver, Lung, Lymph node	Unknown
15272 LK1	*Ptf1a/p48$^{Cre/+}$/ LSL-Kras^{G12}*	Epithelial	Lymph node metastasis	Yes	Lung, Lymph node	Unknown
15272 VB	*Ptf1a/p48$^{Cre/+}$/ LSL-Kras^{G12}*	Epithelial	Circulation	Yes	Liver, Lung	Positive

Cell line ID	Genotype	Phenotype	Source organ	Metastatized in endogenous mouse model (source)	Metastatisized after orthotopic implan-tation into mude mice	Kras WT Status
16990 PPT	*Ptf1a/p48$^{Cre/+}$/ LSL-Kras^{G12}*	Epithelial, some mesen-chymal cells	Non-metastatic primary tumour	No	Unknown	Positive
16992 PPT	*Ptf1a/p48$^{Cre/+}$/ LSL-Kras^{G12}*	Mesenchymal	Primary tumour	Unknown	Liver	Negative
16992 PT K1	*Ptf1a/p48$^{Cre/+}$/ LSL-Kras^{G12}*	Mesenchymal	Primary tumour	Unknown	Liver	Negative
16992 PT K3	*Ptf1a/p48$^{Cre/+}$/ LSL-Kras^{G12}*	Mesenchymal	Primary tumour	Unknown	Unknown	Negative
16992 PT K5	*Ptf1a/p48$^{Cre/+}$/ LSL-Kras^{G12}*	Mesenchymal	Primary tumour	Unknown	Unknown	Negative
17728 PPT	*Ptf1a/p48$^{Cre/+}$/ LSL-Kras^{G12D}*	Mesenchymal	Metastatic primary tumour	Yes	No	Positive
17728 Leber	*Ptf1a/p48$^{Cre/+}$/ LSL-Kras^{G12}*	Mesenchymal	Metastatic primary tumour	Yes	Lung	Positive
53266 PPT	*Ptf1a/p48$^{Cre/+}$/ LSL-Kras^{G12D+}*	Epithelial	Metastatic primary tumour	Yes	Not Implanted	Positive
53268 PPT	*Ptf1a/p48$^{Cre/+}$/ LSL-Kras^{G12D+}*	Epithelial	Metastatic primary tumour	Yes	Unknown	Positive
53268 Leb1	*Ptf1a/p48$^{Cre/+}$/ LSL-Kras^{G12D+}*	Epithelial	Liver metastasis	Yes	Liver, Lung	Negative
53268 Leb2	*Ptf1a/p48$^{Cre/+}$/ LSL-Kras^{G12D+}*	Epithelial	Liver metastasis	Yes	Not Implanted	Positive
53631 PPT	*Ptf1a/p48$^{Cre/+}$/ LSL-Kras^{G12D}*	Unknown	Metastatic primary tumour	Yes	Liver, Lung	Positive
53631 Leb Met I	*Ptf1a/p48$^{Cre/+}$/ LSL-Kras^{G12D+}*	Unknown	Liver metastasis	Yes	Lung, Lymph node	Positive

Cell line ID	Genotype	Phenotype	Source organ	Metastatized in endogenous mouse model (source)	Metastatisized after orthotopic implan-tation into mude mice	Kras WT Status
53631 Lebermet II	*Ptf1a/p48$^{Cre/+}$/ LSL-Kras^{G12D}*	Unknown	Liver metastasis	Yes	Lymph node	Unknown
53631 Lungenmet II	*Ptf1a/p48$^{Cre/+}$/ LSL-Kras^{G12}*	Unknown	Lung metastasis	Yes	Lung, Lymph node	Positive
53631 Lungenmet III	*Ptf1a/p48$^{Cre/+}$/ LSL-Kras^{G12}*	Unknown	Lung metastasis	Yes	Liver, Lung	Positive
53631 VB	*Ptf1a/p48$^{Cre/+}$/ LSL-Kras^{G12D+}*	Unknown	Circulation	Yes	Lung, Lymph node	Positive
53646 PPT	*Ptf1a/p48$^{Cre/+}$/ LSL-Kras^{G12D+}*	Epithelial	Metastatic primary tumour	Yes	Liver, Lung	Negative
53646 Leber1	*Ptf1a/p48$^{Cre/+}$/ LSL-Kras^{G12D+}*	Epithelial	Liver metastasis	Yes	Unknown	Negative
53646 Leber2	*Ptf1a/p48$^{Cre/+}$/ LSL-Kras^{G12D+}*	Epithelial	Liver metastasis	Yes	Not Implanted	Negative
53646 Leber3	*Ptf1a/p48$^{Cre/+}$/ LSL-Kras^{G12D+}*	Epithelial	Liver metastasis	Yes	Not Implanted	Negative
53704 PPT	*Ptf1a/p48$^{Cre/+}$/ LSL-Kras^{G12D+}*	Unknown	Metastatic primary tumour	Yes	Unknown	Negative
53704 LebMet1	*Ptf1a/p48$^{Cre/+}$/ LSL-Kras^{G12D+}*	Unknown	Liver metastasis	Yes	Not Implanted	Negative
53704 LebMet2	*Ptf1a/p48$^{Cre/+}$/ LSL-Kras^{G12D+}*	Unknown	Liver metastasis	Yes	Unknown	Negative
53704 LebMet3	*Ptf1a/p48$^{Cre/+}$/ LSL-Kras^{G12D+}*	Unknown	Liver metastasis	Yes	Not Implanted	Negative
53909 PPT	*Ptf1a/p48$^{Cre/+}$/ LSL-Kras^{G12D+}*	Mesenchymal	Metastatic primary tumour	Yes	Unknown	Negative

Cell line ID	Genotype	Phenotype	Source organ	Metastatized in endogenous mouse model (source)	Metastatisized after orthotopic implan-tation into mude mice	Kras WT Status
53909 Leb Met	*Ptf1a/p48$^{Cre/+}$/ LSL-Kras^{G12D+}*	Mesenchymal	Liver metastasis	Yes	Unknown	Negative
53909 Aszites	*Ptf1a/p48$^{Cre/+}$/ LSL-Kras^{G12D+}*	Mesenchymal	Ascites	Yes	Not Implanted	Negative
54237 Leber	*PDX$^{Cre/+}$/ LSL-Kras^{G12D+}*	Epithelial	Liver metastasis	Yes	Lung	Negative
54394 PPT K2	*Ptf1a/p48$^{Cre/+}$/ LSL-Kras^{G12D}/ LSL-TP53$^{R172H/+}$*	Unknown	Primary tumour	Unknown	Unknown	Negative
54394 PPT K7	*Ptf1a/p48$^{Cre/+}$/ LSL-Kras^{G12D}/ LSL-TP53$^{R172H/+}$*	Unknown	Primary tumour	Unknown	Unknown	Positive
54394 PPT K9	*Ptf1a/p48$^{Cre/+}$/ LSL-Kras^{G12D}/ LSL-TP53$^{R172H/+}$*	Unknown	Primary tumour	Unknown	Unknown	Positive
54394 PPT K10	*Ptf1a/p48$^{Cre/+}$/ LSL-Kras^{G12D}/ LSL-TP53$^{R172H/+}$*	Unknown	Primary tumour	Unknown	Lung	Negative

9 References

Aguirre, A. J., Bardeesy, N., Sinha, M., Lopez, L., Tuveson, D. A., Horner, J., Redston, M. S., and DePinho, R. A. (2003). Activated Kras and Ink4a/Arf deficiency cooperate to produce metastatic pancreatic ductal adenocarcinoma. *Genes Dev,* **17**, 3112-3126.

Al-Hajj, M., and Clarke, M. F. (2004). Self-renewal and solid tumor stem cells. *Oncogene,* **23**, 7274-7282.

Al-Hajj, M., Wicha, M. S., Benito-Hernandez, A., Morrison, S. J., and Clarke, M. F. (2003). Prospective identification of tumorigenic breast cancer cells. *Proc Natl Acad Sci U S A,* **100**, 3983-3988.

Al-Mulla, F., Keith, W. N., Pickford, I. R., Going, J. J., and Birnie, G. D. (1999). Comparative genomic hybridization analysis of primary colorectal carcinomas and their synchronous metastases. *Genes Chromosomes Cancer,* **24**, 306-314.

Almoguera, C., Shibata, D., Forrester, K., Martin, J., Arnheim, N., and Perucho, M. (1988). Most human carcinomas of the exocrine pancreas contain mutant c-K-ras genes. *Cell,* **53**, 549-554.

Argani, P., Rosty, C., Reiter, R. E., Wilentz, R. E., Murugesan, S. R., Leach, S. D., Ryu, B., Skinner, H. G., Goggins, M., Jaffee, E. M.*, et al.* (2001). Discovery of new markers of cancer through serial analysis of gene expression: prostate stem cell antigen is overexpressed in pancreatic adenocarcinoma. *Cancer Res,* **61**, 4320-4324.

Artandi, S. E., Chang, S., Lee, S. L., Alson, S., Gottlieb, G. J., Chin, L., and DePinho, R. A. (2000). Telomere dysfunction promotes non-reciprocal translocations and epithelial cancers in mice. *Nature,* **406**, 641-645.

Balic, M., Lin, H., Young, L., Hawes, D., Giuliano, A., McNamara, G., Datar, R. H., and Cote, R. J. (2006). Most early disseminated cancer cells detected in bone marrow of breast cancer patients have a putative breast cancer stem cell phenotype. *Clin Cancer Res,* **12**, 5615-5621.

Barton, C. M., Staddon, S. L., Hughes, C. M., Hall, P. A., O'Sullivan, C., Kloppel, G., Theis, B., Russell, R. C., Neoptolemos, J., Williamson, R. C., and et al. (1991). Abnormalities of the p53 tumour suppressor gene in human pancreatic cancer. *Br J Cancer,* **64**, 1076-1082.

Bates, M. K., Zhang, G., Sebestyen, M. G., Neal, Z. C., Wolff, J. A., and Herweijer, H. (2006). Genetic immunization for antibody generation in research animals by intravenous delivery of plasmid DNA. *Biotechniques,* **40**, 199-208.

Bates, P., Young, J. A., and Varmus, H. E. (1993). A receptor for subgroup A Rous sarcoma virus is related to the low density lipoprotein receptor. *Cell,* **74**, 1043-1051.

Batlle, E., Sancho, E., Franci, C., Dominguez, D., Monfar, M., Baulida, J., and Garcia De Herreros, A. (2000). The transcription factor snail is a repressor of E-cadherin gene expression in epithelial tumour cells. *Nat Cell Biol,* **2**, 84-89.

Beer, D. G., Kardia, S. L., Huang, C. C., Giordano, T. J., Levin, A. M., Misek, D. E., Lin, L., Chen, G., Gharib, T. G., Thomas, D. G.*, et al.* (2002). Gene-expression

profiles predict survival of patients with lung adenocarcinoma. *Nat Med,* **8**, 816-824.

Berchuck, A., Iversen, E. S., Lancaster, J. M., Pittman, J., Luo, J., Lee, P., Murphy, S., Dressman, H. K., Febbo, P. G., West, M.*, et al.* (2005). Patterns of gene expression that characterize long-term survival in advanced stage serous ovarian cancers. *Clin Cancer Res,* **11**, 3686-3696.

Biankin, A. V., Kench, J. G., Morey, A. L., Lee, C. S., Biankin, S. A., Head, D. R., Hugh, T. B., Henshall, S. M., and Sutherland, R. L. (2001). Overexpression of p21(WAF1/CIP1) is an early event in the development of pancreatic intraepithelial neoplasia. *Cancer Res,* **61**, 8830-8837.

Bonnet, D., and Dick, J. E. (1997). Human acute myeloid leukemia is organized as a hierarchy that originates from a primitive hematopoietic cell. *Nat Med,* **3**, 730-737.

Boschman, C. R., Stryker, S., Reddy, J. K., and Rao, M. S. (1994). Expression of p53 protein in precursor lesions and adenocarcinoma of human pancreas. *Am J Pathol,* **145**, 1291-1295.

Brembeck, F. H., Schreiber, F. S., Deramaudt, T. B., Craig, L., Rhoades, B., Swain, G., Grippo, P., Stoffers, D. A., Silberg, D. G., and Rustgi, A. K. (2003). The mutant K-ras oncogene causes pancreatic periductal lymphocytic infiltration and gastric mucous neck cell hyperplasia in transgenic mice. *Cancer Res,* **63**, 2005-2009.

Campbell, S. L., Khosravi-Far, R., Rossman, K. L., Clark, G. J., and Der, C. J. (1998). Increasing complexity of Ras signaling. *Oncogene,* **17**, 1395-1413.

Cano, A., Perez-Moreno, M. A., Rodrigo, I., Locascio, A., Blanco, M. J., del Barrio, M. G., Portillo, F., and Nieto, M. A. (2000). The transcription factor snail controls epithelial-mesenchymal transitions by repressing E-cadherin expression. *Nat Cell Biol,* **2**, 76-83.

Carriere, C., Seeley, E. S., Goetze, T., Longnecker, D. S., and Korc, M. (2007). The Nestin progenitor lineage is the compartment of origin for pancreatic intraepithelial neoplasia. *Proc Natl Acad Sci U S A,* **104**, 4437-4442.

Carter, S. L., Eklund, A. C., Kohane, I. S., Harris, L. N., and Szallasi, Z. (2006). A signature of chromosomal instability inferred from gene expression profiles predicts clinical outcome in multiple human cancers. *Nat Genet,* **38**, 1043-1048.

Chang, H. Y., Nuyten, D. S., Sneddon, J. B., Hastie, T., Tibshirani, R., Sorlie, T., Dai, H., He, Y. D., van't Veer, L. J., Bartelink, H.*, et al.* (2005). Robustness, scalability, and integration of a wound-response gene expression signature in predicting breast cancer survival. *Proc Natl Acad Sci U S A,* **102**, 3738-3743.

Chang, H. Y., Sneddon, J. B., Alizadeh, A. A., Sood, R., West, R. B., Montgomery, K., Chi, J. T., van de Rijn, M., Botstein, D., and Brown, P. O. (2004). Gene expression signature of fibroblast serum response predicts human cancer progression: similarities between tumors and wounds. *PLoS Biol,* **2**, E7.

Chen, Y. W., Paliwal, S., Draheim, K., Grossman, S. R., and Lewis, B. C. (2008). p19Arf inhibits the invasion of hepatocellular carcinoma cells by binding to C-terminal binding protein. *Cancer Res,* **68**, 476-482.

Chin, L., Artandi, S. E., Shen, Q., Tam, A., Lee, S. L., Gottlieb, G. J., Greider, C. W., and DePinho, R. A. (1999). p53 deficiency rescues the adverse effects of

telomere loss and cooperates with telomere dysfunction to accelerate carcinogenesis. *Cell,* **97**, 527-538.

Collins, A. T., Berry, P. A., Hyde, C., Stower, M. J., and Maitland, N. J. (2005). Prospective identification of tumorigenic prostate cancer stem cells. *Cancer Res,* **65**, 10946-10951.

Crnogorac-Jurcevic, T., Efthimiou, E., Nielsen, T., Loader, J., Terris, B., Stamp, G., Baron, A., Scarpa, A., and Lemoine, N. R. (2002). Expression profiling of microdissected pancreatic adenocarcinomas. *Oncogene,* **21**, 4587-4594.

Du, Y. C., Lewis, B. C., Hanahan, D., and Varmus, H. (2007). Assessing tumor progression factors by somatic gene transfer into a mouse model: Bcl-xL promotes islet tumor cell invasion. *PLoS Biol,* **5**, e276.

Du, Z., Podsypanina, K., Huang, S., McGrath, A., Toneff, M. J., Bogoslovskaia, E., Zhang, X., Moraes, R. C., Fluck, M., Allred, D. C.*, et al.* (2006). Introduction of oncogenes into mammary glands in vivo with an avian retroviral vector initiates and promotes carcinogenesis in mouse models. *Proc Natl Acad Sci U S A,* **103**, 17396-17401.

Dunn, K. J., Incao, A., Watkins-Chow, D., Li, Y., and Pavan, W. J. (2001). In utero complementation of a neural crest-derived melanocyte defect using cell directed gene transfer. *Genesis,* **30**, 70-76.

Dunn, K. J., Williams, B. O., Li, Y., and Pavan, W. J. (2000). Neural crest-directed gene transfer demonstrates Wnt1 role in melanocyte expansion and differentiation during mouse development. *Proc Natl Acad Sci U S A,* **97**, 10050-10055.

Fearon, E. R., and Vogelstein, B. (1990). A genetic model for colorectal tumorigenesis. *Cell,* **61**, 759-767.

Federspiel, M. J., Bates, P., Young, J. A., Varmus, H. E., and Hughes, S. H. (1994). A system for tissue-specific gene targeting: transgenic mice susceptible to subgroup A avian leukosis virus-based retroviral vectors. *Proc Natl Acad Sci U S A,* **91**, 11241-11245.

Feil, R. (2007). Conditional somatic mutagenesis in the mouse using site-specific recombinases. *Handb Exp Pharmacol*, 3-28.

Fidler, I. J., and Kripke, M. L. (1977). Metastasis results from preexisting variant cells within a malignant tumor. *Science,* **197**, 893-895.

Fisher, G. H., Orsulic, S., Holland, E., Hively, W. P., Li, Y., Lewis, B. C., Williams, B. O., and Varmus, H. E. (1999). Development of a flexible and specific gene delivery system for production of murine tumor models. *Oncogene,* **18**, 5253-5260.

Grippo, P. J., Nowlin, P. S., Demeure, M. J., Longnecker, D. S., and Sandgren, E. P. (2003). Preinvasive pancreatic neoplasia of ductal phenotype induced by acinar cell targeting of mutant Kras in transgenic mice. *Cancer Res,* **63**, 2016-2019.

Grutzmann, R., Foerder, M., Alldinger, I., Staub, E., Brummendorf, T., Ropcke, S., Li, X., Kristiansen, G., Jesnowski, R., Sipos, B.*, et al.* (2003). Gene expression profiles of microdissected pancreatic ductal adenocarcinoma. *Virchows Arch,* **443**, 508-517.

Gu, Z., Flemington, C., Chittenden, T., and Zambetti, G. P. (2000). ei24, a p53 response gene involved in growth suppression and apoptosis. *Mol Cell Biol,* **20**, 233-241.

Guz, Y., Montminy, M. R., Stein, R., Leonard, J., Gamer, L. W., Wright, C. V., and Teitelman, G. (1995). Expression of murine STF-1, a putative insulin gene transcription factor, in beta cells of pancreas, duodenal epithelium and pancreatic exocrine and endocrine progenitors during ontogeny. *Development,* **121**, 11-18.

Hahn, S. A., Schutte, M., Hoque, A. T., Moskaluk, C. A., da Costa, L. T., Rozenblum, E., Weinstein, C. L., Fischer, A., Yeo, C. J., Hruban, R. H., and Kern, S. E. (1996). DPC4, a candidate tumor suppressor gene at human chromosome 18q21.1. *Science,* **271**, 350-353.

Han, H., Bearss, D. J., Browne, L. W., Calaluce, R., Nagle, R. B., and Von Hoff, D. D. (2002). Identification of differentially expressed genes in pancreatic cancer cells using cDNA microarray. *Cancer Res,* **62**, 2890-2896.

Hardwick, C., Hoare, K., Owens, R., Hohn, H. P., Hook, M., Moore, D., Cripps, V., Austen, L., Nance, D. M., and Turley, E. A. (1992). Molecular cloning of a novel hyaluronan receptor that mediates tumor cell motility. *J Cell Biol,* **117**, 1343-1350.

He, L., Thomson, J. M., Hemann, M. T., Hernando-Monge, E., Mu, D., Goodson, S., Powers, S., Cordon-Cardo, C., Lowe, S. W., Hannon, G. J., and Hammond, S. M. (2005). A microRNA polycistron as a potential human oncogene. *Nature,* **435**, 828-833.

Hermann, P. C., Huber, S. L., Herrler, T., Aicher, A., Ellwart, J. W., Guba, M., Bruns, C. J., and Heeschen, C. (2007). Distinct populations of cancer stem cells determine tumor growth and metastatic activity in human pancreatic cancer. *Cell Stem Cell,* **1**, 313-323.

Hezel, A. F., Kimmelman, A. C., Stanger, B. Z., Bardeesy, N., and Depinho, R. A. (2006). Genetics and biology of pancreatic ductal adenocarcinoma. *Genes Dev,* **20**, 1218-1249.

Hill, R. P., Chambers, A. F., Ling, V., and Harris, J. F. (1984). Dynamic heterogeneity: rapid generation of metastatic variants in mouse B16 melanoma cells. *Science,* **224**, 998-1001.

Himly, M., Foster, D. N., Bottoli, I., Iacovoni, J. S., and Vogt, P. K. (1998). The DF-1 chicken fibroblast cell line: transformation induced by diverse oncogenes and cell death resulting from infection by avian leukosis viruses. *Virology,* **248**, 295-304.

Hingorani, S. R., Petricoin, E. F., Maitra, A., Rajapakse, V., King, C., Jacobetz, M. A., Ross, S., Conrads, T. P., Veenstra, T. D., Hitt, B. A.*, et al.* (2003). Preinvasive and invasive ductal pancreatic cancer and its early detection in the mouse. *Cancer Cell,* **4**, 437-450.

Hingorani, S. R., Wang, L., Multani, A. S., Combs, C., Deramaudt, T. B., Hruban, R. H., Rustgi, A. K., Chang, S., and Tuveson, D. A. (2005). Trp53R172H and KrasG12D cooperate to promote chromosomal instability and widely metastatic pancreatic ductal adenocarcinoma in mice. *Cancer Cell,* **7**, 469-483.

Hochberg, Y. B. a. Y. (1995). Controlling the false discovery rate: a practical and powerful approach to multiple testing. *Journal of the Royal Statistical Society Series B (Methodological)*, 289–300.

Holgado-Madruga, M., Emlet, D. R., Moscatello, D. K., Godwin, A. K., and Wong, A. J. (1996). A Grb2-associated docking protein in EGF- and insulin-receptor signalling. *Nature,* **379**, 560-564.

Holgado-Madruga, M., Moscatello, D. K., Emlet, D. R., Dieterich, R., and Wong, A. J. (1997). Grb2-associated binder-1 mediates phosphatidylinositol 3-kinase activation and the promotion of cell survival by nerve growth factor. *Proc Natl Acad Sci U S A,* **94**, 12419-12424.

Holland, E. C., Hively, W. P., DePinho, R. A., and Varmus, H. E. (1998). A constitutively active epidermal growth factor receptor cooperates with disruption of G1 cell-cycle arrest pathways to induce glioma-like lesions in mice. *Genes Dev,* **12**, 3675-3685.

Holland, E. C., and Varmus, H. E. (1998). Basic fibroblast growth factor induces cell migration and proliferation after glia-specific gene transfer in mice. *Proc Natl Acad Sci U S A,* **95**, 1218-1223.

Hruban, R. H., Goggins, M., Parsons, J., and Kern, S. E. (2000). Progression model for pancreatic cancer. *Clin Cancer Res,* **6**, 2969-2972.

Hruban, R. H., Takaori, K., Klimstra, D. S., Adsay, N. V., Albores-Saavedra, J., Biankin, A. V., Biankin, S. A., Compton, C., Fukushima, N., Furukawa, T.*, et al.* (2004). An illustrated consensus on the classification of pancreatic intraepithelial neoplasia and intraductal papillary mucinous neoplasms. *Am J Surg Pathol,* **28**, 977-987.

Huang, E., Cheng, S. H., Dressman, H., Pittman, J., Tsou, M. H., Horng, C. F., Bild, A., Iversen, E. S., Liao, M., Chen, C. M.*, et al.* (2003). Gene expression predictors of breast cancer outcomes. *Lancet,* **361**, 1590-1596.

Husemann, Y., Geigl, J. B., Schubert, F., Musiani, P., Meyer, M., Burghart, E., Forni, G., Eils, R., Fehm, T., Riethmuller, G., and Klein, C. A. (2008). Systemic spread is an early step in breast cancer. *Cancer Cell,* **13**, 58-68.

Iacobuzio-Donahue, C. A., Maitra, A., Shen-Ong, G. L., van Heek, T., Ashfaq, R., Meyer, R., Walter, K., Berg, K., Hollingsworth, M. A., Cameron, J. L.*, et al.* (2002). Discovery of novel tumor markers of pancreatic cancer using global gene expression technology. *Am J Pathol,* **160**, 1239-1249.

Iki, K., and Pour, P. M. (2006). Expression of Oct4, a stem cell marker, in the hamster pancreatic cancer model. *Pancreatology,* **6**, 406-413.

Immervoll, H., Hoem, D., Sakariassen, P. O., Steffensen, O. J., and Molven, A. (2008). Expression of the "stem cell marker" CD133 in pancreas and pancreatic ductal adenocarcinomas. *BMC Cancer,* **8**, 48.

Iorio, M. V., Ferracin, M., Liu, C. G., Veronese, A., Spizzo, R., Sabbioni, S., Magri, E., Pedriali, M., Fabbri, M., Campiglio, M.*, et al.* (2005). MicroRNA gene expression deregulation in human breast cancer. *Cancer Res,* **65**, 7065-7070.

Ishikawa, H. O., Takeuchi, H., Haltiwanger, R. S., and Irvine, K. D. (2008). Four-jointed is a Golgi kinase that phosphorylates a subset of cadherin domains. *Science,* **321**, 401-404.

Jackson, E. L., Willis, N., Mercer, K., Bronson, R. T., Crowley, D., Montoya, R., Jacks, T., and Tuveson, D. A. (2001). Analysis of lung tumor initiation and progression using conditional expression of oncogenic K-ras. *Genes Dev,* **15**, 3243-3248.

James, R. M., Arends, M. J., Plowman, S. J., Brooks, D. G., Miles, C. G., West, J. D., and Patek, C. E. (2003). K-ras proto-oncogene exhibits tumor suppressor activity as its absence promotes tumorigenesis in murine teratomas. Mol *Cancer Res,* **1**, 820-825.

Jemal, A., Siegel, R., Ward, E., Hao, Y., Xu, J., and Thun, M. J. (2009). Cancer statistics, 2009. *CA Cancer J Clin,* **59**, 225-249.

Jones, S., Zhang, X., Parsons, D. W., Lin, J. C., Leary, R. J., Angenendt, P., Mankoo, P., Carter, H., Kamiyama, H., Jimeno, A.*, et al.* (2008). Core signaling pathways in human pancreatic cancers revealed by global genomic analyses. *Science,* **321**, 1801-1806.

Jonkers, J., and Berns, A. (2002). Conditional mouse models of sporadic cancer. *Nat Rev Cancer,* **2**, 251-265.

Jonkers, J., Meuwissen, R., van der Gulden, H., Peterse, H., van der Valk, M., and Berns, A. (2001). Synergistic tumor suppressor activity of BRCA2 and p53 in a conditional mouse model for breast cancer. *Nat Genet,* **29**, 418-425.

Kalluri, R., and Weinberg, R. A. (2009). The basics of epithelial-mesenchymal transition. *J Clin Invest,* **119**, 1420-1428.

Kang, Y., and Massague, J. (2004). Epithelial-mesenchymal transitions: twist in development and metastasis. *Cell,* **118**, 277-279.

Kang, Y., Siegel, P. M., Shu, W., Drobnjak, M., Kakonen, S. M., Cordon-Cardo, C., Guise, T. A., and Massague, J. (2003). A multigenic program mediating breast cancer metastasis to bone. *Cancer Cell,* **3**, 537-549.

Kawaguchi, Y., Cooper, B., Gannon, M., Ray, M., MacDonald, R. J., and Wright, C. V. (2002). The role of the transcriptional regulator Ptf1a in converting intestinal to pancreatic progenitors. *Nat Genet,* **32**, 128-134.

Kerbel, R. S., Waghorne, C., Korczak, B., Lagarde, A., and Breitman, M. L. (1988). Clonal dominance of primary tumours by metastatic cells: genetic analysis and biological implications. *Cancer Surv,* **7**, 597-629.

Kerbel, R. S., Waghorne, C., Man, M. S., Elliott, B., and Breitman, M. L. (1987). Alteration of the tumorigenic and metastatic properties of neoplastic cells is associated with the process of calcium phosphate-mediated DNA transfection. *Proc Natl Acad Sci U S A,* **84**, 1263-1267.

Kim, C. F., Jackson, E. L., Woolfenden, A. E., Lawrence, S., Babar, I., Vogel, S., Crowley, D., Bronson, R. T., and Jacks, T. (2005). Identification of bronchioalveolar stem cells in normal lung and lung cancer. *Cell,* **121**, 823-835.

Klimstra, D. S., and Longnecker, D. S. (1994). K-ras mutations in pancreatic ductal proliferative lesions. *Am J Pathol,* **145**, 1547-1550.

Kogan, S. C., Doherty, M., and Gitschier, J. (1987). An improved method for prenatal diagnosis of genetic diseases by analysis of amplified DNA sequences. Application to hemophilia A. *N Engl J Med,* **317**, 985-990.

Krapp, A., Knofler, M., Ledermann, B., Burki, K., Berney, C., Zoerkler, N., Hagenbuchle, O., and Wellauer, P. K. (1998). The bHLH protein PTF1-p48 is essential for the formation of the exocrine and the correct spatial organization of the endocrine pancreas. *Genes Dev,* **12**, 3752-3763.

Kumar, V. A., Abul K; Fausto, Nelson; Robbins, Stanley L; Cotran, Ramzi S (2005). Robbins and Cotran pathologic basis of disease, *7th edn (Philadelphia: Elsevier Saunders)*.

Kuukasjarvi, T., Karhu, R., Tanner, M., Kahkonen, M., Schaffer, A., Nupponen, N., Pennanen, S., Kallioniemi, A., Kallioniemi, O. P., and Isola, J. (1997). Genetic heterogeneity and clonal evolution underlying development of asynchronous metastasis in human breast cancer. *Cancer Res,* **57**, 1597-1604.

Lan, Y., Kingsley, P. D., Cho, E. S., and Jiang, R. (2001). Osr2, a new mouse gene related to Drosophila odd-skipped, exhibits dynamic expression patterns during craniofacial, limb, and kidney development. *Mech Dev,* **107**, 175-179.

Lan, Y., Ovitt, C. E., Cho, E. S., Maltby, K. M., Wang, Q., and Jiang, R. (2004). Odd-skipped related 2 (Osr2) encodes a key intrinsic regulator of secondary palate growth and morphogenesis. *Development,* **131**, 3207-3216.

Lewis, B. C., Chinnasamy, N., Morgan, R. A., and Varmus, H. E. (2001). Development of an avian leukosis-sarcoma virus subgroup A pseudotyped lentiviral vector. *J Virol,* **75**, 9339-9344.

Lewis, B. C., Klimstra, D. S., and Varmus, H. E. (2003). The c-myc and PyMT oncogenes induce different tumor types in a somatic mouse model for pancreatic cancer. *Genes Dev,* **17**, 3127-3138.

Li, C., Heidt, D. G., Dalerba, P., Burant, C. F., Zhang, L., Adsay, V., Wicha, M., Clarke, M. F., and Simeone, D. M. (2007a). Identification of pancreatic cancer stem cells. *Cancer Res,* **67**, 1030-1037.

Li, F., Tiede, B., Massague, J., and Kang, Y. (2007b). Beyond tumorigenesis: cancer stem cells in metastasis. *Cell Res,* **17**, 3-14.

Ling, V., Chambers, A. F., Harris, J. F., and Hill, R. P. (1985). Quantitative genetic analysis of tumor progression. *Cancer Metastasis Rev,* **4**, 173-192.

Lu, J., Getz, G., Miska, E. A., Alvarez-Saavedra, E., Lamb, J., Peck, D., Sweet-Cordero, A., Ebert, B. L., Mak, R. H., Ferrando, A. A.*, et al.* (2005). MicroRNA expression profiles classify human cancers. *Nature,* **435**, 834-838.

Lumelsky, N., Blondel, O., Laeng, P., Velasco, I., Ravin, R., and McKay, R. (2001). Differentiation of embryonic stem cells to insulin-secreting structures similar to pancreatic islets. *Science,* **292**, 1389-1394.

Ma, X. J., Salunga, R., Tuggle, J. T., Gaudet, J., Enright, E., McQuary, P., Payette, T., Pistone, M., Stecker, K., Zhang, B. M.*, et al.* (2003). Gene expression profiles of human breast cancer progression. *Proc Natl Acad Sci U S A,* **100**, 5974-5979.

Maeda, S., Shinchi, H., Kurahara, H., Mataki, Y., Maemura, K., Sato, M., Natsugoe, S., Aikou, T., and Takao, S. (2008). CD133 expression is correlated with lymph node metastasis and vascular endothelial growth factor-C expression in pancreatic cancer. *Br J Cancer,* **98**, 1389-1397.

Malumbres, M., and Barbacid, M. (2003). RAS oncogenes: the first 30 years. *Nat Rev Cancer,* **3**, 459-465.

Marino, S., Vooijs, M., van Der Gulden, H., Jonkers, J., and Berns, A. (2000). Induction of medulloblastomas in p53-null mutant mice by somatic inactivation of Rb in the external granular layer cells of the cerebellum. *Genes Dev,* **14**, 994-1004.

Massague, J., Blain, S. W., and Lo, R. S. (2000). TGFbeta signaling in growth control, cancer, and heritable disorders. *Cell,* **103**, 295-309.

Miller, C. P., McGehee, R. E., Jr., and Habener, J. F. (1994). IDX-1: a new homeodomain transcription factor expressed in rat pancreatic islets and duodenum that transactivates the somatostatin gene. *Embo J,* **13**, 1145-1156.

Minn, A. J., Gupta, G. P., Siegel, P. M., Bos, P. D., Shu, W., Giri, D. D., Viale, A., Olshen, A. B., Gerald, W. L., and Massague, J. (2005a). Genes that mediate breast cancer metastasis to lung. *Nature,* **436,** 518-524.

Minn, A. J., Kang, Y., Serganova, I., Gupta, G. P., Giri, D. D., Doubrovin, M., Ponomarev, V., Gerald, W. L., Blasberg, R., and Massague, J. (2005b). Distinct organ-specific metastatic potential of individual breast cancer cells and primary tumors. *J Clin Invest,* **115**, 44-55.

Missiaglia, E., Blaveri, E., Terris, B., Wang, Y. H., Costello, E., Neoptolemos, J. P., Crnogorac-Jurcevic, T., and Lemoine, N. R. (2004). Analysis of gene expression in cancer cell lines identifies candidate markers for pancreatic tumorigenesis and metastasis. *Int J Cancer,* **112**, 100-112.

Mullendore, M. E., Koorstra, J. B., Li, Y. M., Offerhaus, G. J., Fan, X., Henderson, C. M., Matsui, W., Eberhart, C. G., Maitra, A., and Feldmann, G. (2009). Ligand-dependent Notch signaling is involved in tumor initiation and tumor maintenance in pancreatic cancer. *Clin Cancer Res,* **15**, 2291-2301.

Murphy, G. J., and Leavitt, A. D. (1999). A model for studying megakaryocyte development and biology. *Proc Natl Acad Sci U S A,* **96**, 3065-3070.

Nakamura, T., Furukawa, Y., Nakagawa, H., Tsunoda, T., Ohigashi, H., Murata, K., Ishikawa, O., Ohgaki, K., Kashimura, N., Miyamoto, M*., et al.* (2004). Genome-wide cDNA microarray analysis of gene expression profiles in pancreatic cancers using populations of tumor cells and normal ductal epithelial cells selected for purity by laser microdissection. *Oncogene,* **23**, 2385-2400.

Nakhai, H., Sel, S., Favor, J., Mendoza-Torres, L., Paulsen, F., Duncker, G. I., and Schmid, R. M. (2007). Ptf1a is essential for the differentiation of GABAergic and glycinergic amacrine cells and horizontal cells in the mouse retina. *Development,* **134**, 1151-1160.

Nakhai, H., Siveke, J. T., Klein, B., Mendoza-Torres, L., Mazur, P. K., Algul, H., Radtke, F., Strobl, L., Zimber-Strobl, U., and Schmid, R. M. (2008). Conditional ablation of Notch signaling in pancreatic development. *Development,* **135**, 2757-2765.

National Cancer Institute (2002). What You Need To Know About Cancer of the Pancreas. In.

Offield, M. F., Jetton, T. L., Labosky, P. A., Ray, M., Stein, R. W., Magnuson, M. A., Hogan, B. L., and Wright, C. V. (1996). PDX-1 is required for pancreatic

outgrowth and differentiation of the rostral duodenum. *Development,* **122**, 983-995.

Ohlsson, H., Karlsson, K., and Edlund, T. (1993). IPF1, a homeodomain-containing transactivator of the insulin gene. *Embo J,* **12**, 4251-4259.

Olive, K. P., Tuveson, D. A., Ruhe, Z. C., Yin, B., Willis, N. A., Bronson, R. T., Crowley, D., and Jacks, T. (2004). Mutant p53 gain of function in two mouse models of Li-Fraumeni syndrome. *Cell,* **119**, 847-860.

Ornitz, D. M., Hammer, R. E., Messing, A., Palmiter, R. D., and Brinster, R. L. (1987). Pancreatic neoplasia induced by SV40 T-antigen expression in acinar cells of transgenic mice. *Science,* **238**, 188-193.

Orsulic, S. (2002). An RCAS-TVA-based approach to designer mouse models. *Mamm Genome,* **13**, 543-547.

Orsulic, S., Li, Y., Soslow, R. A., Vitale-Cross, L. A., Gutkind, J. S., and Varmus, H. E. (2002). Induction of ovarian cancer by defined multiple genetic changes in a mouse model system. *Cancer Cell,* **1**, 53-62.

Paik, S., Shak, S., Tang, G., Kim, C., Baker, J., Cronin, M., Baehner, F. L., Walker, M. G., Watson, D., Park, T.*, et al.* (2004). A multigene assay to predict recurrence of tamoxifen-treated, node-negative breast cancer. *N Engl J Med,* **351**, 2817-2826.

Pao, W., Klimstra, D. S., Fisher, G. H., and Varmus, H. E. (2003). Use of avian retroviral vectors to introduce transcriptional regulators into mammalian cells for analyses of tumor maintenance. *Proc Natl Acad Sci U S A,* **100**, 8764-8769.

Perou, C. M., Sorlie, T., Eisen, M. B., van de Rijn, M., Jeffrey, S. S., Rees, C. A., Pollack, J. R., Ross, D. T., Johnsen, H., Akslen, L. A.*, et al.* (2000). Molecular portraits of human breast tumours. *Nature,* **406**, 747-752.

Pittman, J., Huang, E., Dressman, H., Horng, C. F., Cheng, S. H., Tsou, M. H., Chen, C. M., Bild, A., Iversen, E. S., Huang, A. T.*, et al.* (2004). Integrated modeling of clinical and gene expression information for personalized prediction of disease outcomes. *Proc Natl Acad Sci U S A,* **101**, 8431-8436.

Podsypanina, K., Du, Y. C., Jechlinger, M., Beverly, L. J., Hambardzumyan, D., and Varmus, H. (2008). Seeding and propagation of untransformed mouse mammary cells in the lung. *Science,* **321**, 1841-1844.

Ponti, D., Costa, A., Zaffaroni, N., Pratesi, G., Petrangolini, G., Coradini, D., Pilotti, S., Pierotti, M. A., and Daidone, M. G. (2005). Isolation and in vitro propagation of tumorigenic breast cancer cells with stem/progenitor cell properties. *Cancer Res,* **65**, 5506-5511.

Potti, A., Mukherjee, S., Petersen, R., Dressman, H. K., Bild, A., Koontz, J., Kratzke, R., Watson, M. A., Kelley, M., Ginsburg, G. S.*, et al.* (2006). A genomic strategy to refine prognosis in early-stage non-small-cell lung cancer. *N Engl J Med,* **355**, 570-580.

Quaife, C. J., Pinkert, C. A., Ornitz, D. M., Palmiter, R. D., and Brinster, R. L. (1987). Pancreatic neoplasia induced by ras expression in acinar cells of transgenic mice. *Cell,* **48**, 1023-1034.

Ramaswamy, S., Ross, K. N., Lander, E. S., and Golub, T. R. (2003). A molecular signature of metastasis in primary solid tumors. *Nat Genet,* **33**, 49-54.

Rangarajan, A., and Weinberg, R. A. (2003). Opinion: Comparative biology of mouse versus human cells: modelling human cancer in mice. *Nat Rev Cancer,* **3**, 952-959.

Reya, T., Morrison, S. J., Clarke, M. F., and Weissman, I. L. (2001). Stem cells, cancer, and cancer stem cells. *Nature,* **414**, 105-111.

Ross, D. T., Scherf, U., Eisen, M. B., Perou, C. M., Rees, C., Spellman, P., Iyer, V., Jeffrey, S. S., Van de Rijn, M., Waltham, M.*, et al.* (2000). Systematic variation in gene expression patterns in human cancer cell lines. *Nat Genet,* **24**, 227-235.

Rosty, C., Christa, L., Kuzdzal, S., Baldwin, W. M., Zahurak, M. L., Carnot, F., Chan, D. W., Canto, M., Lillemoe, K. D., Cameron, J. L.*, et al.* (2002). Identification of hepatocarcinoma-intestine-pancreas/pancreatitis-associated protein I as a biomarker for pancreatic ductal adenocarcinoma by protein biochip technology. *Cancer Res,* **62**, 1868-1875.

Rozenblum, E., Schutte, M., Goggins, M., Hahn, S. A., Panzer, S., Zahurak, M., Goodman, S. N., Sohn, T. A., Hruban, R. H., Yeo, C. J., and Kern, S. E. (1997). Tumor-suppressive pathways in pancreatic carcinoma. *Cancer Res,* **57**, 1731-1734.

Saiki, R. K., Gelfand, D. H., Stoffel, S., Scharf, S. J., Higuchi, R., Horn, G. T., Mullis, K. B., and Erlich, H. A. (1988). Primer-directed enzymatic amplification of DNA with a thermostable DNA polymerase. *Science,* **239**, 487-491.

Sandgren, E. P., Luetteke, N. C., Palmiter, R. D., Brinster, R. L., and Lee, D. C. (1990). Overexpression of TGF alpha in transgenic mice: induction of epithelial hyperplasia, pancreatic metaplasia, and carcinoma of the breast. *Cell,* **61**, 1121-1135.

Saur, D., Seidler, B., Paehge, H., Schusdziarra, V., and Allescher, H. D. (2002). Complex regulation of human neuronal nitric-oxide synthase exon 1c gene transcription. Essential role of Sp and ZNF family members of transcription factors. *J Biol Chem,* **277**, 25798-25814.

Saur, D., Seidler, B., Schneider, G., Algul, H., Beck, R., Senekowitsch-Schmidtke, R., Schwaiger, M., and Schmid, R. M. (2005). CXCR4 expression increases liver and lung metastasis in a mouse model of pancreatic cancer. *Gastroenterology,* **129**, 1237-1250.

Schaefer-Klein, J., Givol, I., Barsov, E. V., Whitcomb, J. M., VanBrocklin, M., Foster, D. N., Federspiel, M. J., and Hughes, S. H. (1998). The EV-O-derived cell line DF-1 supports the efficient replication of avian leukosis-sarcoma viruses and vectors. *Virology,* **248**, 305-311.

Schmidt-Kittler, O., Ragg, T., Daskalakis, A., Granzow, M., Ahr, A., Blankenstein, T. J., Kaufmann, M., Diebold, J., Arnholdt, H., Muller, P.*, et al.* (2003). From latent disseminated cells to overt metastasis: genetic analysis of systemic breast cancer progression. *Proc Natl Acad Sci U S A,* **100**, 7737-7742.

Schneider, G., Siveke, J. T., Eckel, F., and Schmid, R. M. (2005). Pancreatic cancer: basic and clinical aspects. *Gastroenterology,* **128**, 1606-1625.

Schwarte-Waldhoff, I., Volpert, O. V., Bouck, N. P., Sipos, B., Hahn, S. A., Klein-Scory, S., Luttges, J., Kloppel, G., Graeven, U., Eilert-Micus, C.*, et al.* (2000). Smad4/DPC4-mediated tumor suppression through suppression of angiogenesis. *Proc Natl Acad Sci U S A,* **97**, 9624-9629.

Segal, E., Friedman, N., Koller, D., and Regev, A. (2004). A module map showing conditional activity of expression modules in cancer. *Nat Genet,* **36**, 1090-1098.

Seidler, B., Schmidt, A., Mayr, U., Nakhai, H., Schmid, R. M., Schneider, G., and Saur, D. (2008). A Cre-loxP-based mouse model for conditional somatic gene expression and knockdown in vivo by using avian retroviral vectors. *Proc Natl Acad Sci U S A,* **105**, 10137-10142.

Sharpless, N. E., and DePinho, R. A. (2004). Telomeres, stem cells, senescence, and cancer. *J Clin Invest,* **113**, 160-168.

Shedden, K., Taylor, J. M., Enkemann, S. A., Tsao, M. S., Yeatman, T. J., Gerald, W. L., Eschrich, S., Jurisica, I., Giordano, T. J., Misek, D. E.*, et al.* (2008). Gene expression-based survival prediction in lung adenocarcinoma: a multi-site, blinded validation study. *Nat Med,* **14**, 822-827.

Shi, L., Reid, L. H., Jones, W. D., Shippy, R., Warrington, J. A., Baker, S. C., Collins, P. J., de Longueville, F., Kawasaki, E. S., Lee, K. Y.*, et al.* (2006). The MicroArray Quality Control (MAQC) project shows inter- and intraplatform reproducibility of gene expression measurements. *Nat Biotechnol,* **24**, 1151-1161.

Shipp, M. A., Ross, K. N., Tamayo, P., Weng, A. P., Kutok, J. L., Aguiar, R. C., Gaasenbeek, M., Angelo, M., Reich, M., Pinkus, G. S.*, et al.* (2002). Diffuse large B-cell lymphoma outcome prediction by gene-expression profiling and supervised machine learning. *Nat Med,* **8**, 68-74.

Singh, D., Febbo, P. G., Ross, K., Jackson, D. G., Manola, J., Ladd, C., Tamayo, P., Renshaw, A. A., D'Amico, A. V., Richie, J. P.*, et al.* (2002). Gene expression correlates of clinical prostate cancer behavior. *Cancer Cell,* **1**, 203-209.

Singh, S. K., Hawkins, C., Clarke, I. D., Squire, J. A., Bayani, J., Hide, T., Henkelman, R. M., Cusimano, M. D., and Dirks, P. B. (2004). Identification of human brain tumour initiating cells. *Nature,* **432**, 396-401.

Soriano, P. (1999). Generalized lacZ expression with the ROSA26 Cre reporter strain. *Nat Genet,* **21**, 70-71.

Straight, A. F., Cheung, A., Limouze, J., Chen, I., Westwood, N. J., Sellers, J. R., and Mitchison, T. J. (2003). Dissecting temporal and spatial control of cytokinesis with a myosin II Inhibitor. *Science,* **299**, 1743-1747.

Tan, P. K., Downey, T. J., Spitznagel, E. L., Jr., Xu, P., Fu, D., Dimitrov, D. S., Lempicki, R. A., Raaka, B. M., and Cam, M. C. (2003). Evaluation of gene expression measurements from commercial microarray platforms. *Nucleic Acids Res,* **31**, 5676-5684.

Tapon, N., and Ziebold, U. (2008). Invasion and metastasis: stem cells, screens and survival. Conference on Invasion and Metastasis. *EMBO Rep, 9*, 1078-1083.

Terhune, P. G., Phifer, D. M., Tosteson, T. D., and Longnecker, D. S. (1998). K-ras mutation in focal proliferative lesions of human pancreas. *Cancer Epidemiol Biomarkers Prev,* **7**, 515-521.

Theodoropoulos, P. A., Polioudaki, H., Agelaki, S., Kallergi, G., Saridaki, Z., Mavroudis, D., and Georgoulias, V. (2009). Circulating tumor cells with a putative stem cell phenotype in peripheral blood of patients with breast cancer. *Cancer Lett*.

Thiery, J. P., and Sleeman, J. P. (2006). Complex networks orchestrate epithelial-mesenchymal transitions. *Nat Rev Mol Cell Biol,* **7**, 131-142.

Tse, J. C., and Kalluri, R. (2007). Mechanisms of metastasis: epithelial-to-mesenchymal transition and contribution of tumor microenvironment. *J Cell Biochem,* **101**, 816-829.

van 't Veer, L. J., Dai, H., van de Vijver, M. J., He, Y. D., Hart, A. A., Mao, M., Peterse, H. L., van der Kooy, K., Marton, M. J., Witteveen, A. T.*, et al.* (2002). Gene expression profiling predicts clinical outcome of breast cancer. *Nature,* **415**, 530-536.

van de Vijver, M. J., He, Y. D., van't Veer, L. J., Dai, H., Hart, A. A., Voskuil, D. W., Schreiber, G. J., Peterse, J. L., Roberts, C., Marton, M. J.*, et al.* (2002). A gene-expression signature as a predictor of survival in breast cancer. *N Engl J Med,* **347**, 1999-2009.

Vecchi, M., Confalonieri, S., Nuciforo, P., Vigano, M. A., Capra, M., Bianchi, M., Nicosia, D., Bianchi, F., Galimberti, V., Viale, G.*, et al.* (2008). Breast cancer metastases are molecularly distinct from their primary tumors. *Oncogene,* **27**, 2148-2158.

Vicent, S., Luis-Ravelo, D., Anton, I., Garcia-Tunon, I., Borras-Cuesta, F., Dotor, J., De Las Rivas, J., and Lecanda, F. (2008). A novel lung cancer signature mediates metastatic bone colonization by a dual mechanism. *Cancer Res,* **68**, 2275-2285.

Volinia, S., Calin, G. A., Liu, C. G., Ambs, S., Cimmino, A., Petrocca, F., Visone, R., Iorio, M., Roldo, C., Ferracin, M.*, et al.* (2006). A microRNA expression signature of human solid tumors defines cancer gene targets. *Proc Natl Acad Sci U S A,* **103**, 2257-2261.

Volsky, S.-Y. K. a. D. J. (2005). Page: parametric analysis of gene set enrichment. *BMC Bioinformatics,* **6**.

Wagner, M., Luhrs, H., Kloppel, G., Adler, G., and Schmid, R. M. (1998). Malignant transformation of duct-like cells originating from acini in transforming growth factor transgenic mice. *Gastroenterology,* **115**, 1254-1262.

Walhout, A. J., Temple, G. F., Brasch, M. A., Hartley, J. L., Lorson, M. A., van den Heuvel, S., and Vidal, M. (2000). GATEWAY recombinational cloning: application to the cloning of large numbers of open reading frames or ORFeomes. *Methods Enzymol,* **328**, 575-592.

Wang, Y., Klijn, J. G., Zhang, Y., Sieuwerts, A. M., Look, M. P., Yang, F., Talantov, D., Timmermans, M., Meijer-van Gelder, M. E., Yu, J.*, et al.* (2005). Gene-expression profiles to predict distant metastasis of lymph-node-negative primary breast cancer. *Lancet,* **365**, 671-679.

Wang, Y. H., Li, F., Luo, B., Wang, X. H., Sun, H. C., Liu, S., Cui, Y. Q., and Xu, X. X. (2009). A side population of cells from a human pancreatic carcinoma cell line harbors cancer stem cell characteristics. *Neoplasma,* **56**, 371-378.

Warshaw, A. L., and Fernandez-del Castillo, C. (1992). Pancreatic carcinoma. *N Engl J Med 326*, 455-465.

Weigelt, B., Peterse, J. L., and van 't Veer, L. J. (2005). Breast cancer metastasis: markers and models. *Nat Rev Cancer,* **5**, 591-602.

Weiss, L., Holmes, J. C., and Ward, P. M. (1983). Do metastases arise from pre-existing subpopulations of cancer cells? *Br J Cancer,* **47**, 81-89.

Welsch, T., Keleg, S., Bergmann, F., Degrate, L., Bauer, S., and Schmidt, J. (2009). Comparative analysis of tumorbiology and CD133 positivity in primary and recurrent pancreatic ductal adenocarcinoma. *Clin Exp Metastasis*.

West, M., Blanchette, C., Dressman, H., Huang, E., Ishida, S., Spang, R., Zuzan, H., Olson, J. A., Jr., Marks, J. R., and Nevins, J. R. (2001). Predicting the clinical status of human breast cancer by using gene expression profiles. *Proc Natl Acad Sci U S A,* **98**, 11462-11467.

Wilentz, R. E., Iacobuzio-Donahue, C. A., Argani, P., McCarthy, D. M., Parsons, J. L., Yeo, C. J., Kern, S. E., and Hruban, R. H. (2000). Loss of expression of Dpc4 in pancreatic intraepithelial neoplasia: evidence that DPC4 inactivation occurs late in neoplastic progression. *Cancer Res,* **60**, 2002-2006.

Winklmeier, A., Poser, I., Hoek, K. S., and Bosserhoff, A. K. (2009). Loss of full length CtBP1 expression enhances the invasive potential of human melanoma. *BMC Cancer,* **9**, 52.

Xu, X., Wagner, K. U., Larson, D., Weaver, Z., Li, C., Ried, T., Hennighausen, L., Wynshaw-Boris, A., and Deng, C. X. (1999). Conditional mutation of Brca1 in mammary epithelial cells results in blunted ductal morphogenesis and tumour formation. *Nat Genet,* **22**, 37-43.

Yanaihara, N., Caplen, N., Bowman, E., Seike, M., Kumamoto, K., Yi, M., Stephens, R. M., Okamoto, A., Yokota, J., Tanaka, T.*, et al.* (2006). Unique microRNA molecular profiles in lung cancer diagnosis and prognosis. *Cancer Cell,* **9**, 189-198.

Zavadil, J., and Bottinger, E. P. (2005). TGF-beta and epithelial-to-mesenchymal transitions. *Oncogene,* **24**, 5764-5774.

Zhang, Z., Wang, Y., Vikis, H. G., Johnson, L., Liu, G., Li, J., Anderson, M. W., Sills, R. C., Hong, H. L., Devereux, T. R.*, et al.* (2001). Wildtype Kras2 can inhibit lung carcinogenesis in mice. *Nat Genet,* **29**, 25-33.

10 Acknowledgements

I want to sincerely thank everybody who supported my PhD research in any possible way.

First of all, I want to thank Prof. Dr. Roland M. Schmid for giving me the opportunity to conduct my PhD research in his department and for his strong support.
Along these lines I would like to thank Prof. Dr. Michael Schemann for taking over the external supervision of my thesis.
I want to thank both Prof. Dr. Roland Schmid and Prof. Dr. Micheal Schemann for their extensive scientific support during the TAC meetings which helped me very much in developing and conducting my research.

Especially, I want to thank PD Dr. Dieter Saur for taking me into his group and for offering such an interesting topic. Our scientific discussions were extremely helpful and he was always supportive. I am very grateful that he gave me the opportunity to develop and test my own ideas while his scientific input taught me a great deal about science.

Furthermore, I want to thank Dr. Hans-Jörg Schäffer from the IMPRS who has been a constant source of encouragement, help and support. He was there whenever I needed him for scientific and non-scientific reasons.

For their technical and experimental support I want to thank Uschi Götz, Monika Werb and Kornelia Fritsch. Also for scientific input and discussions I would like to thank Barbara Seidler.

For a great working environment, scientific discussions and especially moral support whenever I needed it for scientific and non-scientific matters I want to cordially thank my PhD mates Christiane Pelz, Mariel Paul and Sandra Baumann. Uschi Götz was also there whenever I was feeling down.
Many thanks to all members of the Saur, the Schneider and the Vogelmann group who added to an enjoyable working atmosphere.

I am very thankful to Dr. Philipp Pagel, Philipp Eser and Andre Aberer for analyzing my microarray data and for their supportive input. Special thanks go to Andre Aberer who helped me with these analyses even when he was half the world away.

For reading and correcting this manuscript, I would like to thank Mariel Paul and my mother.

Finally and most importantly, I would also like to thank my husband Thorsten Gohlke and my parents Günter and Erika Schmidt who helped me mastering any crisis and for constantly supporting me in the best way I could possibly imagine.

Annegret Gohlke

Adresse	Josephsburgstr. 78 81673 München
E-Mail	anne.schmidt@lrz.tum.de
Geburtsort	Quito, Ekuador
Geburtsdatum	3. April 1980
Nationalität	deutsch

BERUFSERFAHRUNG

Seit 11/2009	**Junior Projekt Managerin**, IMS Health GmbH & Co. OHG, München

AUSBILDUNG

10/2005-10/2009	**Doktorarbeit, Klinikum rechts der Isar, im Rahmen der "International Max Planck Research School for Molecular and Cellular Life Sciences", München** Projekt: "Molekulare Analyse der organspezifischen Metastasierung im Pankreaskarzinom – Identifikation und funktionale Charakterisierung metastasierungsrelevanter Gene"
10/1999-05/2005	**Diplomstudium Biologie**, Rheinische Friedrich-Wilhelms-Universität Bonn, Hauptfach Zellbiologie, Note "sehr gut" (1,4) Diplomarbeit: "Einfluss von Claudin-1 auf epithelzelluläre Migration und Invasion – Untersuchungen an Brustdrüsenepithelzellen und Brustdrüsenepitheltumorzellen"
03-12/2002	**Study Abroad Studentin**, University of New South Wales, Sydney, Australien, Kurse: human genetics, molecular cell biology, bacteria and disease
04/2001	**Vordiplom in Biologie**, Rheinische Friedrich-Wilhelms-Universität Bonn, Note "sehr gut“ (1,3)
1999	**Abitur, Albert-Einstein-Gymnasium**, St. Augustin, Note "sehr gut“ (1,1)

PRAKTISCHE ERFAHRUNG

09-11/2003	**Praktikum bei Bayer HealthCare, Leverkusen** Projekt: "Veränderung der Keratinexpression bei Tumorzelllinien und Keratinozyten nach Therapeutikaeinwirkung"
05-06/2003	**Praktikum am Pathologischen Institut der Uniklinik Bonn** Projekt: "Herstellung einer AP-2 überexprimierenden Zelllinie"

05/2001	**Praktikum am Nees-Institut für Biodiversität der Pflanzen der Universität Bonn** Projekt: "Benetzungsverhalten von pflanzlichen und technischen superhydrophoben Oberflächen in Abhängigkeit vom hydrostatischen Druck"

STIPENDIEN

06/2009	**Stipendium von "Keystone Symposia"**
Seit 03/2008	**Stipendium von e-fellows.net**
Seit 10/2005	**Stipendiatin der "International Max Planck Research School for Molecular and Cellular Life Sciences"**
12/2001-04/2005	**Stipendiatin der Stiftung der Deutschen Wirtschaft (sdw)**
03-12/2002	**Stipendiatin des DAAD**, Study Abroad Studentin an der University of New South Wales, Sydney, Australien

PUBLIKATIONEN:

Schmidt, A.*, Seidler, B.*, Mayr, U., Nakhai, H., Schmid, R. M., Schneider, G., and Saur, D. (2008). A Cre-loxP-based mouse model for conditional somatic gene expression and knockdown in vivo by using avian retroviral vectors. *Proc Natl Acad Sci U S A 105*, 10137-10142. (* equally contributed)

von Burstin, J., Eser, S., Seidler, B., Paul, M., Brandl, M., von Werder, A., **Schmidt, A.**, Mages, J., Schmid, R.M., Schneider, G., and Saur, D. (2009). E-cadherin regulates metastasis of pancreatic cancer in vivo and is suppressed by a SNAIL/HDAC2 repressor complex. *Gastroenterology*, 137 (1), 361-71

WEITERE KENNTNISSE

Fremdsprachen	Englisch	fließend
	Spanisch	sehr gut
	Französisch	Grundkenntnisse
EDV-Kenntnisse	Adobe PhotoShop, EndNote, Image-Pro Plus, MS Office (Word, Excel, Powerpoint, Outlook), SigmaPlot	
Workshops	**Scientific Presentation** 2,5 Tage, englischsprachig	
	Intercultural Communication 2,5 Tage, englischsprachig	
	Self-Management for Junior Scientists 2,5 Tage, englischsprachig	
	Führung (sdw Stipendiatenseminar) 2,5 Tage	

ENGAGEMENT

Seit 05/2009	**Vorstand "Projekte" des sdw Alumni e.V.**
06-07/2008	**Organisation eines sozialen Projektes** im Rahmen von "Corporate Volunteering" der Allianz SE
2007	**Mitglied im Hauptorganisationsteam des "PhD Symposium >interact"** im Dezember 2007
07/2001-2005	**Betreuung von Jugendfreizeiten und Familienfreizeiten** des LandesSportBundes NRW e. V.
07/2003-10/2004	**Hauptverantwortliche und selbstständige Organisation eines viertägigen Seminars** zum Thema „Schöne neue Gen-Welt – Ethik in der Biotechnologie“ im Rahmen eines Stipendiatenprojektes der Stiftung der Deutschen Wirtschaft (sdw)
1999-2003	**Mitarbeit in der Fachschaft Biologie**, davon 2 Jahre als stellvertretende Fachschaftsvorsitzende und gewähltes Fachgruppenmitglied
2000	**Koordination von Tutoren** zur akademischen Einarbeitung von Erstsemestern